

**Richard Thorn. "Flow."**

**Copyright 2000 CRC Press LLC. <<http://www.engnetbase.com>>.**

**Richard Thorn**

*University of Derby*

**Adrian Melling**

*Universitaet Erlangen-Nuember*

**Herbert Köchner**

*Universitaet Erlangen-Nuember*

**Reinhard Haak**

*Universitaet Erlangen-Nuember*

**Zaki D. Husain**

*Daniel Flow Products, Inc.*

**Donald J. Wass**

*Daniel Flow Products, Inc.*

**David Wadlow**

*Sensors Research Consulting, Inc.*

**Harold M. Miller**

*Data Industrial Corporation*

**Halit Eren**

*Curtin University of Technology*

**Hans-Peter Vaterlaus**

*Rittmeyer Ltd.*

**Thomas Hossle**

*Rittmeyer Ltd.*

**Paolo Giordano**

*Rittmeyer Ltd.*

**Christophe Bruttin**

*Rittmeyer Ltd.*

**Wade M. Mattar**

*The Foxboro Company*

**James H. Vignos**

*The Foxboro Company*

**Nam-Trung Nguyen**

*University of California at Berkeley*

**Jesse Yoder**

*Automation Research Corporation*

**Rekha Philip-Chandy**

*Liverpool John Moores University*

**Roger Morgan**

*Liverpool John Moores University*

**Patricia J. Scully**

*Liverpool John Moores University*

# Flow Measurement

---

- 28.1 **Differential Pressure Flowmeters**  
Important Principles of Fluid Flow in Pipes • Bernoulli's Equation • Common Differential Pressure Flowmeters • Other Differential Pressure Flowmeters • Performance and Applications • Installation • Differential Pressure Measurement • Standards • Future Developments
- 28.2 **Variable Area Flowmeters**  
General Description of Variable Area Flowmeters • Measuring Principles of Variable Area Flowmeters
- 28.3 **Positive Displacement Flowmeters**  
Design and Construction • Some Commercially Available PD Meter Designs • Advantages and Disadvantages of PD Meters • Applications • Accessories • Price and Performance
- 28.4 **Turbine and Vane Flowmeters**  
Axial Turbine Flowmeters • Insertion Axial Turbine Flowmeters • Angular Momentum Flowmeters • Multijet Turbine Flowmeters • Cylindrical Rotor Flowmeter • Manufacturers • Conclusion
- 28.5 **Impeller Flowmeters**  
Sensing Principles • Flow Ranges • Installation • Manufacturers
- 28.6 **Electromagnetic Flowmeters**  
Faraday's Law of Induction • Construction and Operation of Electromagnetic Flowmeters • Types of Electromagnetic Flowmeters • Installation and Practical Applications of Electromagnetic Flowmeters • Effects of Electric Conductivity of Fluid • Signal Pickup and Demodulation Techniques
- 28.7 **Ultrasonic Flowmeters**  
Transit Time Flowmeter
- 28.8 **Vortex Shedding Flowmeters**  
Principle of Operation • Calculation of Mass Flow and Standard Volume • Flowmeter Construction • Application Considerations • Recent Developments
- 28.9 **Thermal Mass Flow Sensors**  
Principles of Conventional Thermal Mass Flowmeters • Mass and Heat Transfer • Analytical Models for Calorimetric Flowmeters • Principles of Microflow Sensors • Smart Thermal Flow Sensors and Advanced Evaluation Circuits • Calibration Conditions
- 28.10 **Coriolis Effect Mass Flowmeters**  
Theory of Operation • Construction • Advantages • Disadvantages • Applications • A Look Ahead

## 28.1 Differential Pressure Flowmeters

---

*Richard Thorn*

Flow measurement is an everyday event. Whether you are filling up a car with petrol (gasoline) or wanting to know how much water the garden sprinkler is consuming, a flowmeter is required. Similarly, it is also difficult to think of a sector of industry in which a flowmeter of one type or another does not play a part. The world market in flowmeters was estimated to be worth \$2500 million in 1995, and is expected to grow steadily for the foreseeable future. The value of product being measured by these meters is also very large. For example, in the U.K. alone, it was estimated that in 1994 the value of crude oil produced was worth \$15 billion.

Given the size of the flowmeter market, and the value of product being measured, it is somewhat surprising that both the accuracy and capability of many flowmeters are poor in comparison to those instruments used for measurement of other common process variables such as pressure and temperature. For example, the orifice plate flowmeter, which was first used commercially in the early 1900s and has a typical accuracy of  $\pm 2\%$  of reading, is still the only flowmeter approved by most countries for the fiscal measurement of natural gas. Although newer techniques such as Coriolis flowmeters have become increasingly popular in recent years, the flow measurement industry is by nature conservative and still dominated by traditional measurement techniques. For a review of recent flowmeter developments, refer to [1].

Over 40% of all liquid, gas, and steam measurements made in industry are still accomplished using common types of *differential pressure flowmeter*; that is, the orifice plate, Venturi tube, and nozzle. The operation of these flowmeters is based on the observation made by Bernoulli that if an annular restriction is placed in a pipeline, then the velocity of the fluid through the restriction is increased. The increase in velocity at the restriction causes the static pressure to decrease at this section, and a pressure difference is created across the element. The difference between the pressure upstream and pressure downstream of this obstruction is related to the rate of fluid flowing through the restriction and therefore through the pipe. A differential pressure flowmeter consists of two basic elements: an obstruction to cause a pressure drop in the flow (a *differential producer*) and a method of measuring the pressure drop across this obstruction (a *differential pressure transducer*).

One of the major advantages of the orifice plate, Venturi tube, or nozzle is that the measurement uncertainty can be predicted without the need for calibration, if it is manufactured and installed in accordance with one of the international standards covering these devices. In addition, this type of differential pressure flowmeter is simple, has no moving parts, and is therefore reliable. The main disadvantages of these devices are their limited range (typically 3:1), the permanent pressure drop they produce in the pipeline (which can result in higher pumping costs), and their sensitivity to installation effects (which can be minimized using straight lengths of pipe before and after the flowmeter). The combined advantages of this type of flowmeter are still quite hard to beat, and although it has limitations, these have been well investigated and can be compensated for in most circumstances. Unless very high accuracy is required, or unless the application makes a nonintrusive device essential, the differential flowmeter should be considered. Despite the predictions of its demise, there is little doubt that the differential pressure flowmeter will remain a common method of flow measurement for many years to come.

### Important Principles of Fluid Flow in Pipes

There are a number of important principles relating to the flow of fluid in a pipe that should be understood before a differential pressure flowmeter can be used with confidence. These are the difference

between laminar and turbulent flow, the meaning of Reynolds number, and the importance of the flow's velocity profile.

Fluid motion in a pipe can be characterized as one of three types: laminar, transitional, or turbulent. In *laminar flow*, the fluid travels as parallel layers (known as streamlines) that do not mix as they move in the direction of the flow. If the flow is turbulent, the fluid does not travel in parallel layers, but moves in a haphazard manner with only the average motion of the fluid being parallel to the axis of the pipe. If the flow is *transitional*, then both types may be present at different points along the pipeline or the flow may switch between the two.

In 1883, Osborne Reynolds performed a classic set of experiments at the University of Manchester that showed that the flow characteristic can be predicted using a dimensionless number, now known as the Reynolds number. The Reynolds number  $Re$  is the ratio of the inertia forces in the flow ( $\rho\bar{v}D$ ) to the viscous forces in the flow ( $\eta$ ) and can be calculated using:

$$Re = \frac{\rho\bar{v}D}{\eta} \quad (28.1)$$

where  $\rho$  = Density of the fluid

$\bar{v}$  = Mean velocity of the fluid

$D$  = Pipe diameter

$\eta$  = Dynamic viscosity of the fluid

If  $Re$  is less than 2000, viscous forces in the flow dominate and the flow will be laminar. If  $Re$  is greater than 4000, inertia forces in the flow dominate and the flow will be turbulent. If  $Re$  is between 2000 and 4000, the flow is transitional and either mode can be present. The Reynolds number is calculated using mainly properties of the fluid and does not take into account factors such as pipe roughness, bends, and valves that also affect the flow characteristic. Nevertheless, the Reynolds number is a good guide to the type of flow that can be expected in most situations.

The fluid velocity across a pipe cross-section is not constant, and depends on the type of flow present. In laminar flow, the velocity profile is parabolic since the large viscous forces present cause the fluid to move more slowly near the pipe walls. Under these conditions, the velocity at the center of the pipe is twice the average velocity across the pipe cross-section. The laminar flow profile is unaffected by the roughness of the pipe wall. In turbulent flow, inertia forces dominate, pipe wall effects are less, and the flow's velocity profile is flatter, with the velocity at the center being about 1.2 times the mean velocity. The exact flow profile in a turbulent flow depends on pipe wall roughness and Reynolds number. [Figure 28.1](#) shows the "fully developed" flow profiles for laminar and turbulent flow. These are the flow profiles that would be obtained at the end of a very long pipe, thus ensuring that any changes to the flow profile due to pipe bends and fittings are no longer present. To have confidence in the performance of a differential pressure flowmeter, both the characteristic and velocity profile of the flow passing through the flowmeter should be stable and known.

## Bernoulli's Equation

The Bernoulli equation defines the relationship between fluid velocity ( $v$ ), fluid pressure ( $p$ ), and height ( $h$ ) above some fixed point for a fluid flowing through a pipe of varying cross-section, and is the starting point for understanding the principle of the differential pressure flowmeter. For the inclined, tapered pipe shown in [Figure 28.2](#), Bernoulli's equation states that:

$$\frac{p_1}{\rho g} + \frac{v_1^2}{2g} + h_1 = \frac{p_2}{\rho g} + \frac{v_2^2}{2g} + h_2 \quad (28.2)$$

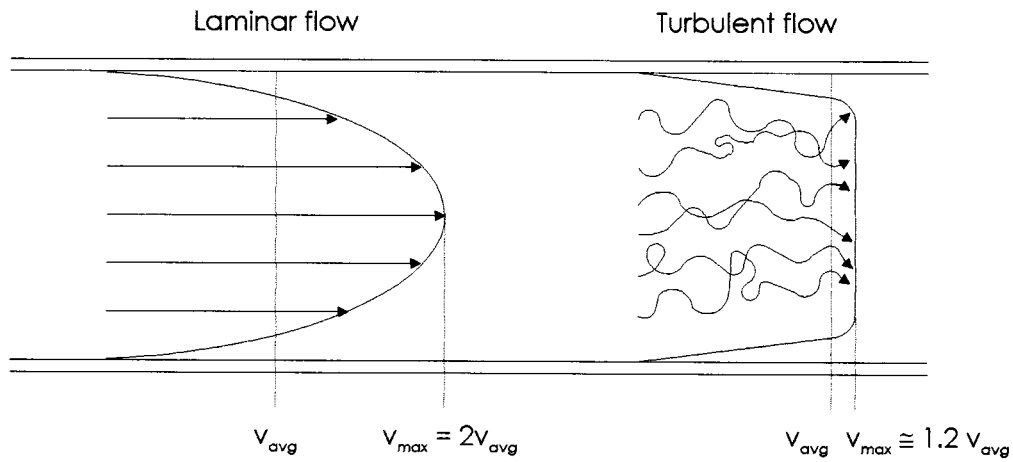


FIGURE 28.1 Velocity profiles in laminar and turbulent flow.

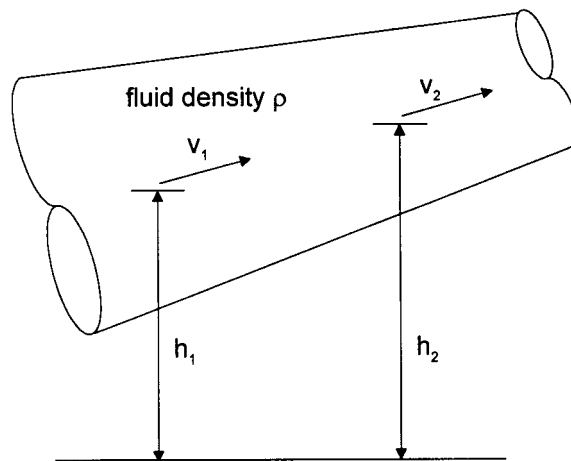


FIGURE 28.2 Flow through an inclined, tapered pipe.

Thus, the sum of the pressure head ( $p/\rho g$ ), the velocity head ( $v/2g$ ), and potential head ( $h$ ) is constant along a flow streamline. The term “head” is commonly used because each of these terms has the unit of meters. Equation 28.2 assumes that the fluid is frictionless (zero viscosity) and of constant density (incompressible). Further details on the derivation and significance of Bernoulli’s equation can be found in most undergraduate fluid dynamics textbooks (e.g., [2]).

Bernoulli’s equation can be used to show how a restriction in a pipe can be used to measure flow rate. Consider the pipe section shown in Figure 28.3. Since the pipe is horizontal,  $h_1 = h_2$ , and Equation 28.2 reduces to:

$$\frac{P_1 - P_2}{\rho} = \frac{v_1^2 - v_2^2}{2} \quad (28.3)$$

The conservation of mass principle requires that:

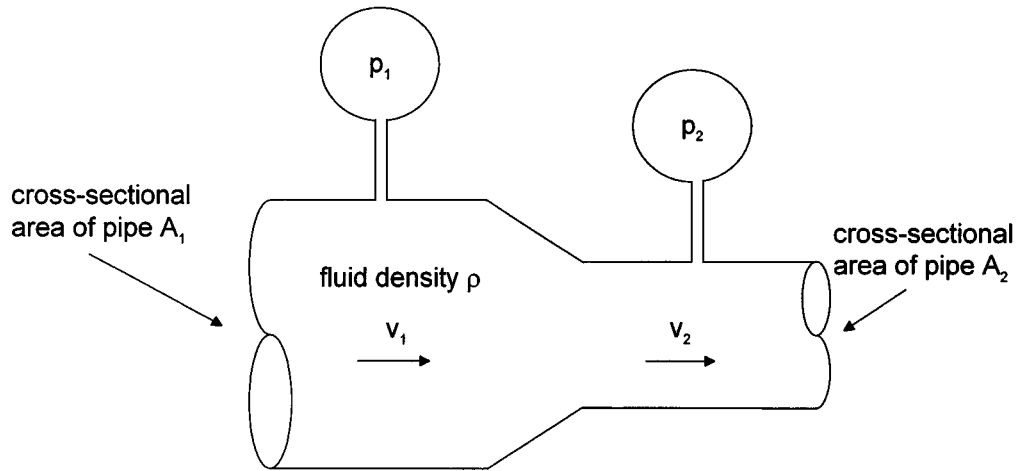


FIGURE 28.3 Using a restriction in a pipe to measure fluid flow rate.

$$v_1 A_1 \rho = v_2 A_2 \rho \quad (28.4)$$

Rearranging Equation 28.4 and substituting for  $v_2$  in Equation 28.3 gives:

$$Q = v_1 A_1 = \frac{A_2}{\sqrt{1 - \left(\frac{A_2}{A_1}\right)^2}} \sqrt{\frac{2(p_1 - p_2)}{\rho}} \quad (28.5)$$

This shows that the volumetric flow rate of fluid  $Q$  can be determined by measuring the drop in pressure ( $p_1 - p_2$ ) across the restriction in the pipeline — the basic principle of all differential pressure flowmeters. Equation 28.5 has limitations, the main ones being that it is assumed that the fluid is incompressible (a reasonable assumption for most liquids), and that the fluid has no viscosity (resulting in a flat velocity profile). These assumptions need to be compensated for when Equation 28.5 is used for practical flow measurement.

## Common Differential Pressure Flowmeters

### The Orifice Plate

The orifice plate is the simplest and cheapest type of differential pressure flowmeter. It is simply a plate with a hole of specified size and position cut in it, which can then clamped between flanges in a pipeline (Figure 28.4). The increase that occurs in the velocity of a fluid as it passes through the hole in the plate results in a pressure drop being developed across the plate. After passing through this restriction, the fluid flow jet continues to contract until a minimum diameter known as the vena contracta is reached. If Equation 28.5 is used to calculate volumetric flow rate from a measurement of the pressure drop across the orifice plate, then an error would result. This is because  $A_2$  should strictly be the area of the vena contracta, which of course is unknown. In addition, turbulence between the vena contracta and the pipe wall results in an energy loss that is not accounted for in this equation.

To overcome the problems caused by the practical application of Equation 28.5, two empirically determined correction factors are added. After some reorganization Equation 28.5 can be written as:

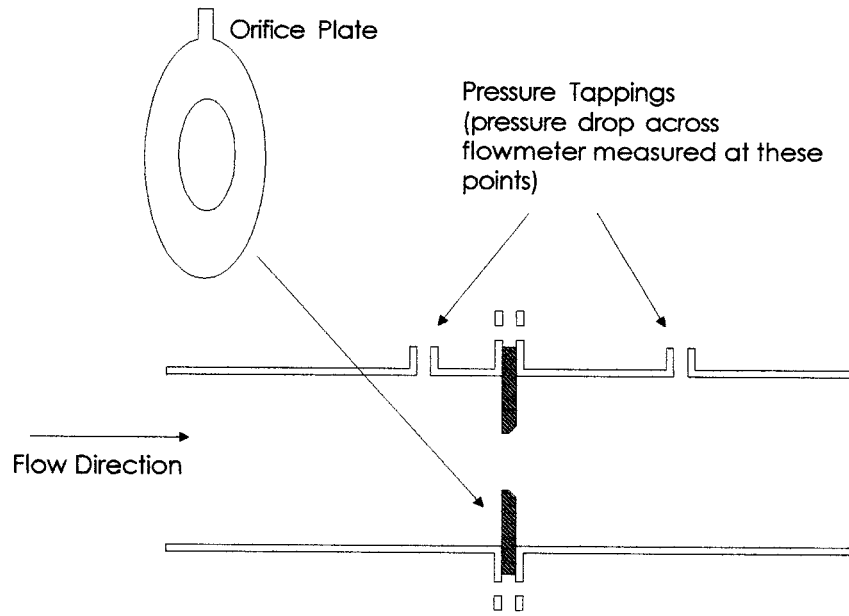


FIGURE 28.4 A square-edged orifice plate flowmeter.

$$Q = \frac{C}{\sqrt{1-\beta^4}} \varepsilon \frac{\pi}{4} d^2 \sqrt{\frac{2(p_1 - p_2)}{\rho}} \quad (28.6)$$

where  $\rho$  = Density of the fluid upstream of the orifice plate

$d$  = Diameter of the hole in the orifice plate

$\beta$  = Diameter ratio  $d/D$ , where  $D$  is the upstream internal pipe diameter

The two empirically determined correction factors are  $C$  the discharge coefficient, and  $\varepsilon$  the expansibility factor.  $C$  is affected by changes in the diameter ratio, Reynolds number, pipe roughness, the sharpness of the leading edge of the orifice, and the points at which the differential pressure across the plate are measured. However, for a fixed geometry, it has been shown that  $C$  is only dependent on Reynolds number and so this coefficient can be determined for a particular application.  $\varepsilon$  is used to account for the compressibility of the fluid being monitored. Both  $C$  and  $\varepsilon$  can be determined from equations and tables in a number of internationally recognized documents known as standards. These standards not only specify  $C$  and  $\varepsilon$ , but also the geometry and installation conditions for the square-edged orifice plate, Venturi tube, and nozzle, and are essentially a design guide for the use of the most commonly used types of differential pressure flowmeter. Installation recommendations are intended to ensure that fully developed turbulent flow conditions exist within the measurement section of the flowmeter. The most commonly used standard in Europe is ISO 5167-1 [3], while in the U.S., API 2530 is the most popular [4]. There are differences between some of the recommendations in these two standards (e.g., the minimum recommended length of straight pipe upstream of the flowmeter), but work is underway to resolve these.

Equation 28.6 illustrates perhaps the greatest strength of the orifice plate, which is that measurement performance can be confidently predicted without the need for calibration if the device is manufactured, installed, and operated in accordance with one of the international standards. In addition, the device is cheap to manufacture, has no moving parts, is reliable, and can be used for metering most clean gases, liquids, and steam.

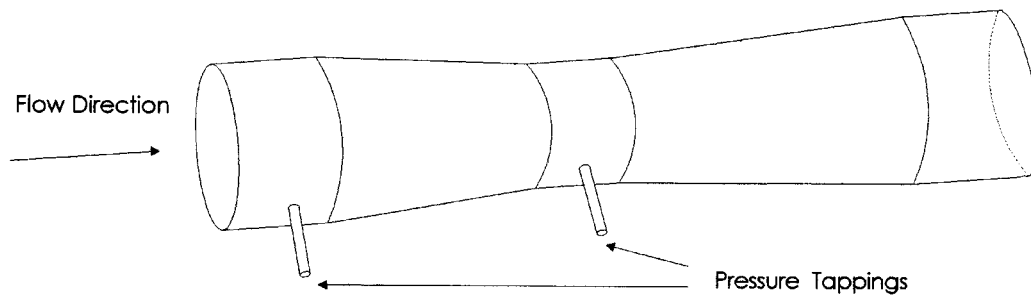


FIGURE 28.5 A Venturi tube flowmeter.

The major disadvantages of the orifice plate are its limited range and sensitivity to flow disturbances. The fact that fluid flow rate is proportional to the square root of the measured differential pressure limits the range of a one plate/one differential pressure transmitter combination to about 3:1. The required diameter ratio (also known as beta ratio) of the plate depends on the maximum flow rate to be measured and the range of the differential pressure transducer available. Sizing of the orifice plate is covered in most of the books in the further reading list, and nowadays computer programs are also available to help perform this task. The flow measurement range can be increased by switching; ways in which this may be achieved are described in [5]. Equation 28.6 assumes a fully developed and stable flow profile, and so installation of the device is critical, particularly the need for sufficient straight pipework upstream of the meter. Wear of the leading edge of the orifice plate can severely alter measurement accuracy; thus, this device is normally only used with clean fluids.

Only one type of orifice plate, the square-edged concentric, is covered by the standards. However, other types exist, having been designed for specific applications. One example is the eccentric orifice plate, which is suited for use with dirty fluids. Details of these other types of orifice plate can be found in [6].

### The Venturi Tube

The classical or Herschel Venturi tube is the oldest type of differential pressure flowmeter, having first been used in 1887. As Figure 28.5 shows, a restriction is introduced into the flow in a more gradual way than for the orifice plate. The resulting flow through a Venturi tube is closer to that predicted in theory by Equation 28.5 and so the discharge coefficient  $C$  is much nearer unity, being typically 0.95. In addition, the permanent pressure loss caused by the Venturi tube is lower, but the differential pressure is also lower than for an orifice plate of the same diameter ratio. The smooth design of the Venturi tube means that it is less sensitive to erosion than the orifice plate, and thus more suitable for use with dirty gases or liquids. The Venturi tube is also less sensitive to upstream disturbances, and therefore needs shorter lengths of straight pipework upstream of the meter than the equivalent orifice plate or nozzle. Like the orifice plate and nozzle, the design, installation, and use of the Venturi tube is covered by a number of international standards.

The major disadvantages of the Venturi tube flowmeter are its size and cost. It is more difficult, and therefore more expensive to manufacture than the orifice plate. Since a Venturi tube can be typically 6 diameters long, it can become cumbersome to use with larger pipe sizes, with associated maintenance of upstream and downstream pipe lengths also becoming a problem.

### The Nozzle

The nozzle (Figure 28.6) combines some of the best features of the orifice plate and Venturi tube. It is compact and yet, because of its curved inlet, has a discharge coefficient close to unity. There are a number of designs of nozzle, but one of the most commonly used in Europe is the ISA-1932 nozzle, while in the U.S., the ASME long radius nozzle is more popular. Both of these nozzles are covered by international standards.



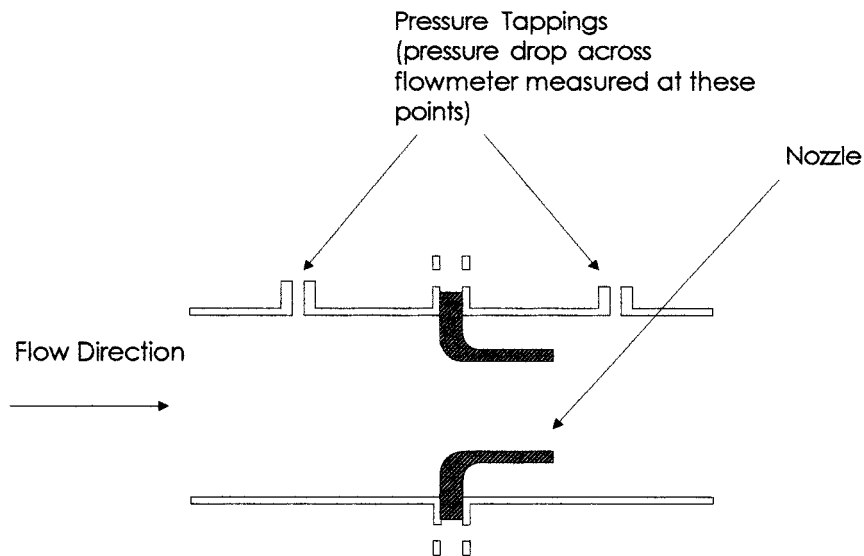


FIGURE 28.6 A nozzle flowmeter.

The smooth inlet of the nozzle means that it is more expensive to manufacture than the orifice plate as the curvature of the inlet changes with diameter ratio, although it is cheaper than the Venturi tube. The device has no sharp edges to erode and cause changes in calibration, and thus is well suited for use with dirty and abrasive fluids. The nozzle is also commonly used for high-velocity, high-temperature applications such as steam metering.

A variation of the nozzle is the sonic (or critical flow Venturi) nozzle, which has been used both as a calibration standard for testing gas meters and a transfer standard in interlaboratory comparisons [7].

### Other Differential Pressure Flowmeters

There are many other types of differential pressure flowmeter, including the segmental wedge, V-cone, elbow, and Dall tube. Each of these has advantages over the orifice plate, Venturi tube, and nozzle for specific applications. For example, the segmental wedge can be used with flows having a low Reynolds number, and a Dall tube has a lower permanent pressure loss than a Venturi tube. However, none of these instruments are yet covered by international standards and, thus, calibration is needed to determine their accuracy. Further information on these, and other less-common types of differential pressure flowmeter, can be found in [8].

### Performance and Applications

Table 28.1 shows the performance characteristics and main application areas of the square-edged orifice plate, Venturi tube, and nozzle flowmeters. Compared to other types of flowmeters on the market, these differential pressure flowmeters only have moderate accuracy, typically  $\pm 2\%$  of reading; but of course, this can be improved if the device is calibrated after installation. Although in some circumstances these flowmeters can be used with dirty gases or liquids, usually only small amounts of a second component can be tolerated before large measurement errors occur. When calculating the cost and performance of a differential flowmeter, both the primary element and the differential pressure transducer should be taken into account. Although the orifice plate is the cheapest of the primary elements, the cost of the fitting needed to mount it in the pipeline, particularly if on-line removal is required, can be significant.

Choosing which flowmeter is best for a particular application can be very difficult. The main factors that influence this choice are the required performance, the properties of the fluid to be metered, the

**TABLE 28.1** The Performance and Application Areas of Common Differential Pressure Flowmeters

	Performance					Applications				
	Typical uncalibrated accuracy	Typical range	Typical pipe diameter (mm)	Permanent pressure loss	Comparative cost	Clean gas	Dirty gas	Clean liquid	Slurry	Steam
Orifice plate	±2%	3:1	10–1000	High	Low	Yes	No	Yes	No	Yes
Venturi tube	±2%	3:1	25–500	Low	High	Yes	Maybe	Yes	Maybe	Maybe
Nozzle	±2%	3:1	25–250	High	Medium	Yes	Maybe	Yes	No	Yes

**TABLE 28.2** A Selection of Companies That Supply Differential Pressure Flowmeters

ABB Kent-Taylor Oldens Lane, Stonehouse Gloucestershire, GL10 3TA England Tel: + 44 1453 826661 Fax: + 44 1453 826358	ISA Controls Ltd. Hackworth Industrial Park Sildon County Durham DL4 1LH England Tel: + 44 1388 773065 Fax: + 44 1388 774888
Daniel Industries Inc. 9720 Katy Road P.O. Box 19097 Houston, TX 77224 Tel: (713) 467-6000 Fax: (713) 827-3880	Perry Equipment Corporation Wolters Industrial Park P.O. Box 640 Mineral Wells, TX 76067 Tel: (817) 325-2575 Fax: (817) 325-4622
Hartmann & Braun (UK) Ltd. Bush Beach Engineering Division Stanley Green Trading Estate, Cheadle Hulme Cheshire SK8 6RN England Tel: + 44 161 4858151 Fax: + 44 161 4884048	

installation requirements, the environment in which the instrument is to be used, and, of course, cost. There are two standards that can be used to help select a flowmeter: BS 1042: Section 1.4, which is a guide to the use of the standard differential pressure flowmeters [9]; and BS 7405, which is concerned with the wider principles of flowmeter selection [10].

Because all three flowmeters have similar accuracy, one strategy for selecting the most appropriate instrument is to decide if there are any good reasons for not using the cheapest flowmeter that can be used over the widest range of pipe sizes: the orifice plate. Where permanent pressure loss is important, the Venturi tube should be considered, although the high cost of this meter can only usually be justified where large quantities of fluid are being metered. For high-temperature or high-velocity applications, the nozzle should be considered because under these conditions, it is more predictable than the orifice plate. For metering dirty fluids, either the Venturi tube or the nozzle should be considered in preference to the orifice plate, the choice between the two depending on cost and pressure loss requirements. [Table 28.2](#) lists some suppliers of differential pressure flowmeters.

## Installation

Correct installation is essential for successful use of a differential pressure flowmeter because the predicted uncertainty in the flow rate/differential pressure relationship in Equation 28.6 assumes a steady flow,

**TABLE 28.3** The Minimum Straight Lengths of Pipe Required between Various Fittings and an Orifice Plate or Venturi Tube (as recommended in ISO 5167-1) to Ensure That a Fully Developed Flow Profile Exists in the Measurement Section. All Lengths Are Multiples of the Pipe Diameter

Diameter Ratio $\beta$	Upstream of the flowmeter			Downstream of the flowmeter	
	Single 90° bend	Two 90° bends in the same plane	Two 90° bends in different planes	Globe valve fully open	For any of the fittings shown to the left
0.2	10	14	34	18	4
0.4	14	18	36	20	6
0.6	18	26	48	26	7
0.8	46	50	80	44	8

with a fully developed turbulent velocity profile, is passing through the flowmeter. Standards contain detailed recommendations for the minimum straight lengths of pipe required before and after the flowmeter, in order to ensure a fully developed flow profile. Straight lengths of pipe are required after the flowmeter because disturbances caused by a valve or bend can travel upstream and thus also affect the installed flowmeter. Table 28.3 gives examples of installation requirements taken from ISO 5167-1. If it is not possible to fit the recommended lengths of straight pipe before and after the flowmeter, then the flowmeter must be calibrated once it has been installed.

The other major problem one faces during installation is the presence of a rotating flow or swirl. This condition distorts the flow velocity profile in a very unpredictable way, and is obviously not desirable. Situations that create swirl, such as two 90° bends in different planes, should preferably be avoided. However, if this is not possible, then swirl can be removed by placing a flow conditioner (also known as a flow straightener) between the source of the swirl and the flowmeter. There are a wide range of flow conditioner designs, some of which can be used to both remove swirl and correct a distorted velocity profile [11]. Because they obstruct the flow, all flow conditioners produce an unrecoverable pressure loss, which in general increases with their capability (and complexity).

## Differential Pressure Measurement

Apart from the differential producer, the other main element of a differential pressure flowmeter is the *transducer* needed to measure the pressure drop across the producer. The correct selection and installation of the differential pressure transducer plays an important part in determining the accuracy of the flow rate measurement.

The main factors that should be considered when choosing a differential pressure transducer for a flow measurement application are the differential pressure range to be covered, the accuracy required, the maximum pipeline pressure, and the type and temperature range of the fluid being metered.

Most modern differential pressure transducers consist of a pressure capsule in which either capacitance, strain gage, or resonant wire techniques are used to detect the movement of a diaphragm. Using these techniques, a typical accuracy of  $\pm 0.1\%$  of full scale is possible. See Chapter 26, Section 1 for further details of pressure transducers. The transducer is usually part of a unit known as a transmitter, which converts differential pressure, static pressure, and ambient temperature measurements into a standardized analog or digital output signal. “Smart” transmitters use a local, dedicated microprocessor to condition signals from the individual sensors and compute volumetric or mass flow rate. These devices can be remotely configured, and a wide range of diagnostic and maintenance functions are possible using their built-in “intelligence.”

As far as installation is concerned, the transmitter should be located as close to the differential producer as possible. This helps ensure a fast dynamic response and reduces problems caused by vibration of the connecting tubes. The position of the pressure tapings is also important. If liquid flow in a horizontal pipe is being measured, then the pressure tapings should be located at the side of the pipe so that they cannot be blocked with dirt or filled with air bubbles. For horizontal gas flows, if the gas is clean, the pressure tapings should be vertical; if steam or dirty gas is being metered, then the tapings should be

**TABLE 28.4** Standards Related to Differential Pressure Flow Measurement

---

<b>American National Standards Institute, New York</b>	
ANSI/ASHRAE 41.8	Standard methods of measurement of flow of liquids in pipes using orifice flowmeters.
ANSI/ASME MFC-7M	Measurement of gas flow by means of critical flow Venturi nozzles.
ANSI/ASME MFC-14M	Measurement of fluid flow using small bore precision orifice meters.
<b>American Petroleum Institute, Washington, D.C.</b>	
API 2530	Manual of Petroleum Measurement Standards, Chapter 14 — Natural gas fluids measurement, Section 3 — Orifice metering of natural gas and other related hydrocarbon fluids.
<b>American Society of Mechanical Engineers, New York</b>	
ASME MFC-3M	Measurement of fluid flow in pipes using orifice, nozzle and Venturi.
ASME MFC-8M	Fluid flow in closed conduits — Connections for pressure signal transmissions between primary and secondary devices.
<b>British Standards Institution, London</b>	
BS 1042	Measurement of fluid flow in closed conduits.
<b>International Organization for Standardization, Geneva</b>	
ISO 2186	Fluid flow in closed conduits — connections for pressure transmissions between primary and secondary elements.
ISO TR 3313	Measurement of pulsating fluid flow in a pipe by means of orifice plates, nozzles or Venturi tubes.
ISO 5167-1	Measurement of fluid flow by means of pressure differential devices.
ISO 9300	Measurement of gas flow by means of critical flow Venturi nozzles.

---

located at the side of the pipe. These general guidelines show that considerable care must be taken with the installation of the differential pressure transmitter if large measurement errors are to be avoided. For further details on the installation of differential pressure transmitters, see ISO 2186 [12].

## Standards

International standards that specify the design, installation, and use of the orifice plate, Venturi tube, and nozzle, and allow their accuracy to be calculated without the need for calibration, are probably the main reason for the continuing use of this type of flowmeter. Table 28.4 gives details of the most common standards related to differential pressure flowmeters. There are still inconsistencies in the various standards. For example, ISO 5167-1 states that any flow conditioner should be preceded by at least 22 diameters of straight pipe and followed by at least 20 diameters of straight pipe. This would seem to contradict one application of a flow conditioner, which is to reduce the length of straight pipe required upstream of a flowmeter.

Despite the occasional inconsistency and difference between the standards, they are the internationally accepted rules for the installation and use of the square-edged orifice plate, Venturi tube, and nozzle.

## Future Developments

In spite of the vast amount of published data available on differential pressure flowmeters, continued research is needed to improve the understanding of the effect of flow conditions, and flowmeter geometry, on the uncalibrated accuracy of these devices. For example, work has been recently undertaken to derive an improved equation for the discharge coefficient of an orifice plate [13].

The metering of multiphase flow is an area of increasing importance. In addition to developing new measurement techniques, many people are investigating ways in which traditional flowmeters can be used to meter multiphase flows. A good review of the use of differential pressure flowmeters for multiphase flow measurement can be found in [14].

The development of “smart” differential pressure transmitters has overcome the limitations of differential pressure flowmeters in some applications. For example, these devices are being used to linearize and extend the range of differential pressure flowmeters.

The above developments should help to ensure the continued popularity of the differential pressure flowmeter for the foreseeable future, despite increasing competition from newer types of instrument.

## Defining Terms

**Differential pressure flowmeter:** A flowmeter in which the pressure drop across an annular restriction placed in the pipeline is used to measure fluid flow rate. The most common types use an orifice plate, Venturi tube, or nozzle as the primary device.

**Orifice plate:** Primary device consisting of a thin plate in which a circular aperture has been cut.

**Venturi tube:** Primary device consisting of a converging inlet, cylindrical mid-section, and diverging outlet.

**Nozzle:** Primary device consisting of a convergent inlet connected to a cylindrical section.

**Differential pressure transmitter:** Secondary device that measures the differential pressure across the primary device and converts it into an electrical signal.

## References

1. R. A. Furness, Flowmetering: evolution or revolution, *Measurement and Control*, 27 (8), 15-18, 1994.
2. B. S. Massey, *Mechanics of Fluids*, 6th ed., London: Chapman and Hall, 1989.
3. International Organization for Standardization, ISO 5167-1, Measurement of Fluid Flow by Means of Pressure Differential Devices — Part 1 Orifice plates, nozzles and Venturi tubes inserted in circular cross-section conduits running full, Geneva, Switzerland, 1991.
4. American Petroleum Institute, API 2530, Manual of Petroleum Measurement Standards Chapter 14 — Natural Gas Fluids Measurement, Section 3 — Orifice Metering of Natural Gas and Other Related Hydrocarbon Fluids, Washington, 1985.
5. E. L. Upp, *Fluid Flow Measurement*, Houston: Gulf Publishing, 1993.
6. H. S. Bean, *Fluid Meters Their Theory and Application*, 6th ed., New York: American Society of Mechanical Engineers, 1983.
7. P. H. Wright, The application of sonic (critical flow) nozzles in the gas industry, *Flow Meas. Instrum.*, 4 (2), 67-71, 1993.
8. D. W. Spitzer, *Industrial Flow Measurement*, 2nd ed., Research Triangle Park, NC: ISA, 1990.
9. British Standards Institution, BS 1042, Measurement of Fluid Flow in Closed Conduits — Part 1 Pressure differential devices — Section 1.4 Guide to the use of devices specified in Sections 1.1 and 1.2, London, 1992.
10. British Standards Institution, BS7405, Guide to the Selection and Application of Flowmeters for Measurement of Fluid Flow in Closed Conduits, London, 1991.
11. E. M. Laws and A. K. Ouazzane, Compact installations for differential pressure flow measurement, *Flow Meas. Instrum.*, 5 (2), 79-85, 1994.
12. International Organization for Standardization, ISO 2186, Fluid Flow in Closed Conduits — Connections for Pressure Signal Transmissions Between Primary and Secondary Elements, Geneva, Switzerland, 1973.
13. M. J. Reader-Harris, J. A. Slattery, and E. P. Spearman, The orifice plate discharge coefficient equation — further work, *Flow. Meas. Instrum.*, 6 (2), 101-114, 1995.
14. F. C. Kinghorn, Two-phase flow measurement using differential pressure meters, *Multi-Phase Flow Measurement Short Course*, London, 17th-18th June 1985.

## Further Information

- R. C. Baker, *An Introductory Guide to Flow Measurement*, London: Mechanical Engineering Publications, 1989, a good pocket sized guide on the choice and use of flowmeters commonly used in industry.
- A. T. J. Hayward, *Flowmeters — A Basic Guide and Source-Book for Users*, London: Macmillan, 1979, an overview of the important areas of flow measurement which is a joy to read.
- R. W. Miller, *Flow Measurement Engineering Handbook*, 3rd ed., New York: McGraw-Hill, 1996, a thorough reference book particularly on differential pressure flowmeters, covers European and U.S. standards with calculations using both U.S. and SI units.
- D. W. Spitzer, *Flow Measurement: Practical Guides for Measurement and Control*, Research Triangle Park, NC: ISA, 1991, intended for practicing engineers, this book covers most aspects of industrial flow measurement.
- E. L. Upp, *Fluid Flow Measurement*, Houston: Gulf Publishing, 1993, contains a lot of practical advice on the use of differential pressure flowmeters.
- Flow Measurement and Instrumentation*, UK: Butterworth-Heinemann, a quarterly journal covering all aspects of flowmeters and their applications. A good source of information on current research activity.

## 28.2 Variable Area Flowmeters

---

*Adrian Melling, Herbert Köchner, and Reinhard Haak*

The term *variable area flowmeters* refers to those meters in which the minimum cross-sectional area available to the flow through the meter varies with the flow rate. Meters of this type that are discussed in this section include the rotameter and the movable vane meter used in pipe flows, and the weir or flume used in open-channel flows. The measure of the flow rate is a geometrical quantity such as the height of a bob in the rotameter, the angle of the vane, or the change in height of the free surface of the liquid flowing over the weir or through the flume.

Most of the discussion here is devoted to the rotameter, firstly because the number of installed rotameters and movable vane meters is large relative to the number of weirs and flumes, and secondly because the movable vane is often used simply as a flow indicator rather than as a meter.

The following section includes basic information describing the main constructional features and applications of each type of meter. In the third section, the principles of measurement and design of rotameters and open-channel meters are described in some detail; the movable vane meter is not considered further because most design aspects are similar to those of rotameters. Then, the contribution of modern computational and experimental methods of fluid mechanics to flowmeter design is discussed, using the results of a detailed investigation of the internal flow.

Details of manufacturers of rotameters and movable vane meters, together with approximate costs of these meters, are also tabulated in [Tables 28.5 through 28.7](#).

### General Description of Variable Area Flowmeters

#### Rotameter

The *rotameter* is a robust and simple flowmeter for gases and liquids, and holds a large share of the market for pipe diameters smaller than about 100 mm. In its basic form, the rotameter consists of a conical transparent vertical glass tube containing a “bob” ([Figure 28.7](#)), which rises in the tube with increasing flow rate until a balance is reached between gravitational, buoyancy, and drag forces on the bob. Within the range of a particular flowmeter (depending on the bob shape and density, the tube shape and the fluid density and viscosity), the flow rate is linearly proportional to the height of the bob in the tube and is determined simply by reading the level of the upper edge of the bob. The rotameter is also

**TABLE 28.5** Approximate Rotameter Prices

Type	Size	Price (plastic)	Price (stainless steel, borosilicate glass)
Glass	< 1/2 in. (12.7 mm)	\$50	\$200
Plastic	1/2 in. (12.7 mm)	\$50	\$200
	1 in. (25.4 mm)	\$70	\$150
	2 in. (50.8 mm)	\$200	\$500
Metal	1/2 in. (12.7 mm)		\$500
	1 in. (25.4 mm)		\$600
	2 in. (50.8 mm)		\$700
	3 in. (76.2 mm)		\$1100
	4 in. (101.6 mm)		\$1400
Additional costs			
	Electric limit switch	\$100	
	Current transducer	\$500	
	Pneumatic	\$1200	

**TABLE 28.6** Approximate Movable Vane Meter Prices

Type	Price
Plastic versions (small scale)	From \$10
Direct coupled pointer versions incl. electric flow switch: Metal, screw connections 1/2 in. (12.7 mm) to 2 in. (50.8 mm)	\$400 (brass) to \$600 (stainless steel)
Flanged versions	Add \$200 (1/2 in., 12.7 mm) to \$400 (2 in., 50.8 mm)
Magnetic coupled indicator, stainless steel	\$1200 (1/2 in., 12.7 mm) to \$2100 (8 in., 203 mm)

known as “floating element flowmeter,” although the buoyancy force on the “floating element” is not sufficient to make it float.

The bob is commonly formed of a combination of cylindrical and conical sections, but a spherical bob is often used in small diameter tubes (see [Figures 28.8](#)). More complicated bob geometries can reduce the sensitivity to viscosity of the fluid. Frequently, the bob has several shallow inclined grooves around the upper rim that induce a slow rotation (frequency about 1 Hz) of the bob, which helps to maintain a stable position of the bob. In larger rotameters where the additional friction is acceptable, the bob can be allowed to slide up and down a rod on the tube axis to prevent any sideways motion.

Various tube geometries are in use. The basic requirement for an increase in the cross-sectional area up the height of the tube leads to the conical tube. An alternative form uses three ribs arranged circumferentially around the tube to guide the bob; the flow area between the ribs increases along the tube height. For spherical bobs, a triangular tube in which the bob remains in contact with three surfaces over the whole height of the tube prevents lateral movement of the bob with minimum friction. Commonly, the tube is made of glass to facilitate the reading of the flow rate from a scale engraved on the tube. For general-purpose applications, the scale can be marked in millimeters; the flow rate is then determined by a conversion factor depending on the tube dimensions, the mass of the bob, the pressure and temperature, and the properties of the fluid. For specific application to a single fluid under controlled conditions, it is more convenient to have the flow rate directly marked on the tube.

For laboratory use, medical equipment, and other applications with small flow rates, the glass tube is almost universal. Laboratory meters are often equipped with a flow valve that allows direct flow setting and reading. For many small rotameters, integrated flow controllers are offered; these hold the pressure drop and the flow setting constant, even with changing upstream or downstream pressure.

For most rotameters, electric limit switches or analog electric signal transducers are available. For glass and plastic meters, inductive or optical switches are used that can be positioned to the desired level of

**TABLE 28.7** Manufacturers of Rotameters and Movable Vane Meters

---

Tokyo Keiso Co. Ltd. Shiba Toho Building 1-7-24, Shibakoen Minato-ku Tokyo 105, Japan Tel: +81-3-3431-1625 Fax: +81-3-3433-4922	Porter Instruments Co. 245 Township Line Road Hatfield, PA 19440 Tel: (215) 723-4000 Fax: (215) 723-2199
Brooks Instrument Division Emerson Electric 407 W. Vine St. Hatfield, PA 19440 Tel: (215) 362-3500 Fax: (215) 362-3745	Wallace & Tiernan, Inc. 25 Main St. St. Belleville, NJ 07109 Tel: (201) 759-8000 Fax: (201) 759-9333
Krohne America Inc. 7 Dearborn Rd. Peabody, MA 01960 Tel: (508) 535-6060, (800) 356-9464 Fax: (508) 535-1720	KDG-Mobrey Ltd. Crompton Way Crawley West Sussex RH10 2YZ, Great Britain Tel: +44-1293-518632 Fax: +44-1293-533095
Bailey Fischer & Porter Co. County Line Rd. Warminster, PA 18974 Tel: (215) 674-6000 Fax: (215) 674-7183	CT Platon Jays Close Viabes Basingstoke, Hampshire RG22 4BS, Great Britain Tel: +44-1256-470456 Fax: +44-1256-363345
Bopp & Reuther Heinrichs Messtechnik GmbH Stolberger Str. 393 D-50933 Köln, Germany Tel: +49-221-49708-0 Fax: +49-221-497088	Kobold Messring GmbH Nordring 22-24 D-65719 Hofheim/Taunus, Germany Tel: +49 6192 2990 Fax: +49 6192 23398
Rota Yokogawa GmbH & Co. KG Rheinstrasse 8 D-79664 Wehr, Germany Tel: +49-7761-567-0 Fax: +49-7761-567-126	

---

the bob. While some units just detect the bob within their active area, other switches have bistable operation, wherein the switch is toggled by the float passing the switch.

For industrial applications, the metering of corrosive fluids or fluids at high temperature or pressure leads to the use of stainless steel tubes or a wide range of other materials chosen to suit the application requirements (e.g., temperature, pressure, corrosion). Most metal rotameters use a permanent magnetic coupling between the float and the pointer of the indicator, enabling a direct analog flow reading without electric supply. Electric switches can, however, be added to the indicator, and electric and pneumatic transmitters for the flow reading are offered by most producers. Some units are equipped with options such as flow totalizers, mass flow calculation units for gas applications in conjunction with temperature and pressure sensors, or energy calculation units. Due to the frequent application of the rotameter in the chemical and petrochemical industry, electric options are often designed for use in hazardous areas.

The rotameter is characterized by:

- Simple and robust construction
- High reliability
- Low pressure drop



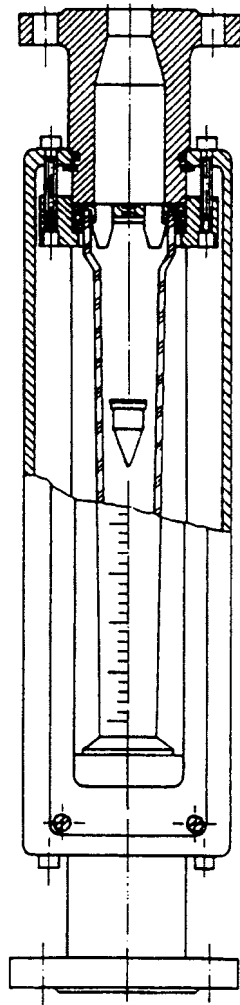


**FIGURE 28.7** Cross-section of a rotameter. The level of the bob rises linearly with increasing flow rate.

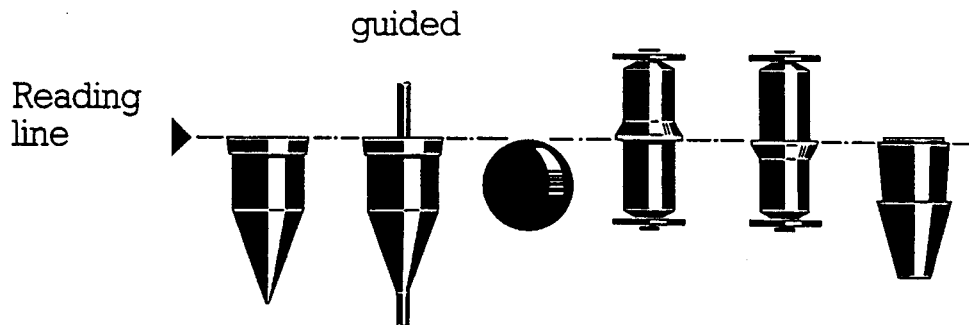


**FIGURE 28.8** Typical rotameter bob geometries.

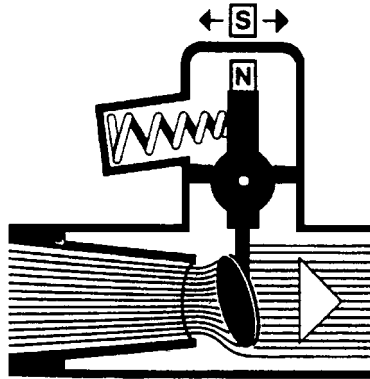


FIGURE 28.9 Movable vane meter. The magnet (N,S) transmits the vane position to an indicator.

- Applicable to a wide variety of gases and liquids
- Flow range typically  $0.04 \text{ L h}^{-1}$  to  $150 \text{ m}^3 \text{ h}^{-1}$  for water
- Flow range typically  $0.5 \text{ L h}^{-1}$  to  $3000 \text{ m}^3 \text{ h}^{-1}$  for air
- 10:1 flow range for given bob-tube combination
- Uncertainty 0.4% to 4% of maximum flow
- Insensitivity to nonuniformity in the inflow (no upstream straight piping needed)
- Typical maximum temperature  $400^\circ\text{C}$
- Typical maximum pressure 4 MPa (40 bar)
- Low investment cost
- Low installation cost

### Movable Vane Meter

The movable vane meter is a robust device suitable for the measurement of high flow rates where only moderate requirements on the measurement accuracy are made. Dirty fluids can also be metered. It contains a flap that at zero flow is held closed by a weight or a spring (Figure 28.9). A flow forces the vane open until the dynamic force of the flow is in balance with the restoring force of the weight or the spring. The angle of the vane is thus a measure of the flow rate, which can be directly indicated by a pointer attached to the shaft of the vane on a calibrated scale. The resistance provided by the vane depends on the vane position and hence on the flow rate or Reynolds number; a recalibration is therefore necessary when the fluid is changed. An important application is the metering of the air flow in automotive engines with fuel injection.

In low-cost flow indicators, a glass or plastic window allows a direct view of the flap (Figure 28.10). Sometimes, optical or reed switches in combination with a permanent magnet attached to the flap are used as electric flow switches. All-metal units use a magnetic coupling between the vane and the pointer of the indicator, thus avoiding most of the friction and material selection problems. Many applications use the movable vane meter as a flow switch with appropriate mechanical, magnetic, inductive, or optical switches. The setting of the switch is done once for all during the installation. Since a continuous flow indication is not needed, flow reading uncertainties are not of concern.

Most aspects of design and application of rotameters can be applied to movable vane meters, although the latter are characterized by a higher uncertainty of the flow reading. General features of both types of variable area flowmeter are summarized, for example, in reference [1]. Since the basic construction of the two meter types is very similar, the unit costs also lie in the same range.

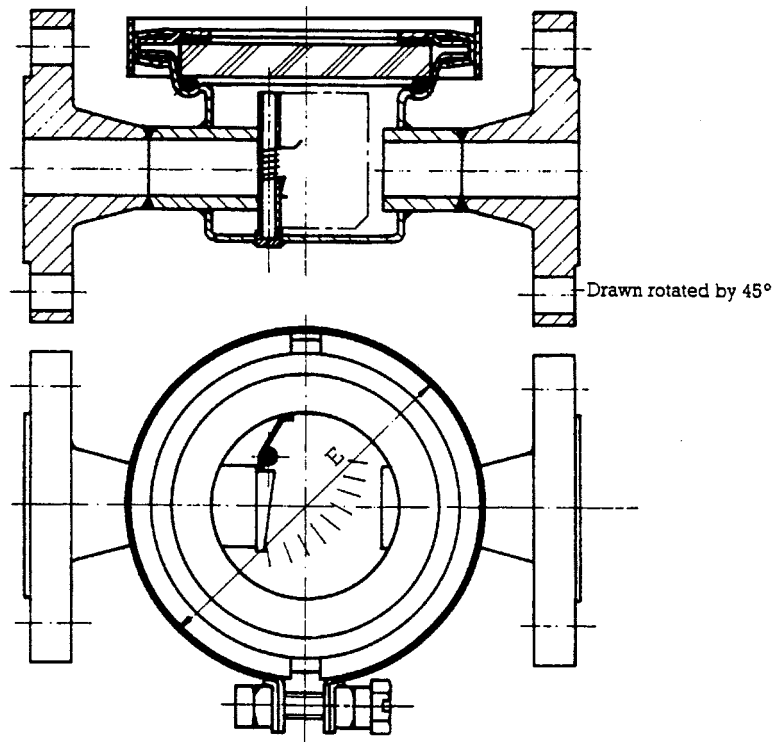
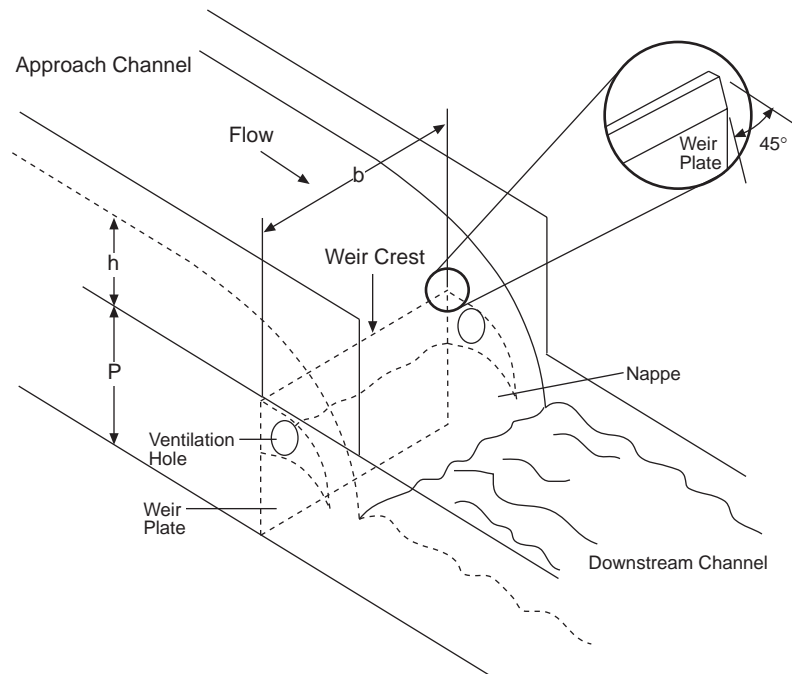


FIGURE 28.10 Flow indicator. The angle of the vane provides a measure of the flow rate.

### Weir, Flume

Of the methods available for the metering of a liquid (generally water) in open-channel flow, the weir and the flume fall within the scope of this discussion on variable area flowmeters. In each case, the flow metering depends on measurement of the difference in height  $h$  of the water surface over an obstruction across the channel and the surface sufficiently far upstream. There is a wide variety of geometries in use (see reference [2]), but most of these can be described as variants of three basic types. In the sharp crested weir, also known as the thin plate weir (Figure 28.11), the sill or crest is only about 1 mm to 2 mm thick. The sheet of liquid flowing over the weir, called the nappe or vein, separates from the weir body after passing over the crest. An air-filled zone at atmospheric pressure is formed underneath the outflowing jet, and the streamlines above the weir are strongly curved. If the width of the weir is less than that of the upstream channel (Figures 28.12 and 28.13), the term “notch” is frequently used. A broad crested weir (Figure 28.14) has a sill which is long enough for straight, parallel streamlines to form above the crest. In this review, the term “weir” is applied generally to both the weir and the notch.

The resistance to flow introduced by the weir causes the water level upstream to rise. If it is assumed that the flow velocity some distance upstream of the weir is zero, then a simple measure of the upstream water level suffices to determine the discharge over a weir of known geometry. As in the case of an orifice in pipe flow, there will be a contraction of the nappe and a frictional resistance at the sides as water flows over a weir. The actual discharge is less than the theoretical discharge according to an empirically determined coefficient of discharge  $C_d$ . In the analysis of rectangular notches and weirs, it is frequently assumed that the channel width remains constant so that a contraction of the nappe occurs only in the vertical direction as the water accelerates over the obstacle. When the weir is narrower than the upstream channel, there is an additional horizontal contraction. The effect of a significant upstream velocity is accounted for empirically.



**FIGURE 28.11** Full-width thin plate weir. Flow rate  $\dot{Q}$  varies with water level  $h$  above the weir crest ( $\dot{Q} \sim h^{3/2}$ ) and with a flow-dependent discharge coefficient  $C_d$ .

As an alternative to the weir, the flume (Figure 28.15) provides a method for flow metering with relatively low pressure loss. By restricting the channel width, analogous to the Venturi tube used in pipe flow, the flow velocity in the narrow portion of the channel is increased and the water level sinks accordingly. Most of the head of water is recovered in the diffusing section of the weir. The water levels upstream and in the throat of the weir can be determined by simple floats and recorded on a chart by pens driven mechanically from the floats. For remote monitoring, the use of echo sounders is advantageous.

The weir is preferentially used in natural river beds and the flume in canalized water courses. The flume must be used in streams with sediment transport to avoid the accumulation of deposits that would occur at the approach to a weir. Weirs and flumes are characterized by

- Simple measurement of the water level
- Simple maintenance
- Reliable measurement of large flow rates at low stream velocity
- Limited measurement accuracy (at best about 2%)
- High installation costs, particularly for flumes

Recommendations for installation of weirs and flumes, for the location of the head measuring station upstream, and for determining the discharge from the measured head are given, for example, in [2] and [3] as well as in appropriate standards (e.g., [4–6]).

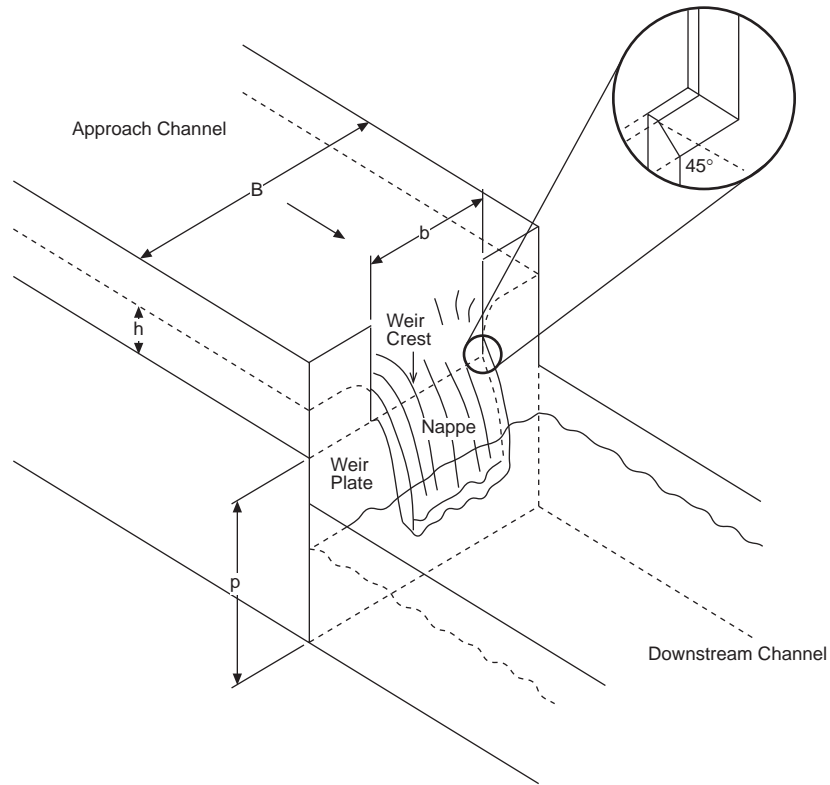


FIGURE 28.12 Thin plate rectangular notch weir: discharge coefficient  $C_d$  is flow dependent.

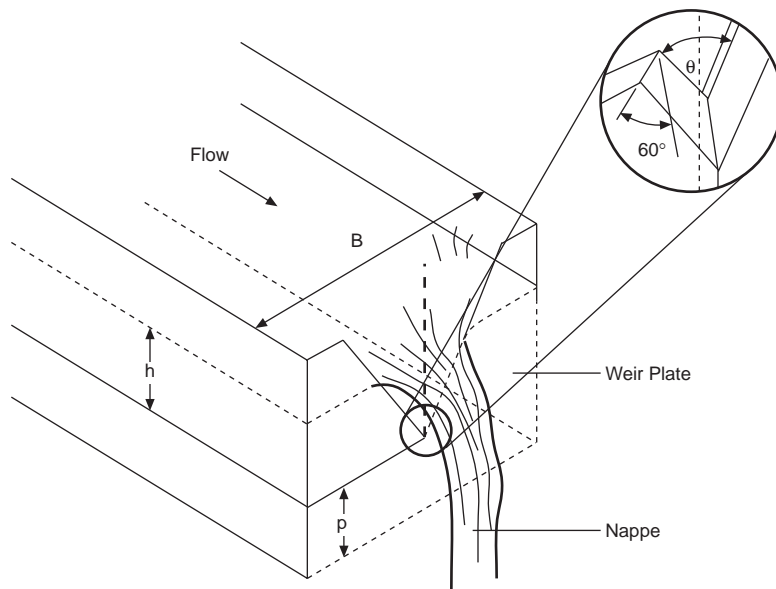


FIGURE 28.13 Thin plate V-notch weir: discharge coefficient  $C_d$  is almost independent of the flow.

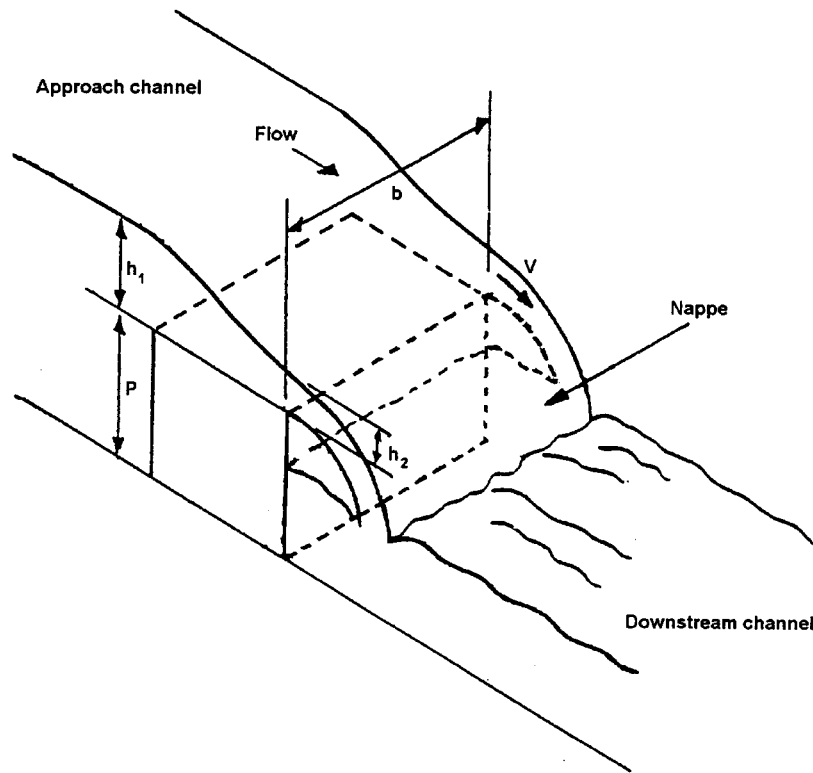


FIGURE 28.14 Broad-crested weir: maximum discharge when  $h_2 = 2h_1/3$ .

## Measuring Principles of Variable Area Flowmeters

### Rotameter

Flow Rate Analysis.

The forces acting on the bob lead to equilibrium between the weight of the bob  $\rho_b g V_b$  acting downwards and the buoyancy force  $\rho g V_b$  and the drag force  $F_d$  acting upwards, where  $V_b$  is the volume and  $\rho_b$  is the density of the bob,  $\rho$  is the density of the fluid, and  $g$  is the gravitational acceleration:

$$\rho_b g V_b = \rho g V_b + F_d \quad (28.7)$$

The drag force results from the flow field surrounding the bob and particularly from the wake of the bob. In flow analyses based on similarity principles, these influences are accounted for by empirical coefficient  $C_L$  or  $C_T$  in the drag law for:

$$\text{Laminar flow } F_d = C_L \mu D_b U \quad (28.8)$$

$$\text{Turbulent flow } F_d = C_T \rho D_b^2 U^2 \quad (28.9)$$

where  $\mu$  = Fluid viscosity

$D_b$  = Maximum bob diameter

$U$  = Velocity in the annular gap around the bob at the minimum cross-section

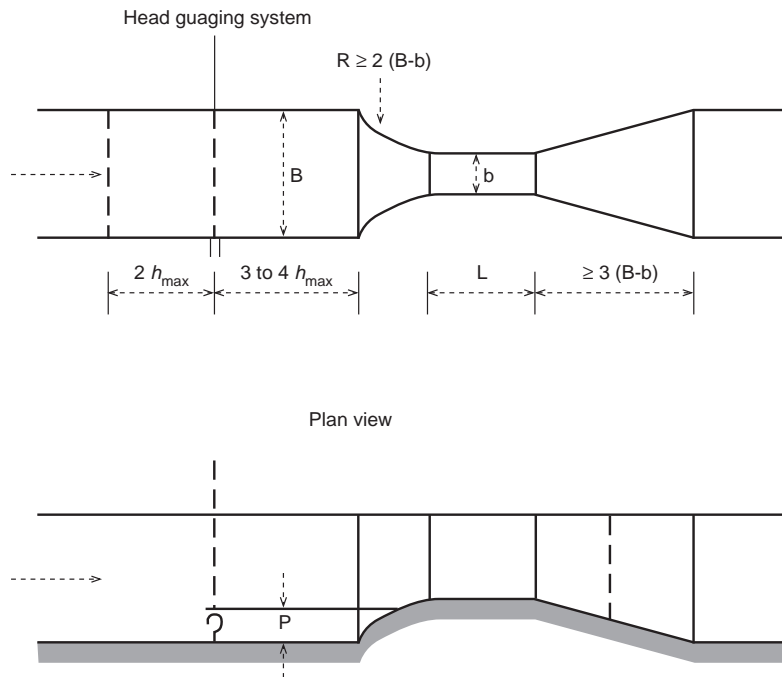


FIGURE 28.15 Venturi flume: maximum discharge when throat depth =  $2/3 \times$  total head.

The volume flow rate through the rotameter is:

$$\dot{Q} = \frac{\pi}{4} (D^2 - D_b^2) U \quad (28.10)$$

or

$$\dot{Q} = m \frac{\pi}{4} D_b^2 U \quad (28.11)$$

where  $m$  is the open area ratio, defined as:

$$m = \frac{D^2 - D_b^2}{D_b^2} \quad (28.12)$$

and  $D$  is the tube diameter at the height of the bob.

Combining Equations 28.7, 28.8, and 28.10 gives for laminar flow:

$$\dot{Q}_L = \alpha D_b^4 \frac{(\rho_b - \rho)g}{\mu} \quad (28.13)$$

where the parameter  $\alpha$  is defined in terms of a constant  $K = V_b/D_b^3$  characteristic of the shape of the bob:

$$\alpha = \frac{\pi m K}{4 C_L} \quad (28.14)$$

Using Equation 28.9 instead of Equation 28.8 yields for turbulent flow:

$$\dot{Q}_T = \beta D_b^{5/2} \sqrt{\frac{(\rho_b - \rho)g}{\rho}} \quad (28.15)$$

where

$$\beta = \frac{\pi m}{4} \sqrt{\frac{K}{C_T}} \quad (28.16)$$

With either laminar or turbulent flow through the rotameter, it is clear from Equations 28.13 and 28.15 that the flow rate is proportional to  $m$ . If the cross-sectional area of the tube is made to increase linearly with length, i.e.,

$$D = D_b (1 + h \tan \phi) \quad (28.17)$$

then since the cone angle  $\phi$  of the tube is small, Equation 28.12 can be written as:

$$m = 2h \tan \phi \quad (28.18)$$

and the flow rate is directly proportional to the height  $h$  of the bob.

Similarity Analysis.

In early studies of floating element flowmeters, Ruppel and Umpfenbach [7] proposed the introduction of characteristic dimensionless quantities, to permit the use of experimentally determined flow coefficients in flowmeter analysis. Lutz [8] extended these ideas by showing that the transfer of flow coefficients from one flowmeter to another is possible if geometrical similarity exists. More recent works [9–12] have used these principles to produce graphical or computer-based design schemes and have proposed general guidelines for laying out practical flow metering systems.

The basic scaling parameter for flow is the Reynolds number, defined as:

$$Re = \frac{\rho U_{IN} D_b}{\mu} \quad (28.19)$$

where  $U_{IN}$  is the velocity at the rotameter inlet, and the tube diameter  $D$  is represented by its value at the inlet, equal to the bob diameter  $D_b$ . Through the Reynolds number regimes of laminar or turbulent flow, and particularly important for the rotameter flow regimes with strong or weak viscosity dependence, can be distinguished. Originating in the work [7], it has been found to be practical for rotameters to use an alternative characteristic number, the Ruppel number, defined as:

$$Ru = \frac{\mu}{\sqrt{m_b g \rho (1 - \rho/\rho_b)}} \quad (28.20)$$



where  $m_b = \rho_b D_b^3$  is the mass of the bob. By combining Equations 28.15, 28.16, and 28.20, the mass flow  $\dot{m}$  through the rotameter can be written as:

$$\dot{m} = \frac{\pi}{4} \frac{m D_b \mu}{\sqrt{C_T} Ru} \quad (28.21)$$

Alternatively, from the definition:

$$\dot{m} = \rho \dot{Q} = \rho U_{IN} \frac{\pi}{4} D_b^2 \quad (28.22)$$

and Equation 28.19, the flow rate is:

$$\dot{m} = \frac{\pi}{4} D_b \mu Re \quad (28.23)$$

Equations 28.21 and 28.23 give the following relationship between the Ruppel number and the Reynolds number:

$$Ru = \frac{m}{\sqrt{C_T} Re} \quad (28.24)$$

An analysis for laminar flow leads to the relationship:

$$Ru = \sqrt{\frac{m}{C_L Re}} \quad (28.25)$$

The advantage of the Ruppel number is its independence of the flow rate. Since the Ruppel number contains only fluid properties and the mass and the density of the bob, it is a constant for a particular instrument.

At low Ruppel numbers the linear resistance law assumed in Equation 28.8 applies and  $\alpha$  is a constant for given  $m$ , as shown in Figure 28.16. At higher Ruppel numbers, the flow is transitional or turbulent, and  $\log \alpha$  decreases linearly with  $\log Ru$ . In Figure 28.17, curves for  $\beta$  against Ruppel number show a linear increase of  $\log \beta$  with  $\log Ru$  in the laminar region, followed by a gradual transition to horizontal curves in fully turbulent flow.

Similarity analysis of rotameters allows the easy calculation of the flow reading with changing density and viscosity of the fluid. For lower viscosities, only the density effect has to be taken into account; hence, for most gas measurements, simple conversion factors can be used. With higher viscosity, manufacturers offer either Ruppel number-related conversion factors or two-dimensional tables of conversion factors to be applied to different heights of the bob. Some manufacturers offer recalibration services, allowing the user to order new scales for instruments to be used in changed applications and environments. For large-order users, simple computer programs are available from some manufacturers for scale calculations.

Theories based on similarity considerations can predict the variation of the flow coefficient with the Ruppel number in the laminar and turbulent flow regimes but not in laminar-turbulent transitional flow. Detailed experimental and computational studies can assist the flow analysis of floating element flowmeters. An example is given in the section "Rotameter Internal Flow Analysis."

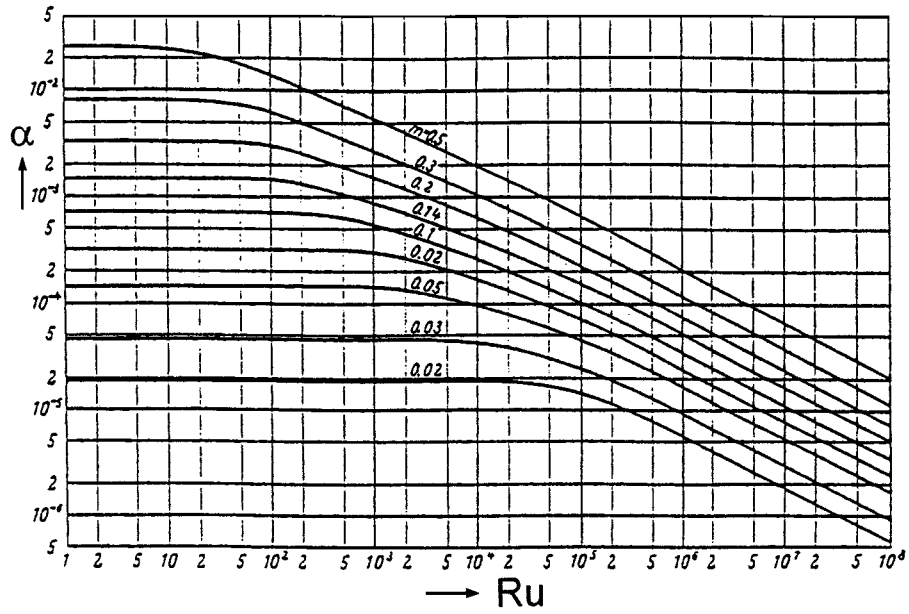


FIGURE 28.16 Rotameter flow coefficient  $\alpha$  as a function of Ruppel number  $Ru$  and open area ratio  $m$ . For a given geometry,  $\alpha$  is constant for low  $Ru$  (laminar flow).

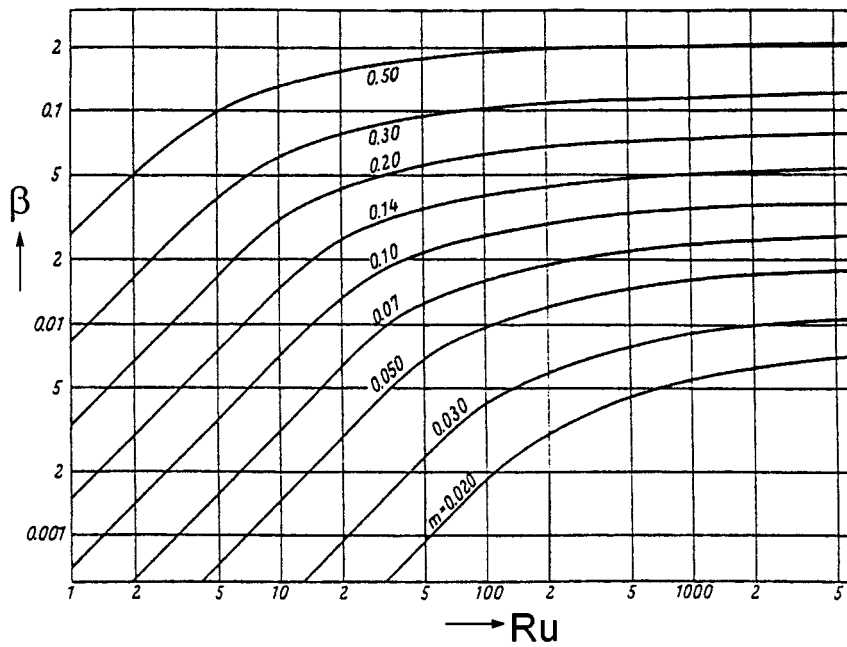


FIGURE 28.17 Rotameter flow coefficient  $\beta$  as a function of Ruppel number  $Ru$  and open area ratio  $m$ . For a given geometry,  $\beta$  is constant for high  $Ru$  (turbulent flow).

## Weir, Flume

Flow Rate Analysis for Weirs.

Although the determination of the discharge across a weir or a flume generally requires the knowledge of one or more empirical coefficients, the basic equations describing the head-discharge characteristics of the various geometrical forms are readily derived from simple fluid mechanics considerations.

The discharge over a sharp crested weir of width  $b$  (Figure 28.11) when the water level over the sill is  $h$  is analyzed by considering a horizontal strip of water of thickness  $\delta y$  at a depth  $y$  below the water surface. Since the velocity of the water through this strip is  $\sqrt{2gy}$ , the discharge is:

$$\delta\dot{Q} = b\delta y\sqrt{2gy} \quad (28.26)$$

The total discharge is obtained by integration, introducing a coefficient of discharge  $C_d$ :

$$\dot{Q} = C_d \sqrt{2gb} \int_0^h \sqrt{y} dy \quad (28.27)$$

$$\dot{Q} = \frac{2}{3} C_d \sqrt{2gb} h^{3/2} \quad (28.28)$$

Empirical corrections to Equation 28.28 to account for the weir height  $p$  are given, for example, in [3], but provided  $h/p$  does not exceed 0.5, it is adequate to use Equation 28.28 with a discharge coefficient of 0.63 to achieve a flow rate tolerance of 3%.

For the rectangular notch, Equation 28.28 also applies with a discharge coefficient of 0.59 and a flow rate tolerance of 3%. Since in practice the discharge coefficient varies slightly with the head of water for both weirs and notches, it is sometimes preferred to replace Equation 28.28 by  $\dot{Q} = Kbh^n$ , where  $K$  and  $n$  are determined by calibration.

The triangular notch (Figure 28.13) offers the advantage that the length of the wetted edge varies with the head of water, in contrast with the rectangular notch where it is constant. Consequently, the discharge coefficient of the triangular notch is constant for all heads. Furthermore, the achievable range (ratio of maximum to minimum flow rates) is higher for the triangular geometry. If  $h$  is the height of the water surface and  $\theta$  is the angle of the notch, then a horizontal strip of the notch of thickness  $\delta y$  at depth  $y$  has a width  $2(h-y)\tan(\theta/2)$ . The discharge through this strip is

$$\delta\dot{Q} = 2(h-y)\tan\frac{\theta}{2}\delta y\sqrt{2gy}C_d \quad (28.29)$$

giving a total discharge through the notch:

$$\dot{Q} = 2C_d\sqrt{2g}\tan\frac{\theta}{2}\int_0^h(h-y)\sqrt{y}dy \quad (28.30)$$

$$\dot{Q} = \frac{8}{15}C_d\sqrt{2g}\tan\frac{\theta}{2}h^{5/2} \quad (28.31)$$

The discharge coefficient is about 0.58.

Commonly used notch angles are  $90^\circ$  ( $\tan \theta/2 = 1$ ,  $C_d = 0.578$ ),  $53.13^\circ$  ( $\tan \theta/2 = 0.5$ ,  $C_d = 0.577$ ), and  $28.07^\circ$  ( $\tan \theta/2 = 0.25$ ,  $C_d = 0.587$ ). Notches with  $\theta = 53.13^\circ$  and  $\theta = 28.07^\circ$  deliver, respectively, one half and one quarter of the discharge of the  $90^\circ$  notch at the same head.

The above derivations assume that the water is discharging from a reservoir with cross-sectional area far exceeding the flow area at the weir, so that the velocity upstream is negligible. When the weir is built into a channel of cross-sectional area  $A$ , the water will have a finite velocity of approach  $v_1 = \dot{Q}/A$ . As a first approximation,  $\dot{Q}$  is obtained from Equation 28.28 assuming zero velocity of approach. Assuming further that  $v_1$  is uniform over the weir, there will be an additional head  $v_1^2/2g$  acting over the entire weir. Referring to Figure 28.11, the total discharge is then:

$$\dot{Q} = C_d \sqrt{2gb} \int_{v_1^2/2g}^{h+v_1^2/2g} \sqrt{y} dy \quad (28.32)$$

$$\dot{Q} = \frac{2}{3} C_d \sqrt{2gb} \left[ \left( h + v_1^2/2g \right)^{3/2} - \left( v_1^2/2g \right)^{3/2} \right] \quad (28.33)$$

From Equation 28.33, a corrected value of  $v_1$  can be determined. Further iterations converge rapidly to the final value of the discharge  $\dot{Q}$ . Equation 28.33 can be written as:

$$\dot{Q} = \frac{2}{3} C_v C_d \sqrt{2gb} h^{3/2} \quad (28.34)$$

where

$$C_v = \left( 1 + \frac{v_1^2}{2gh} \right)^{3/2} - \left( \frac{v_1^2}{2gh} \right)^{3/2} \quad (28.35)$$

is the coefficient of velocity, which is frequently determined empirically.

Over a broad-crested weir (Figure 28.14), the discharge depends on the head  $h_1$ , the width  $b$ , and the length  $l$  of the sill. There is also a dependence on the roughness of the sill surface and the viscosity. Consequently, there is a loss of head as the water flows over the sill. It is assumed that the sill is of sufficient length to allow the velocity to be uniform at a value  $v$  throughout the depth  $h_2$  of the water at the downstream edge of the sill. Neglecting losses

$$v = \sqrt{2g(h_1 - h_2)}$$

and the discharge is:

$$\dot{Q} = C_d b h_2 v = C_d b \sqrt{2g(h_1 h_2^2 - h_2^3)} \quad (28.36)$$

From Equation 28.36, the discharge is a maximum when  $(h_1 h_2^2 - h_2^3)$  reaches a maximum, i.e., when  $h_2 = 2h_1/3$ . This discharge is then:

$$\dot{Q} = \left( \frac{2}{3} \right)^{3/2} C_d b \sqrt{g} h_1^{3/2} \quad (28.37)$$

The stable condition of the weir lies at the maximum discharge.

Flow Rate Analysis for Flumes.

The discharge through a flume depends on the water level  $h$ , the channel width  $b$ , and velocity  $v$  at each of the stations 1 (upstream) and 2 (at the minimum cross-section) in Figure 28.15. Applying Bernoulli's equation to the inlet and the throat, neglecting all losses, one obtains:

$$\rho g H = \rho g h_1 + \frac{1}{2} \rho v_1^2 = \rho g h_2 + \frac{1}{2} \rho v_2^2 \quad (28.38)$$

where  $H$  is the total head. The analysis is then formally the same as that for the broad-crested weir, giving the same expression for the discharge as in Equation 28.37. The flow through the flume is a maximum when the depth at the throat is two thirds of the total head. Normally, a coefficient of velocity is introduced so that the discharge equation is:

$$\dot{Q} = \left(\frac{2}{3}\right)^{3/2} C_v C_d b \sqrt{g h_1^3} \quad (28.39)$$

The combined coefficient is determined empirically. In [3], a value  $C_v C_d = 1.061 \pm 0.085$  is quoted.

The validity of the empirical coefficients quoted above, or of other coefficients given in the various standards for metering of open-channel flows, can only be guaranteed with a given confidence level for meter installations satisfying certain geometrical constraints. Limits on quantities such as  $b$ ,  $h$ ,  $h/b$ , etc. are given in [3] and the standards.

### Rotameter: Internal Flow Analysis

Computation of Internal Flow.

Improvement of rotameter design could be assisted by detailed knowledge of the internal flow field, which is characterized by steep velocity gradients and regions of separated flow. Measurements of the internal flow field are complicated by the small dimensions of the gap around the bob and the strongly curved glass tube. Bückle et al. [13] successfully used laser Doppler anemometry [14] for velocity measurements in a rotameter. The working fluid was a glycerine solution with an index of refraction (1.455) close to that of glass (1.476). Problems with refraction of the laser beams at the curved tube wall were thus avoided, but the high viscosity of glycerine restricted the experiments to laminar flow at Reynolds numbers  $Re = \rho U_{IN} D_b / \mu < 400$ .

The application of computational fluid dynamics to the flow in a rotameter [13] involves the finite volume solution of the conservation equations for mass and momentum. For a two-dimensional laminar flow, these equations can be written in a cylindrical polar coordinate system as:

$$\frac{\partial \rho}{\partial t} + \frac{\partial(\rho u)}{\partial z} + \frac{1}{r} \frac{\partial(\rho r v)}{\partial r} = 0 \quad (28.40)$$

$$\frac{\partial(\rho u)}{\partial t} + \frac{\partial}{\partial z} \left( \rho u u - 2\mu \frac{\partial u}{\partial z} \right) + \frac{1}{r} \frac{\partial}{\partial r} \left( \rho r u v - \mu r \left( \frac{\partial u}{\partial r} + \frac{\partial v}{\partial z} \right) \right) = -\frac{\partial p}{\partial z} \quad (28.41)$$

$$\frac{\partial(\rho v)}{\partial t} + \frac{\partial}{\partial z} \left( \rho u v - \mu r \left( \frac{\partial u}{\partial r} + \frac{\partial v}{\partial z} \right) \right) + \frac{1}{r} \frac{\partial}{\partial r} \left( \rho r v v - 2\mu r \frac{\partial v}{\partial r} \right) = -\frac{\partial p}{\partial r} \quad (28.42)$$

where  $\rho$  is the density,  $u$ ,  $v$  and  $r$ ,  $z$  are the velocity components and coordinate directions in the axial and radial directions, respectively,  $\mu$  is the dynamic viscosity, and  $p$  is the pressure.

For the numerical solution, the governing equations for a generalized transport variable  $\phi$  (i.e.,  $u$  or  $v$ ) are formally integrated over each control volume (CV) of the computational grid. The resulting flux balance equation can in turn be discretized as an algebraic equation for  $\phi$  at the center P of each CV in terms of the values  $\phi_{nb}$  at the four nearest neighbors of point P and known functions A:

$$A_{p\phi p} + \sum_{nb} A_{nb} \phi_{nb} = S_{\phi} \quad (28.43)$$

For the whole solution domain, a system of equations results that can be solved by a suitable algorithm (e.g. [15]).

For a rotameter, the symmetry of the problem allows the computational solution domain to be chosen as one half diametral plane of the rotameter. The boundary conditions are:

$$u = v = 0 \quad (28.44)$$

along the walls, and

$$\frac{\partial u}{\partial r} = v = 0 \quad (28.45)$$

along the axis of symmetry. At the input boundary, the initial profile for the  $u$ -velocity is taken from the experiment. At the outlet boundary, zero gradient is assumed for all dependent variables.

#### Computed Flow Field.

Representative calculations for Reynolds number 220 are shown as velocity vectors (Figure 28.18) and streamlines (Figure 28.19). Experimental and computed velocity profiles over a radius of the flowmeter tube are shown in Figure 28.20.

At  $z = 45$  mm, the computations indicate a stagnation point at the bob tip, but the measurements show a low but finite axial velocity. The deviation from zero is attributable to slight unsteadiness in the position of the bob and to smearing of the steep radial velocity gradient along the measuring volume. This effect is also apparent at radii up to about 5 mm, where the computations show a notably steeper velocity gradient than the measurements. The measured and computed peak velocities agree well, although the measured peak is located at a larger radius.

In the strongly converging annulus between the bob and the tube wall ( $z = 65$  mm) and in the plane  $z = 88$  mm, the computations reproduce well the trend of the measured results, particularly near the flowmeter wall. Discrepancies in the region adjacent to the bob are attributable to asymmetry in measured profiles arising from the piping upstream of the rotameter tube.

Above the bob ( $z = 110$  mm), there is a strong upward flow in an annular region near the tube wall and a recirculation region around the axis occupying almost half the tube cross-section. The forward velocities show a good match between computations and measurements, but there is a very marked discrepancy in the recirculation zone. At  $z = 135$  mm, the recirculation zone is finished, but the wake of the bob is still very evident. Except for a discrepancy of about 10% on the axis, the results from the two methods agree remarkably well.

The effect of rotation of the bob on the flow field was considered by computations, including an equation for the azimuthal velocity component  $w$ .

$$\frac{\partial(\rho w)}{\partial t} + \frac{\partial}{\partial z} \left( \rho u w - \mu \frac{\partial w}{\partial z} \right) + \frac{1}{r} \frac{\partial}{\partial r} \left( \rho r v w - \mu r \frac{\partial w}{\partial r} \right) = -\rho \frac{v w}{r} - \mu \frac{w}{r^2} \quad (28.46)$$

Calculations for 1 Hz rotation frequency showed the highest swirl velocities close to the axis above the bob. There was no observable influence of the rotation on the  $u$ - and  $v$ -velocity components [16].

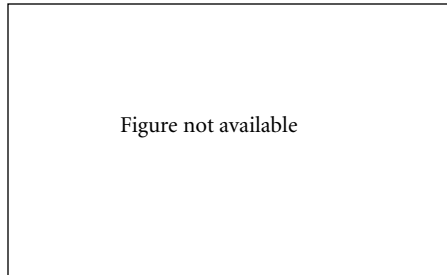


**FIGURE 28.18** Computed velocity vectors for laminar flow through a rotameter. Computations in a half diametral plane for axisymmetric flow at Reynolds number 220.

## Summary

For pipe flows, variable area flowmeters are most suitable for low flow rates of gases or liquids at moderate temperatures and pressures. Favorable features include rugged construction, high reliability, low pressure drop, easy installation, and low cost. Disadvantages include measurement uncertainty of 1% or more, limited range (10:1), slow response, and restrictions on the meter orientation. A generally good price/performance ratio has led to widespread use of these meters in numerous scientific and medical instruments and in many industrial applications for flow monitoring.

Variable area flowmeters in open-channel flows have applications for flow measurements in waste water plants, waterworks, rivers and streams, irrigation, and drainage canals. Hydrological applications of weirs with adjustable sill or crest height include flow regulation, flow measurement, upstream water level control, and discharge of excess flow in streams, rivers, and canals. Ruggedness, simplicity, and low maintenance costs are favorable characteristics for field applications of these meters.

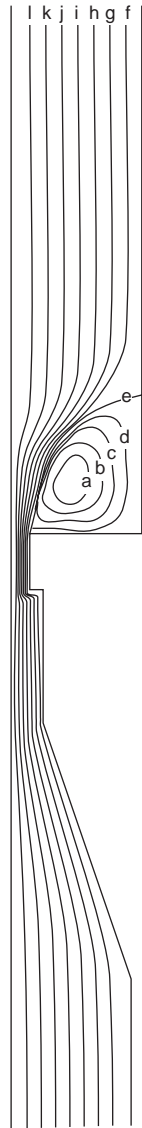


**FIGURE 28.19** Computed streamlines for laminar flow through a rotameter (Reynolds number 220).



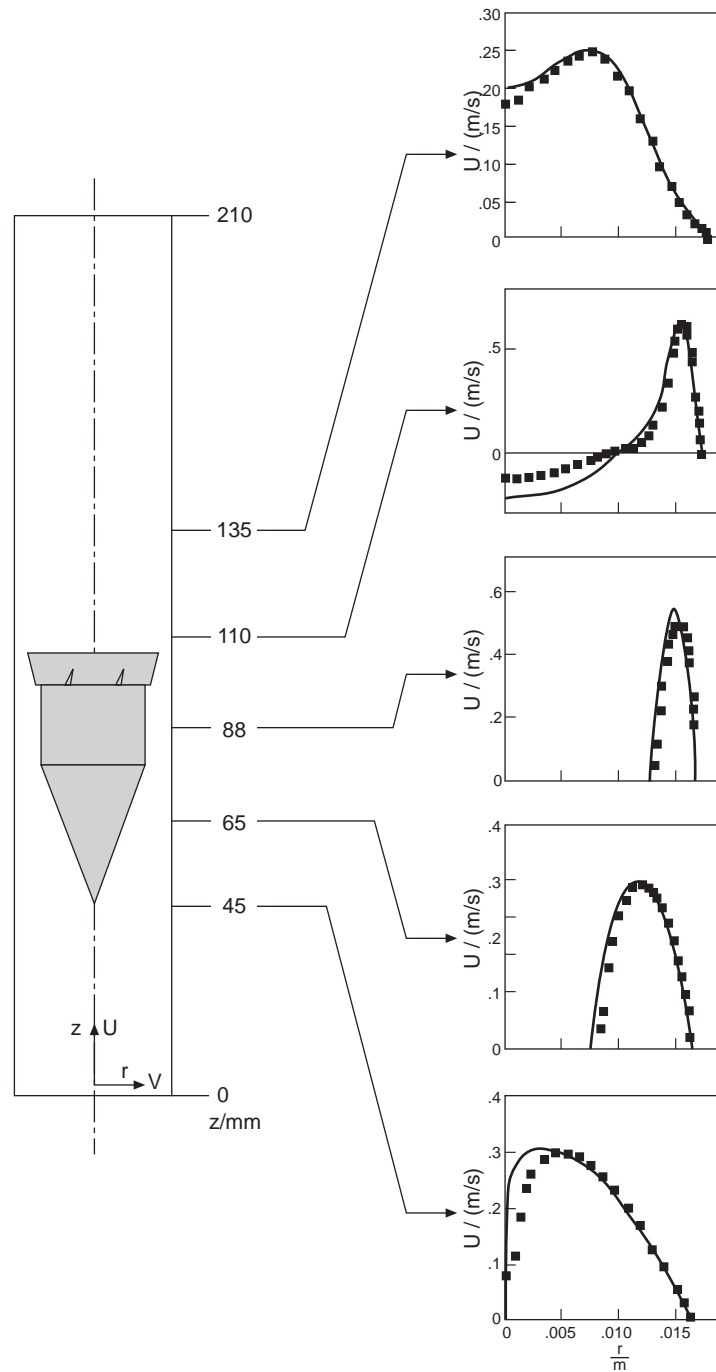


**FIGURE 28.20** Comparison of measured and computed velocity profiles for laminar flow through a rotameter (Reynolds number 220).  $U$  = axial component (m/s),  $z$  = axial position (mm),  $r$  = radial position (m).

## References

1. R. A. Furness, BS7045: the principles of flowmeter selection, *Flow Meas. Instrum.*, 2, 233–242, 1991.
2. W. Boiten, Flow-measuring structures, *Flow Meas. Instrum.*, 4, 17–24, 1993.
3. R. Hershey, General purpose flow measurement equations for flumes and thin plate weirs, *Flow Meas. Instrum.*, 6, 283–293, 1995.
4. ISO 1438, Thin Plate Weirs, International Standards Organisation, Geneva, 1980.
5. ISO 4359, Rectangular, Trapezoidal and U-shaped Flumes, International Standards Organisation, Geneva, 1983.
6. ISO 8368, Guidelines for the Selection of Flow Gauging Structures, International Standards Organisation, Geneva, 1985.
7. G. Ruppel and K. J. Umpfenbach, Strömungstechnische Untersuchungen an Schwimmermessern, *Technische Mechanik und Thermodynamik*, 1, 225–233, 257–267, 290–296, 1930.
8. K. Lutz, Die Berechnung des Schwebekörper-Durchflußmessers, *Regelungstechnik*, 10, 355–360, 1959.
9. D. Bender, Ähnlichkeitsparameter und Durchflußgleichungen für Schwebekörperdurchflußmesser, *ATM-Archiv für Technisches Messen*, 391, 97–102, 1968.
10. VDE/VDI-Fachgruppe Meßtechnik 3513, *Schwebekörperdurchflußmesser, Berechnungsverfahren*, VDE/VDI 3513, 1971.
11. H. Nikolaus, Berechnungsverfahren für Schwebekörperdurchflußmesser, theoretische Grundlagen und Aufbereitung für die Datenverarbeitungsanlage, *ATM-Archiv für Technisches Messen*, 435, 49–55, 1972.
12. H. Nikolaus and M. Feck, Graphische Verfahren zur Bestimmung von Durchflußkennlinien für Schwebekörperdurchflußmeßgeräte, *ATM-Archiv für Technisches Messen*, 1247-5, 171–176, 1974.
13. U. Bückle, F. Durst, B. Howe, and A. Melling, Investigation of a floating element flow meter, *Flow Meas. Instrum.*, 3, 215–225, 1992.
14. F. Durst, A. Melling, and J. H. Whitelaw, *Principles and Practice of Laser-Doppler Anemometry*, 2nd ed., London: Academic Press, 1981.
15. M. Perić, M. Schäfer, and E. Schreck, Computation of fluid flow with a parallel multigrid solver, *Proc. Conf. Parallel Computational Fluid Dynamics*, Stuttgart, 1991.
16. U. Bückle, F. Durst, H. Köchner, and A. Melling, Further investigation of a floating element flowmeter, *Flow Meas. Instrum.*, 6, 75–78, 1995.

## 28.3 Positive Displacement Flowmeters

---

*Zaki D. Husain and Donald J. Wass*

A *positive displacement flowmeter*, commonly called a PD meter, measures the volume flow rate of a continuous flow stream by momentarily entrapping a segment of the fluid into a chamber of known volume and releasing that fluid back into the flow stream on the discharge side of the meter. By monitoring the number of entrapments for a known period of time or number of entrapments per unit time, the total volume of flow or the flow rate of the stream can be ascertained. The total volume and the flow rate can then be displayed locally or transmitted to a remote monitoring station.

The positive displacement flowmeter has been in use for many decades to measure both liquid and gas flows. A PD meter can be viewed as a hydraulic motor with high volumetric efficiency that generally absorbs a small amount of energy from the flowing fluid. The energy absorption is primarily to overcome the internal resistance of the moving parts of the meter and its accessories. This loss of energy is observed as the pressure drop across the meter. The differential pressure across the meter is the driving force for the internals of the PD meter.

## Design and Construction

A positive displacement meter has three basic components: an outer housing, the internal mechanism that creates the dividing chamber through its repetitive motion, and the display or counter accessories that determines the number of entrapments of fluid in the dividing chamber and infers the flow rate and the total volume of flow through the meter.

The external housing acts as the holding chamber of the flowing fluid before and after the entrapments by the internals. For low line pressures, the housing is usually single walled while, for higher operating pressures, the housing is double walled where the inner wall is the containment wall for the entrapment chamber and the outer wall is the pressure vessel. For the double-walled housing, the entrapment chamber walls are subjected to the differential pressure across the meter while the external housing is subjected to the total line pressure. This allows fabrication of a thin-walled inner chamber that can retain its precise shape and dimensions independent of line pressure.

The measuring mechanism consists of precise metering elements that require tight tolerances on the mating parts. The metering elements consist of the containment wall of the metering chamber and the moving components of the meter that forms the entrapment volume of the flowing fluid by cyclic or repetitive motion of those elements. The most common types of positive displacement meters are the oscillating piston, nutating disk, oval gear, sliding vane, birotor, trirotor, and diaphragm designs.

The counter or output mechanism converts the motion of the internal measuring chamber of a PD meter and displays the flow rate or total flow by correlating the number of entrapments and each entrapped volume. Many positive displacement meters have a mechanical gear train that requires seals and packing glands to transmit the motion of the inner mechanism to the outside counters. This type of display requires more driving power to overcome resistance of the moving parts and the seals, which results in an additional pressure drop for the meter. Many PD meters transmit the motion of the inner mechanism to the counters through switch output utilizing electromechanical, magnetic, optical, or purely electronic techniques in counting the entrapments and displaying the flow rate and total flow volume. The latter processing techniques normally have less pressure drop than the all-mechanical or part-mechanical transmission methods. All-mechanical drive counters do not require external power and, through proper selection of gear train, can display the actual flow volume or the flow rate. Thus, meters can be installed at remote locations devoid of any external power source. Meters with mechanical display cannot easily correct for the changes in volume due to thermal expansion or contraction of the measuring chamber due to flow temperature variation and, in the case of single-walled housing, the changes in the entrapment volume due to variations of the line pressure. An electronically processed output device could monitor both the pressure and temperature of the meter and provide necessary corrections to the meter output. With constantly changing and improving electronics technology, many PD meters are now installed with solar or battery-powered electronic output for installations at remote locations with no external power source. Many electronic displays allow access to meter data from a central monitoring station via radio or satellite communication.

## Some Commercially Available PD Meter Designs

Commercially available PD meters have many noticeably different working mechanisms and a few designs are unique and proprietary. Although each design and working mechanism can be noticeably different from another, all positive displacement meters have a stationary fluid retaining wall and a mechanism that momentarily entraps inlet fluid into a partitioned chamber before releasing it to the downstream side of the meter. This entrapment and release of the flowing fluid occur with such repetitive and sweeping motion that, for most practical purposes, the flow rate appears to be uniform and steady, even though, in reality, the exit flow does have some pulsation. The flow pulsation out of the meter may be more pronounced for some designs of positive displacement meters than others. These flow pulsations are more pronounced at the lower flow rates for all designs. Some designs are more suitable for either liquid or gas flows, while some designs can measure both gas and liquid. For liquid applications, PD meters

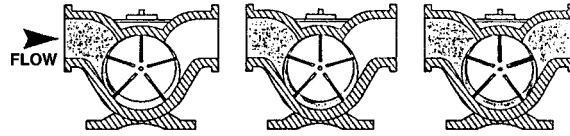


FIGURE 28.21 Sliding-vane type PD meter. (Courtesy of Daniel Industries, Inc.)



FIGURE 28.22 Trirotor type PD meter. (Courtesy of Liquid Controls LLC.)

work best for liquids with heavy viscosities. Almost all PD meters require precisely machined, high-tolerance mating parts; thus, measured fluid must be clean for longevity of the meter and to maintain the measurement precision.

### Sliding-Vane Type Positive Displacement Meter

Figure 28.21 shows a working cycle of a sliding-vane type PD meter where vanes are designed to move in and out of the rotating inner mechanism. The position of each sliding vane relative to specific angular rotation of the rotor is usually maintained by a mechanical cam. In the design shown in Figure 28.21, each blade is independently retained in the slots. There are designs with even numbers of blades where diametrically opposite blades are one integral unit. High-pressure application would utilize dual wall construction.

### Tri-Rotor Type PD Meter

This design has three rotating parts that entrap fluid between the rotors and an outer wall. The working cycle of this type of meter is shown Figure 28.22. In this design, for one rotation of the top mechanism, two blades rotate twice. The driving mechanism and rotation of each blade with respect to the others is maintained by a three-gear assembly where each rotating blade shaft is connected to one gear of the three-gear assembly to maintain relative rotational speed. This design is used to measure liquid flows.

### Birotor PD Meter

The measuring unit of the birotor PD meter has two spiral type rotors kept in perfect timing by a set of precision gears and is used to measure liquid flows. Flow can enter the meter either perpendicular or parallel to the axis of rotation of the mating rotors, as shown in Figure 28.23. The axial design birotor is identical to the standard model in component parts and in principle; however, it utilizes a measuring unit mounted parallel, rather than perpendicular, to flow. Meter output is registered mechanically through a gear train located outside the measuring chamber or, electronically, using a pickup assembly mounted with a timing gear. Axial orientation results in compact installation, improved accuracy, and low pressure loss. The axial design is ideal for high flow rate applications.

### Piston Type PD Meter

A typical design of a piston type PD meter is shown in Figure 28.24. A centrally located rotating part generates the reciprocating motion for each of the four pistons of the meter. The reciprocating motion of each of the piston is timed such that the discharge from an individual piston cylinder occurs in a cycle to generate a semicontinuous discharge from the meter. These PD meters are used for very low flow rates of liquid flows. A piston-cylinder design can withstand large differential pressures across the meter, so high viscous liquids can be measured by this type of meters and measurements are very precise. Mechanical

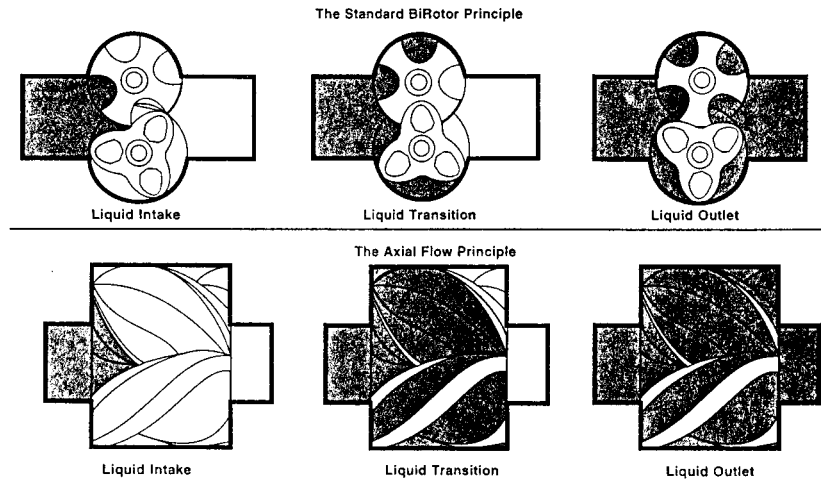


FIGURE 28.23 BiRotor type PD meter. (Courtesy of Brooks Instruments Division, Emerson Electric Company.)

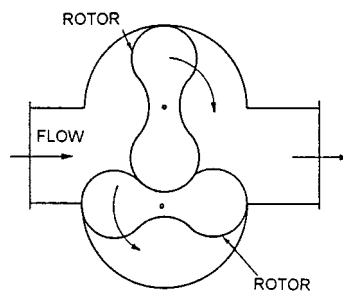


FIGURE 28.24 Piston-type PD meter. (Courtesy of Pierburg Instruments, Inc.)



FIGURE 28.25 Oval Gear Meter. (Courtesy of Daniel Industries, Inc.)

components of this type of meter require very precise mechanical tolerances, which increase the product cost.

### Oval Gear PD Meter

The measurement of volumetric flow of an oval gear meter is obtained by separating partial volumes formed between oval gears and the measuring chamber wall, as shown in Figure 28.25. The rotation of the oval gears results from the differential pressure across the flowmeter. During one revolution of the oval gears, four partial volumes are transferred. The rotation of the gears is transmitted from the measuring chamber to the output shaft directly with mechanical seals or via a magnetic coupling. This type of meter is used to measure liquids having a wide range of viscosity.

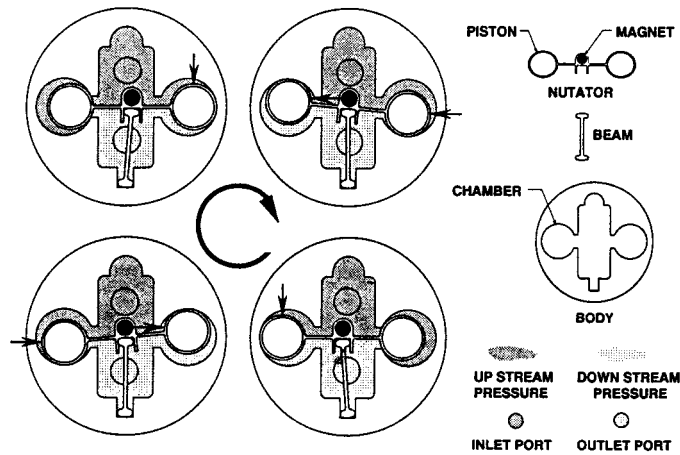


FIGURE 28.26 Nutating-disk type PD meter. (Courtesy of DEA Engineering Company.)

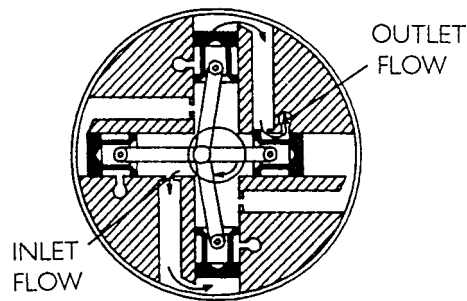


FIGURE 28.27 Schematic diagram of roots meter.

### Nutating-Disk Type PD Meters

A disk placed within the confines of a boundary wall at a specific orientation can induce a flow instability that can generate a wobbling or nutating motion to the disk. The operating cycle of one such design is shown in Figure 28.26. The entrapment and discharge of the fluid to and from the two chambers occur during different phases of the repetitive cycle of the nutating disk. This type of meter is used to measure liquids. The design provides economic flow measurement where accuracy is not of great importance and is often used in water meters.

Meter designs described hereafter are for gas flows. PD meters for gas flows require very tight tolerances of the moving parts to reduce leak paths and, therefore, the gas must be clean because the meters are less tolerant to solid particles.

### Roots PD Meter

The roots meter design is shown in Figure 28.27. This is the most commonly used PD meter to measure gas flows. This is one of the oldest designs of a positive displacement meter. The mechanical clearance between the rotors and the housing requires precisely machined parts. Roots meters are adversely affected if inlet flow to the meter has a relatively high level of pulsation. The main disadvantage of this meter is that it introduces cyclic pulsations into the flow. This meter cannot tolerate dirt and requires filtering upstream of the meter. A roots meter in single-case design is used at near-ambient line pressures. This

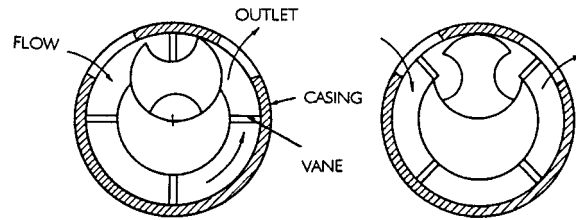


FIGURE 28.28 Operation of CVM meter.

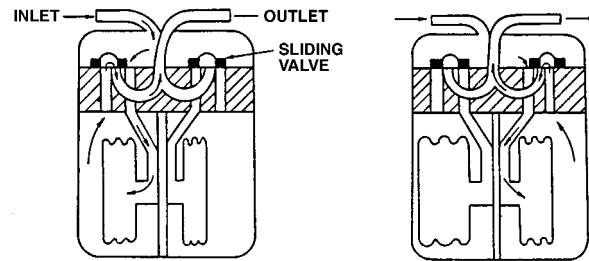


FIGURE 28.29 Operation of a diaphragm meter.

meter design is very widely used in the low-pressure transmission and distribution market of natural gas. If this meter ever seizes up at any position, the flow is completely blocked.

### The CVM Meter

The CVM meter (Figure 28.28) is a proprietary design of a positive displacement meter used to measure gas flows. This meter has a set of four vanes rotating in an annular space about the center of the circular housing. A gate similar in shape to the center piece of the trirotor design (Figure 28.22) allows the vanes to pass — but not the gas. The measurement accuracy of the CVM meter is similar to the roots meter, but the amplitude of exit pulsation is lower than the roots meter for similar meter size and flow rate. This design is also not as sensitive to inlet flow fluctuations, and is widely used in the low-pressure, natural gas distribution market in Europe.

### Diaphragm Meter

The diaphragm meter, also known as a bellows-type meter, is simple, relatively inexpensive, has reliable metering accuracy, and is widely used as a domestic gas meter. This design, shown in Figure 28.29, acts like a reciprocating piston meter, where the bellows act as the piston. The operation is controlled by a double slide valve. In one position, the slide valve connects the inlet to the inside of the bellow, while the outside of the bellow is open to the outlet. In the other position, the outside is connected to the inlet while the inside of the bellow is open to the outlet. This design can measure extremely low flow rates (e.g., pilot light of a gas burner).

### Advantages and Disadvantages of PD Meters

High-quality, positive displacement meters will measure with high accuracy over a wide range of flow rates, and are very reliable over long periods. Unlike most flowmeters, a positive displacement meter is insensitive to inlet flow profile distortions. Thus, PD meters can be installed in close proximity to any upstream or downstream piping installations without any loss of accuracy. In general, PD meters have minimal pressure drop across the meter; hence, they can be installed in a pipeline with very low line pressures. Until the introduction of electronic correctors and flow controls on other types of meters, PD

meters were most widely used in batch loading and dispensing applications. All mechanical units can be installed in remote locations.

Positive displacement meters are generally bulky, especially in the larger sizes. Due to the tight clearance necessary between mating parts, the fluid must be clean for measurement accuracy and longevity of the meter. More accurate PD meters are quite expensive. If a PD meter ever seizes up, it would completely block the flow. Many PD meters have high inertia of the moving parts; therefore, a sudden change in the flow rate can damage the meter. PD meters are normally suitable over only limited ranges of pressure and temperature. Some designs will introduce noticeably high pulsations into the flow. Most PD meters require a good maintenance schedule and are high repair and maintenance meters. Recurring costs in maintaining a positive displacement flowmeter can be a significant factor in overall flowmeter cost.

## Applications

Liquid PD meters are capable of measuring fluids with a wide range of viscosity and density. Minor changes in viscosity of the fluid have minimal influence on the accuracy of a PD meter. However, no one specific design of PD meter is capable of such a broad application range. The physical properties of the fluid, especially the fluid viscosity, must be reviewed for proper selection of a meter for the application. Many PD meter designs accurately measure flow velocities over a wide range.

Careful dimensional control is required to produce well-regulated clearances around the moving parts of the PD meter. The clearances provide a leakage path around the flow measurement mechanism, and the amount of leakage depends on the relative velocity of the moving parts, the viscosity of the fluid, and the clearances between parts. In general, the leakage flow rate follows the Poiseuille equation; that is, leakage is directly proportional to the differential pressure and inversely proportional to the absolute viscosity and the length of the leakage path.

The leakage flow, in percentage of the total flow rate, is useful information for error measurement. At low flow rates, percent leakage error can be significant; while with modest flow rates, leakage can be insignificant. However, the differential pressure across the PD meter increases exponentially with increasing flow rates. Therefore, at very high flow rates, leakage flow can again be a significant portion of the total flow. As a result, PD meters tend to dispense more fluid than is indicated by the register at the very low and very high flow rates. The amount of error due to leakage depends on the meter design and on the viscosity of the fluid.

PD meters are driven by the differential pressure across the meter. The primary losses within the meter can be attributed to the friction losses and the viscous drag of the fluid on the moving parts. At very low flow rates, the bearing losses are predominant, while at high flow rates, the viscous drags predominate. The viscous drag is directly proportional to the fluid viscosity and the relative velocity of the moving parts and inversely proportional to the clearance. Within each design, the differential pressure is limited to a predetermined value. Excessive differential pressures can damage the meter. High differential pressure can be avoided by limiting the maximum flow rate, lowering viscosity by heating the fluid, increasing clearances, or by various combinations of these techniques. In general, if the differential pressure limit can be addressed, PD meters measuring high-viscosity fluids have less measurement error over a wide flow rate range.

The viscosity of most gases is too low to cause application problems relating to viscous drag of the form discussed for liquid PD meters. Gas PD meters utilize smaller clearances than liquid PD meters; therefore, gas must be very clean. Even small particles of foreign material can damage gas PD meters. PD meters used in gas flow measurement are primarily in the low line pressure application.

## Accessories

Many accessories are available for PD meters. Among the most common and useful accessories for liquid PD meters are the automatic air eliminator and the direct-coupled shut-off valve for batch loading operations. The automatic air eliminator consists of a pressure-containing case surrounding a float valve.



When gas in the liquid flow enters the chamber, the float descends by gravity and allows the float valve to open and purge the gas. An air eliminator improves the precision of flow measurement in many applications and is an absolute necessity in applications where air or gas is trapped in the flow stream. The direct-coupled shut-off valve is directly linked to the mechanical register. A predetermined fluid quantity can be entered into the register. When the dispensed amount equals the amount entered in the register, the mechanical linkage closes the valve. Two-stage shut-off valves are often used to avoid line shock in high flow rate dispensing applications. Similarly, all-electronic units can control batch operations. The all-electronic units provide great convenience in the handling of data. However, the register-driven mechanical valves have advantages in simplicity of design, field maintenance or repair, and initial cost.

Gas PD meters can be equipped with mechanical registers that correct the totals for pressure and temperature. The pressure and temperature compensation range is limited in the mechanical units but with appropriate application; the range limitation is not a problem. Electronic totalizers for gas PD meters can correct for broad ranges of temperature and pressure. Electronic accessories can provide various data storage, logging, and remote data access capabilities.

### Price and Performance

In general, the accuracy of the PD meter is reflected in the sales price. However, several additional factors influence the cost. The intended application, the materials of construction, and the pressure rating have a strong influence on the cost. Although they provide excellent accuracy, small PD meters for residential water or residential natural gas service are very inexpensive. Meters produced for the general industrial market provide good accuracy at a reasonable cost, and meters manufactured for the pipeline or petrochemical markets provide excellent accuracy and are expensive.

Very inexpensive PD meters are available with plastic cases or plastic internal mechanisms. Aluminum, brass, ductile iron, or cast iron PD meters are moderately priced. Steel PD meters are relatively expensive, especially for high-pressure applications. If stainless steel or unusual materials are necessary for corrosive fluids or special service requirements, the costs are very high. PD meters are manufactured in a wide range of sizes, pressure ratings, and materials, with a multitude of flow rate ranges, and with an accuracy to match most requirements. The cost is directly related to the performance requirements.

### Further Information

- D. W. Spitzer, Ed., *Flow Measurement: Practical Guides for Measurement and Control*, Research Triangle Park, NC: ISA, 1991.
- R. W. Miller, *Flow Measurement Engineering Handbook*, New York: McGraw-Hill, 1989.
- Fluid Meters: Their Theory and Application, 6th ed., Report of ASME Research Committee on Fluid Meters, American Society of Mechanical Engineers, 1971.
- V. L. Streeter, *Fluid Mechanics, 4th ed.*, New York: McGraw-Hill, 1966.
- V. L. Streeter, *Handbook of Fluid Dynamics*, New York: McGraw-Hill, 1961.
- Measurement of Liquid Hydrocarbons by Displacement Meters, Manual of Petroleum Measurement Standard, Chapter 5.2, American Petroleum Institute, 1992.

## 28.4 Turbine and Vane Flowmeters

---

*David Wadlow*

This section describes a range of closed-conduit flowmeters that utilize rotating vaned transduction elements, with particular emphasis on axial turbine flowmeters. Single jet and insertion tangential turbines, also known as paddlewheel flowmeters, are described in another section. The various vaned flowmeters used for open-channel and free-field flow measurement are not included in this section.

## Axial Turbine Flowmeters

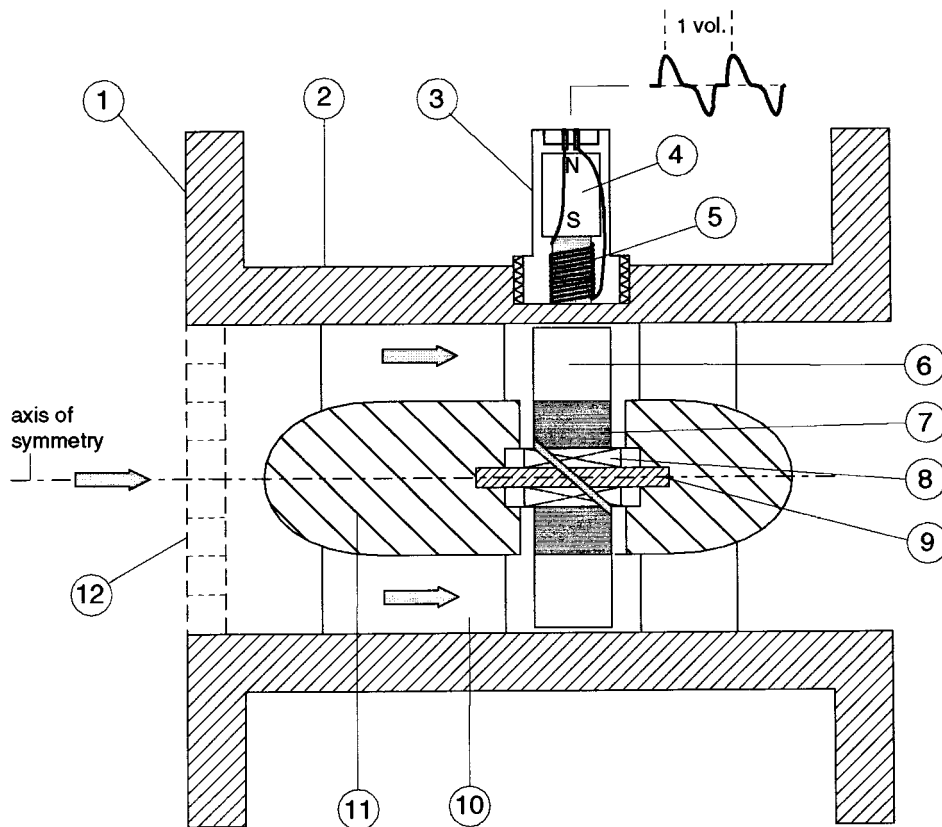
The modern axial turbine flowmeter, when properly installed and calibrated, is a reliable device capable of providing the highest accuracies attainable by any currently available flow sensor for both liquid and gas volumetric flow measurement. It is the product of decades of intensive innovation and refinements to the original axial vaned flowmeter principle first credited to Woltman in 1790, and at that time applied to measuring water flow. The initial impetus for the modern development activity was largely the increasing needs of the U.S. natural gas industry in the late 1940s and 1950s for a means to accurately measure the flow in large-diameter, high-pressure, interstate natural gas lines. Today, due to the tremendous success of this principle, axial turbine flowmeters of different and often proprietary designs are used for a variety of applications where accuracy, reliability, and rangeability are required in numerous major industries besides water and natural gas, including oil, petrochemical, chemical process, cryogenics, milk and beverage, aerospace, biomedical, and others.

Figure 28.30 is a schematic longitudinal section through the axis of symmetry depicting the key components of a typical meter. As one can see, the meter is an in-line sensor comprising a single turbine rotor, concentrically mounted on a shaft within a cylindrical housing through which the flow passes. The shaft or shaft bearings are located by end supports inside suspended upstream and downstream aerodynamic structures called diffusers, stators, or simply cones. The flow thus passes through an annular region occupied by the rotor blades. The blades, which are usually flat but can be slightly twisted, are inclined at an angle to the incident flow velocity and hence experience a torque that drives the rotor. The rate of rotation, which can be up to several  $\times 10^4$  rpm for smaller meters, is detected by a pickup, which is usually a magnetic type, and registration of each rotor blade passing infers the passage of a fixed volume of fluid.

### General Performance Characteristics

Axial turbines perform best when measuring clean, conditioned, steady flows of gases and liquids with low kinematic viscosities (below about  $10^{-5}$  m<sup>2</sup>s<sup>-1</sup>, 10 cSt, although they are used up to  $10^{-4}$  m<sup>2</sup>s<sup>-1</sup>, 100 cSt), and are linear for subsonic, turbulent flows. Under these conditions, the inherent mechanical stability of the meter design gives rise to excellent repeatability performance. Not including the special case of water meters, which are described later, the main performance characteristics are:

- Sizes (internal diameter) range from 6 mm to 760 mm, (1/4 in. to 30 in.).
- Maximum measurement capacities range from 0.025 Am<sup>3</sup> h<sup>-1</sup> to 25,500 Am<sup>3</sup> h<sup>-1</sup>, (0.015 ACFM to 15,000 ACFM), for gases and 0.036 m<sup>3</sup> h<sup>-1</sup> to 13,000 m<sup>3</sup> h<sup>-1</sup>, (0.16 gpm to 57,000 gpm or 82,000 barrels per hour), for liquids, where A denotes actual.
- Typical measurement repeatability is  $\pm 0.1\%$  of reading for liquids and  $\pm 0.25\%$  for gases with up to  $\pm 0.02\%$  for high-accuracy meters. Typical linearities (before electronic linearization) are between  $\pm 0.25\%$  and  $\pm 0.5\%$  of reading for liquids, and  $\pm 0.5\%$  and  $\pm 1.0\%$  for gases. High-accuracy meters have linearities of  $\pm 0.15\%$  for liquids and  $\pm 0.25\%$  for gases, usually specified over a 10:1 dynamic range below maximum rated flow. Traceability to NIST (National Institute of Standards and Technology) is frequently available, allowing one to estimate the overall absolute accuracy performance of a flowmeter under specified conditions. Under ideal conditions, absolute accuracies for optimum designs and installations can come close to the accuracy capabilities at the NIST, which are stated as  $\pm 0.13\%$  for liquid flows and  $\pm 0.25\%$  for air.
- Rangeability, when defined as the ratio of flow rates over which the linearity specification applies, is typically between 10:1 and 100:1.
- Operating temperature ranges span  $-270^\circ\text{C}$  to  $650^\circ\text{C}$ , ( $-450^\circ\text{F}$  to  $1200^\circ\text{F}$ ).
- Operating pressure ranges span coarse vacuum to 414 MPa (60,000 psi).
- Pressure drop at the maximum rated flow rate ranges from around 0.3 kPa (0.05 psi) for gases to in the region of 70 kPa (10 psi) for liquids.



**FIGURE 28.30** Longitudinal section of an axial turbine flowmeter depicting the key components. The flowmeter body is usually a magnetically transparent stainless steel such as 304. Common end-fittings include face flanges (depicted), various threaded fittings and tri-clover fittings. The upstream and downstream diffusers are the same in bidirectional meters, and generally supported by three or more flat plates, or sometimes tubular structures, aligned with the body, which also act as flow straighteners. The relative size of the annular flow passage at the rotor varies among different designs. Journal rotor bearings are frequently used for liquids, while ball bearings are often used for gases. Magnetic reluctance pickups (depicted) are frequently used. Others types include mechanical and modulated carrier pickups. (1) End fitting — flange shown; (2) flowmeter body; (3) rotation pickup — magnetic, reluctance type shown; (4) permanent magnet; (5) pickup cold wound on pole piece; (6) rotor blade; (7) rotor hub; (8) rotor shaft bearing — journal type shown; (9) rotor shaft; (10) diffuser support and flow straightener; (11) diffuser; (12) flow conditioning plate (dotted) — optional with some meters.

### Theory

There are two approaches described in the current literature for analyzing axial turbine performance. The first approach describes the fluid driving torque in terms of momentum exchange, while the second describes it in terms of aerodynamic lift via airfoil theory. The former approach has the advantage that it readily produces analytical results describing basic operation, some of which have not appeared via airfoil analysis. The latter approach has the advantage that it allows more complete descriptions using fewer approximations. However, it is mathematically intensive and leads rapidly into computer-generated solutions. One prominent pioneer of the momentum approach is Lee [1] who, using this approach, later went on to invent one of the few, currently successful, dual rotor turbine flowmeters, while Thompson and Grey [2] provided one of the most comprehensive models currently available using the airfoil

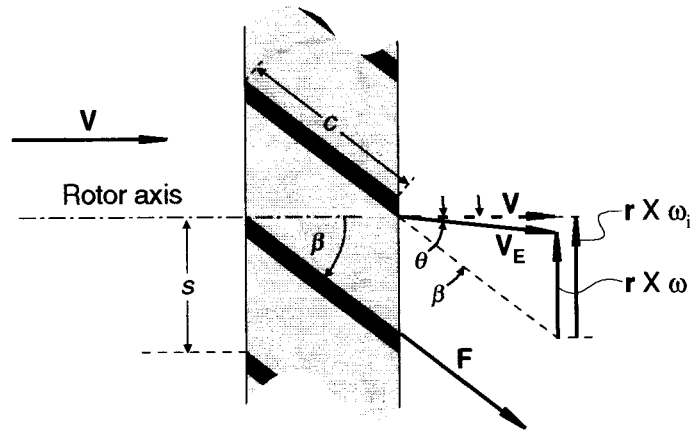


**FIGURE 28.31** Vector diagram for a flat-bladed axial turbine rotor. The difference between the ideal (subscript *i*) and actual tangential velocity vectors is the rotor slip velocity and is caused by the net effect of the rotor retarding torques. This gives rise to linearity errors and creates swirl in the exit flow.  $V$ , incident fluid velocity vector;  $V_E$ , exit fluid velocity vector;  $\theta$ , exit flow swirl angle due to rotor retarding torques;  $\beta$ , blade pitch angle, same as angle of attack for parallel flow;  $\omega$ , rotor angular velocity vector;  $r$ , rotor radius vector;  $F$ , flow-induced drag force acting on each blade surface;  $c$ , blade chord;  $s$ , blade spacing along the hub;  $c/s$ , rotor solidity factor.

approach, which for example, took into account blade interference effects. In the following, the momentum exchange approach is used to highlight the basic concepts of the axial turbine flowmeter.

In a hypothetical situation, where there are no forces acting to slow down the rotor, it will rotate at a speed that exactly maintains the fluid flow velocity vector at the blade surfaces. Figure 28.31 is a vector diagram for a flat-bladed rotor with a blade pitch angle equal to  $\beta$ . Assuming that the rotor blades are flat and that the velocity is everywhere uniform and parallel to the rotor axis, then referring to Figure 28.31, one obtains:

$$r\omega_i = \frac{\tan\beta}{V} \quad (28.47)$$

When one introduces the total flow rate, this becomes:

$$\frac{\omega_i}{Q} = \frac{\tan\beta}{\bar{r}A} \quad (28.48)$$

where  $\omega_i$  = "Ideal" rotational speed

$Q$  = Volumetric flow rate

$A$  = Area of the annular flow cross-section

$\bar{r}$  = Root-mean-square of the inner and outer blade radii, ( $R, a$ )

Eliminating the time dimension from the left-hand-side quantity reduces it to the number of rotor rotations per unit fluid volume, which is essentially the flowmeter  $K$  factor specified by most manufacturers. Hence, according to Equation 28.48, in the ideal situation, the meter response is perfectly linear and determined only by geometry. (In some flowmeter designs, the rotor blades are helically twisted to improve efficiency. This is especially true of blades with large radius ratios, ( $R/a$ ). If the flow velocity profile is assumed to be flat, then the blade angle in this case can be described by  $\tan\beta = \text{constant} \times r$ . This is sometimes called the "ideal" helical blade.) In practice, there are instead a number of rotor

retarding torques of varying relative magnitudes. Under steady flow, the rotor assumes a speed that satisfies the following equilibrium:

$$\begin{aligned} \text{Fluid driving torque} = & \text{rotor blade surfaces fluid drag torque} + \text{rotor hub} \\ & \text{and tip clearance fluid drag torque} + \text{rotation sensor} \\ & \text{drag torque} + \text{bearing friction retarding torque} \end{aligned} \quad (28.49)$$

Referring again to Figure 28.31, the difference between the actual rotor speed,  $r\omega$ , and the ideal rotor speed,  $r\omega_i$ , is the rotor slip velocity due to the combined effect of all the rotor retarding torques as described in Equation 28.49, and as a result of which the fluid velocity vector is deflected through an exit or swirl angle,  $\theta$ . Denoting the radius variable by  $r$ , and equating the total rate of change of angular momentum of the fluid passing through the rotor to the retarding torque, one obtains:

$$\int_a^R \frac{\rho Q 2\pi r^2 (r\omega_i - r\omega)}{\pi(R^2 - a^2)} dr = N_T \quad (28.50)$$

which yields:

$$\bar{r}^2 \rho Q (\omega_i - \omega) = N_T \quad (28.51)$$

where  $\rho$  is the fluid density and  $N_T$  is the total retarding torque. Combining Equations 28.47 and 28.51 and rearranging, yields:

$$\frac{\omega}{Q} = \frac{\tan\beta}{\bar{r}A} - \frac{N_T}{\bar{r}^2 \rho Q^2} \quad (28.52)$$

The trends evident in Equation 28.52 reflect the characteristic decline in meter response at very low flows and why lower friction bearings and lower drag pickups tend to be used in gas vs. liquid applications and small diameter meters. In most flowmeter designs, especially for liquids, the latter three of the four retarding torques described in Equation 28.49 are small under normal operating conditions compared with the torque due to induced drag across the blade surfaces. As shown in Figure 28.31, the force,  $F$ , due to this effect acts in a direction along the blade surface and has a magnitude given by:

$$F = \frac{\rho V^2}{2} C_D S \quad (28.53)$$

where  $C_D$  is the drag coefficient and  $S$  is the blade surface area per side. Using the expression for drag coefficient corresponding to turbulent flow, selected by Pate et al. [3] and others, this force can be estimated by:

$$F = \rho V^2 0.074 \text{Re}^{-0.2} S \quad (28.54)$$

where  $\text{Re}$  is the flow Reynolds number based on the blade chord shown as dimension  $c$  in Figure 28.31. Assuming  $\theta$  is small compared with  $\beta$ , then after integration, the magnitude of the retarding torque due to the induced drag along the blade surfaces of a rotor with  $n$  blades is found to be:

$$N_D = n(R+a)\rho V^2 0.037 \text{Re}^{-0.2} S \sin\beta \quad (28.55)$$

Combining Equations 28.55 and 28.52, and rearranging yields:

$$\frac{\omega}{Q} = \frac{\tan\beta}{\bar{r}A} - \frac{0.036n(R+a)SA^2 \text{Re}^{-0.2} \sin\beta}{\bar{r}^2} \quad (28.56)$$

Equation 28.56 is an approximate expression for the  $K$  factor because it neglects the effects of several of the rotor retarding torques, and a number of important detailed meter design and aerodynamic factors, such as rotor solidity and flow velocity profile. Nevertheless, it reveals that linearity variations under normal, specified operating conditions are a function of certain basic geometric factors and Reynolds number. These results reflect general trends that influence design and calibration. Additionally, the marked departure from an approximate  $\rho V^2$  (actually  $\rho^{0.8} V^{1.8} \mu^{-0.2}$  via  $\text{Re}$  in Equation 28.54) dependence of the fluid drag retarding torque on flow properties under turbulent flow, to other relationships under transitional and laminar flow, gives rise to major variations in the  $K$  factor vs. flow rate and media properties for low-flow Reynolds numbers. This is the key reason why axial turbine flowmeters are generally recommended for turbulent flow measurement.

### Calibration, Installation, and Maintenance

Axial turbine flowmeters have a working dynamic range of at least 10:1 over which the linearity is specified. The maximum flow rate is determined by design factors related to size vs. maximum pressure drop and maximum rotor speed. The minimum of the range is determined by the linearity specification itself. Due to small, unavoidable, manufacturing variances, linearity error curves are unique to individual meters and are normally provided by the manufacturer. However, although recommended where possible, the conditions of the application cannot usually and need not necessarily duplicate those of the initial or even subsequent calibrations. This has pivotal importance in applications where actual operating conditions are extreme or the medium is expensive or difficult to handle. Figure 28.32 depicts a typically shaped calibration curve of linearity vs. flow rate expressed in terms of multiple alternative measures, various combinations of which can be found in current use. The vertical axis thus represents either the linearity error as a percentage of flow rate, a  $K$  factor expressed in terms of the number of pulses from the rotation sensor output per volume of fluid, or the deviation from 100% registration; the latter only applies to flowmeters with mechanical pickups. The horizontal axis can be expressed in terms of flow rate in volume units/time, Reynolds number ( $\text{Re}$ ), or pulse frequency (from the rotation sensor for nonmechanical) divided by kinematic viscosity, ( $f/\nu$ ), in units of  $\text{Hz}/\text{m}^2\text{s}^{-1}$ , ( $\text{Hz}/\text{cSt}$  or  $\text{Hz}/\text{SSU}$ ;  $10^{-6} \text{m}^2\text{s}^{-1} = 1 \text{ centistoke} = 31.0 \text{ seconds, Saybolt Universal}$ ), and where kinematic viscosity is the ratio of absolute viscosity ( $\mu$ ) to density. Calibrations are preferably expressed vs.  $\text{Re}$  or  $f/\nu$ , which is proportional to  $\text{Re}$ . The hump shown in the curve is a characteristic frequently observed at lower  $\text{Re}$  and is due to velocity profile effects.  $K$  factor vs.  $f/\nu$  calibration curves are specifically called universal viscosity curves (UVC) and, for most meters, are available from the manufacturer for an extra charge. A key utility of UVC is that where media type and properties differ significantly from those of the original calibration, accuracies much greater than the overall linearity error can still readily be obtained via the flowmeter UVC if the kinematic viscosity of the application is known. An alternative, advanced calibration technique [4] is to provide response in terms of Strouhal number vs.  $\text{Re}$  or Roshko number. This approach is not widely adopted, but it is particularly relevant to high-accuracy and extreme temperature applications because it further allows correct compensation for flowmeter thermal expansion errors.

The accuracy of axial turbine flowmeters is reduced by unconditioned flow, especially swirl. An installation incorporating flow conditioners along with specific upstream and downstream straight pipe lengths is generally recommended [5]. Some axial turbine flowmeters can be purchased with additional large flow straighteners that mount directly ahead of the flowmeter body or conditioning plates that are integral to the body. The manufacturer is the first source of information regarding installation. Errors due to flow velocity pulsations are another concern, particularly in certain gas installations. However, no standard technique for effectively counteracting this source of error has yet been adopted. Periodic

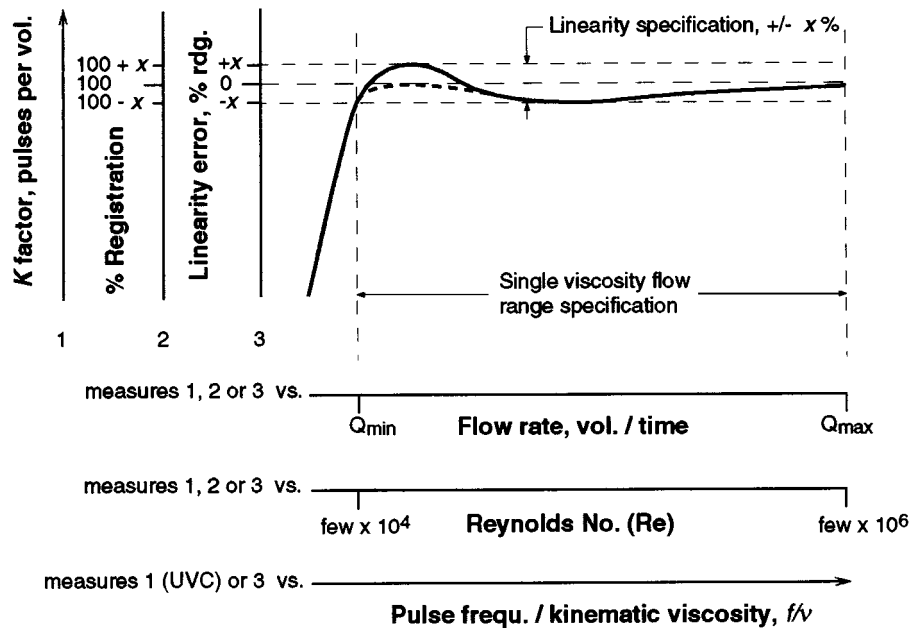


**FIGURE 28.32** A typical single rotor axial turbine linearity error, or calibration, curve for a low-viscosity fluid showing the main alternative presentations in current use. Higher accuracy specifications usually correspond to a 10:1 flow range down from  $Q_{\max}$ , while extended operating ranges usually correspond to reduced accuracies. The hump in the depicted curve is a characteristic feature caused by flow velocity profile changes as  $Re$  approaches the laminar region. This feature varies in magnitude between meters. Sensitivity and repeatability performance degrade at low  $Re$ . Percent registration is only used with meters that have mechanical pickups. All other meters have a  $K$  factor. Universal viscosity curve (UVC) and  $Re$  calibrations remain in effect at different known media viscosities provided  $Re$  or  $f/\nu$  stays within the specified range.  $Re$  is referenced to the connecting conduit diameter and is less within the flowmeter. The  $Re$  range shown is therefore approximate and can vary by an order of magnitude, depending on the meter. Linearity error can also be expressed in terms of Strouhal number ( $fD/V$ ) vs.  $Re$  ( $VD/\nu$ ) or Roshko number ( $fD^2/\nu$ ), when instead  $D$  is a flowmeter reference diameter [4]. UVC, Universal Viscosity Curve; - - -, the effect of a rotor shroud in a viscosity compensated flowmeter.

maintenance, testing, and recalibration is required because the calibration will shift over time due to wear, damage, or contamination. For certain applications, especially those involving custody transfer of oil and natural gas, national standards, international standards, and other recommendations exist that specify the minimum requirements for turbine meters with respect to these aspects [6–10].

### Design and Construction

There are numerous, often proprietary, designs incorporating variations in rotors, bearings, pickups, and other components in format and materials that are tailored to different applications. Meter bodies are available with a wide range of standard end-fittings. Within application constraints, the primary objective is usually to optimize the overall mechanical stability and fit in order to achieve good repeatability performance. Design for performance, application, and manufacture considerations impacts every internal component, but most of all the rotor with respect to blade shape and pitch, blade count, balance and rigidity vs. drag, stress, and inertia, bearings with respect to precision vs. friction, speed rating and durability, and rotation pickup vs. performance and drag.

Most low-radius ratio blades are machined flat, while high-ratio blades tend to be twisted. The blade count varies from about 6 to 20 or more, depending on the pitch angle and blade radius ratio so that the required rotor solidity is achieved. Rotor solidity is a measure of the “openness” to the flow such that higher solidity rotors are more highly coupled to the flow and achieve a better dynamic range. The pitch

angle, which primarily determines the rotor speed, is typically 30° to 45° but can be lower in flowmeters designed for low-density, gas applications. Rotor assemblies are usually a close fit to the inside of the housing. In large-diameter meters, the rotor often incorporates a shroud around the outer perimeter for enhanced stability. Also, since large meters are often used for heavy petroleum products, via selection of a suitable wall clearance, the fluid drag resulting from this clearance gap is often designed to offset the tendency at high media viscosities for the meter to speed up at lower Reynolds numbers. The materials of construction range from nonmagnetic to magnetic steels to plastics.

Stainless steel ball bearings tend to be used for gas meters and low lubricity liquids such as cryogenic liquids and freon, while combination tungsten carbide or ceramic journal and thrust bearings are often considered best for many other liquid meters, depending on the medium lubricity. Fluid bearings (sometimes called “bearingless” designs) are often used in conjunction with the latter, but also sometimes with gases, for reducing the drag. They operate by various designs that use flow-induced forces to balance the rotor away from the shaft ends. Bearing lubrication is either derived from the metered medium or an internal or external system is provided. The more fragile, jeweled pivot bearings are also used in certain gas applications and small meters. Sanitary meters can incorporate flush holes in the bearing assembly to meet 3A crack and crevice standards.

The most common types of rotation sensor are magnetic, modulated carrier, and mechanical, while optical, capacitive, and electric resistance are also used. In research, a modulated nuclear radiation flux rotation sensor for use in certain nuclear reactors has also been reported [11, 12]. Mechanical pickups, which sometimes incorporate a magnetic coupling, are traditional in some applications and can have high resolution; one advantage is that they require no electric power. However, the pickup drag tends to be high. The magnetic and modulated carrier types utilize at least a coil in a pickup assembly that screws into the meter housing near the rotor. In magnetic inductance types, which are now less common, the blades or shroud carry magnetized inserts, and signals are induced in the coil by the traversing magnetic fields. In the more prevalent magnetic reluctance type, an example of which is schematically depicted in Figure 28.30, the coil is wrapped around a permanent magnet or magnet pole piece in the pickup assembly which is mounted next to a high magnetic permeability bladed rotor (or machined shroud). The latter is then typically made of a magnetic grade of stainless steel such as 416, 430, or 17-4Ph. As the rotor turns, the reluctance of the magnetic circuit varies, producing signals at the coil. In the more expensive modulated carrier types, the rotor need only be electrically conductive. The coil is part of a radio frequency (RF) oscillator circuit and the proximity of the rotor blades changes the circuit impedance, giving rise to modulation at a lower frequency that is recovered. The RF types have much lower drag, higher signal levels at low flow, and can operate at temperatures above the Curie point of typical ferromagnetic materials. They are preferred for wide dynamic range and high-temperature applications. Bidirectional flowmeters usually have two magnetic pickups to determine flow direction. This is useful, for example, in the monitoring of container filling and emptying operations often encountered in sanitary applications. Multiple magnetic pickups are also used in some designs to provide increased measurement resolution. Regarding output, various pulse amplifiers, totalizers, flow computers for gas pressure and temperature correction, along with 4–20 mA and other standard interface protocols, are available to suit particular applications. As an example of advanced transmitters, at least one manufacturer (EG&G Flow Technology, Inc.) provides a real-time, miniature, reprogrammable, “smart” transmitter that is integrated into the pickup housing along with a meter body temperature sensor, for full viscosity compensation and UVC linearization. These are for use in dedicated applications, such as airborne fuel management, where the medium viscosity–temperature relationship is known.

Certain applications have uniquely different design requirements and solutions, and two are discussed separately in the following.

#### Propeller Meters.

Propeller meters are used in either municipal, irrigation, or wastewater measurement. Although in some designs, propeller and turbine meters look almost identical and operate on the same axial rotor principle, this type of flowmeter is currently commercially and officially [13, 14] distinguished as a separate category



distinct from the axial turbine. Diameters up to 2440 mm (96 in.) are available. The flow rate capacity of a 1800 mm (72 in.) diameter propeller meter is up to about 25,000 m<sup>3</sup> h<sup>-1</sup>, (110,000 gpm). Typical accuracies are  $\pm 2\%$  of reading. A primary requirement is ruggedness, and it is in the designs most suited to harsh environments that the formats are most distinctive. Rotor and pickup assemblies are generally flanged to the housing and removable. The rotors have large clearances, are often cantilevered into the flow, and supported via a sealed bearing without stators. The rotors are typically made of plastic or rubber and carry as few as three highly twisted, high radius ratio blades. Pickups are always mechanical and frequently have magnetic couplings.

#### Spirometers.

Monitoring spirometers measure the volumes of gas flows entering and leaving the lungs and can also be incorporated in ventilator circuits. Diagnostic spirometers are used to monitor the degree and nature of respiration. With these, a clinician can determine patient respiratory condition by various measures and clinical maneuvers. Low cost, light weight, speed of response, and patient safety are major considerations. Measurement capabilities include the gas volume of a single exhalation and also the peak expiratory flow for diagnostic types, measured in liters and liters per second, respectively. Various technologies are used. However, the Wright respirometer, named after the original inventor [15], today refers to a type of hand-held monitoring spirometer that utilizes a special type of tangential turbine transducer with a two-bladed rotor connected to a mechanical pickup and a dial readout for the volume. These particular spirometers are routinely used by respiratory therapists for patient weaning and ventilator checking. Other axial turbine-based flowmeters are available for ventilation measurements involving, for example, patient metabolics measurements. One axial turbine-based diagnostic spirometer made by Micro Medical, Ltd., currently claims most of the European market. This device utilizes an infrared, optical pickup and has a battery-powered microprocessor-controlled display. In these medical devices, rotors tend to be plastic with a large blade radius ratio. Flow conditioning is minimal or absent. The meters are typically accurate to  $\pm$  a few percent of reading. In the U.S., spirometers are designated as class 2 medical devices and as such certain FDA approvals are required concerning manufacture and marketing. In the EU they are class IIb medical devices under a different system, and other approvals are required.

#### Dual-Rotor Axial Turbines

Dual-rotor axial turbines have performance features not found in single rotor designs. In 1981, Lee et al. [16] were issued a U.S. patent for a self-correcting, self-checking dual-rotor turbine flowmeter that is currently manufactured exclusively by Equimeter, Inc. and sold as the Auto-Adjust. This is a high-accuracy flowmeter primarily intended for use on large natural gas lines where even small undetected flow measurement errors can be costly. It incorporates two closely coupled turbine rotors that rotate in the same direction. The upstream rotor is the main rotor and the second rotor, which has a much shallower blade angle, is the sensor rotor. Continuous and automatic correction of measurement errors due to varying bearing friction is achieved by calculating the flow rate based on the difference between the rotor speeds. As shown in Figure 28.31 and discussed in the theory section, the flow exit angle is due to the net rotor retarding torque. If this torque increases in the main rotor, thereby reducing its speed, the exit angle increases and the speed of the sensor rotor is then also reduced. The meter is also insensitive to inlet swirl angle because the swirl affects both rotor speeds in the same sense and the effect is then subtracted in the flow calculation. The meter also checks itself for wear and faults by monitoring the ratio of the two rotor speeds and comparing this number with the installation value [17].

A dual-rotor liquid flowmeter, invented by Ruffner et al. [18], was recently introduced by Exact Flow, LLC. It is being offered as a high-accuracy flowmeter (up to  $\pm 0.1\%$  accuracy and  $\pm 0.02\%$  repeatability), which has an extraordinarily wide dynamic range of 500:1 with a single-viscosity liquid. This flowmeter has had early commercial success in fuel flow measurement in large jet engine test stands where the wide dynamic range is particularly useful [19]. The meter comprises two, closely and hydraulically coupled rotors that rotate in opposite directions. Due to the exit angle generated by the first rotor, the second rotor continues to rotate to much lower flow rates compared with the first.

## Two-Phase Flow Measurement Using Axial Turbines

A differential pressure producing flowmeter such as a venturimeter in series with a turbine is known to be a technically appropriate and straightforward method for measuring the volumetric and mass flow rates of some fine, solid aerosols. However, this section highlights a current research area in the application of axial rotor turbine meters to a range of industrial flow measurement problems where gas/liquid, two-phase flows are encountered. Customarily, turbine meters are not designed for and cannot measure such flows accurately. Errors of the order 10% arise in metering liquids with void fractions of around 20%. Such flows are normally measured after gas separators. Although this problem is not restricted to these industries, the current main impetuses for research are the direct measurement of crude oil in offshore multiphase production systems, the measurement of water/steam mixtures in the cooling loops of nuclear reactors, and the measurement of freon liquid–vapor flows in refrigeration and air conditioning equipment. Several techniques investigated thus far use an auxiliary sensor. This can either be a void fraction sensor or a pressure drop device such as a venturimeter or drag disk, of which the pressure drop approach appears to be technically more promising [20, 21]. Also, from a practical standpoint, gamma densitometers for measuring void fraction are additional and expensive equipment and not, for example, well adapted for use in undersea oil fields. Two techniques currently being studied do not require an auxiliary in-line sensor. The first uses the turbine meter itself as the drag body and combines the output of the turbine with that of a small differential pressure sensor connected across the inlet and outlet regions. This technique requires a homogenizer ahead of the turbine, and measurement accuracies of  $\pm 3\%$  for the volumetric flow rates of both phases have recently been reported for air/water mixtures up to a void fraction of 80% [22]. The second technique is based entirely on analysis of the turbine output signal and has provided significant correlations of the signal fluctuations with void fraction. Accuracies of water volumetric flow rate measurement of  $\pm 2\%$  have been reported when using air/water mixtures with void fractions of up to 25% [23].

## Insertion Axial Turbine Flowmeters

These flowmeters comprise a small axial rotor mounted on a stem that is inserted radially through the conduit wall, often through a shut-off valve. They measure the flow velocity at the rotor position from which the volumetric flow rate is inferred. They are an economical solution to flow measurement problems where pipe diameters are high and accuracy requirements are moderate, and also may be technically preferred where negligible pressure drop is an advantage, as in high-speed flows. They are typically more linear than insertion tangential turbine flowmeters and compete also with magnetic and vortex shedding insertion flowmeters. They are available for the measurement of a range of liquids and gases, including steam, similar to the media range of full bore axial turbines, and have a similarly linear response. Flow Automation, Inc., is currently the leading manufacturer. The rotors, which are usually metal but can be plastic, typically have diameters of 25 mm to 51 mm (1 in. to 2 in.). They can be inserted into pipes with diameters ranging from 51 mm to 2032 mm (2 in. to 80 in.). Velocity measurement ranges cover  $0.046 \text{ ms}^{-1}$  to  $91 \text{ ms}^{-1}$ , (9 fpm to 18,000 fpm) for gases and  $0.03 \text{ ms}^{-1}$  to  $30 \text{ ms}^{-1}$  (6 fpm to 6000 fpm) for liquids. Dynamic ranges vary between 10:1 and 100:1. The maximum flow rate measurement capacity in a 1836 mm (72 in.) diameter pipe can be as high as nearly  $56,500 \text{ m}^3 \text{ h}^{-1}$ , (about 250,000 gpm). Since these devices are local velocity sensors, calculating the volumetric flow rate requires a knowledge of the area velocity profile and the actual flow area. Flow conditioning is therefore particularly important for accurate volumetric measurements, while radial positioning, which is a further responsibility of the user, must be according to the manufacturer's recommendation, which can either be centerline, one third of the diameter, 12% of the diameter, or determined by "profiling." Quick [24] discusses operation and installation for natural gas measurement. Although linearities or "accuracies" can be quoted up to  $\pm 1\%$  of velocity, achieving the same accuracy for the volumetric flow rate, although possible, can be difficult or impractical. In this respect, a unique dual rotor design, exclusive to Onicon, Inc., and primarily used for chilled-water flow measurement in HVAC systems, requires less flow conditioning than single rotor designs. An Onicon dual rotor turbine assembly is depicted in [Figure 28.33](#). It comprises two rotors that

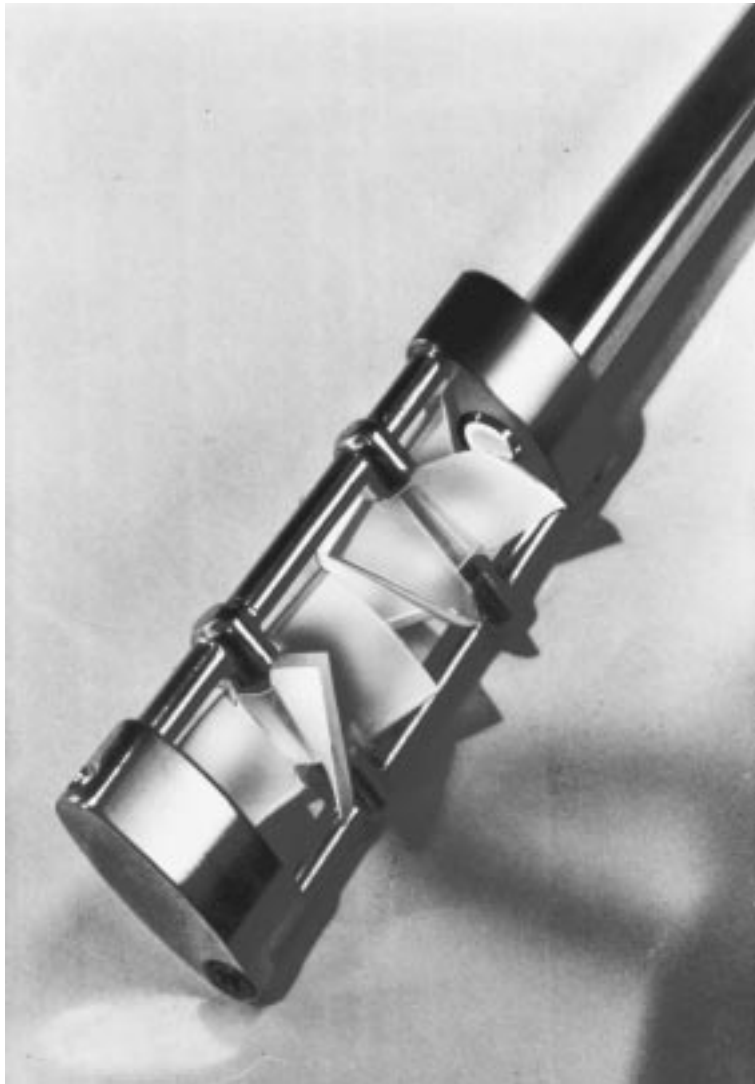


**FIGURE 28.33** The rotor assembly of a dual rotor, insertion axial turbine flowmeter for water flow measurement. This patented design renders the flowmeter insensitive to errors due to flow swirl; an important source of potential error in single rotor axial turbine flowmeters. The rotations are sensed by two separate, electric impedance sensors. (Courtesy of Onicon Incorporated.)

rotate in opposite directions. The output is based on the average rotor speed. Any flow swirl present due to poor flow conditioning changes the speed of rotation of each rotor by the same but opposite amounts. Swirl-induced error is thus virtually absent in the averaged output. Also, flow profile sampling is improved over that of a single rotor. The devices are calibrated using a volumetric prover and the specified accuracy of  $\pm 2\%$  of reading is for volumetric flow rate rather than velocity. This is the total error and includes an allowance for dimensional variations in industry standard pipes.

### **Angular Momentum Flowmeters**

These are accurate, linear, liquid mass flowmeters that utilize vaned components and are used in aerospace applications. They are currently the instrument of choice for airborne, jet engine fuel flow measurement

for large commercial aircraft and some military aircraft for afterburner applications. They are more expensive than the equivalent turbine flowmeters for this application, but they provide mass flow rate measurements directly and are unaffected by fuel density variations. Typical accuracies lie between  $\pm 0.5\%$  and  $\pm 1.0\%$  over a 40:1 or greater dynamic range. Measurement ranges are available for fuel flows from about  $0.01$  to  $6 \text{ kg s}^{-1}$  (70 to 46,000 PPH).

The principle of operation is long established and based on imparting angular momentum to the fluid flow using a driven, flat-bladed impeller. The force required to drive the impeller at constant speed is monitored as a proportional indication of mass flow rate as this quantity varies. Some designs use an electric motor to drive the impeller. However, the current trend in design is motorless. In such a device, a constant driving speed in the region of 100 rpm to 200 rpm is provided by one or more turbine rotors driven by the flow. A variable shunt metering valve assembly adjacent to the turbine rotor mechanically opens and closes in response to flow dynamic pressure and thereby automatically maintains a constant speed of rotation provided that the flow rate is above the minimum of the range. The driven impeller carries vanes that are parallel to the flow, and resides on a common axis with the turbine rotor. A flow straightener ensures parallel flow past the impeller. There is a carefully engineered constant rate spring connection between the turbine shaft and the impeller so that the angular deflection between the two is proportional to the applied torque, and this quantity is directly proportional to the mass flow rate. Two pickup coils sense the rotations of the turbine and the vaned impeller, and only the time difference between the pulses in these two signals is measured and used to calculate the flow rate. Chiles et al. [25] provide a detailed illustration and explanation of the intricate mechanism.

### **Multijet Turbine Flowmeters**

These are linear, volumetric flowmeters designed for liquids measurements and comprise a single, radial-vaned impeller, vertically mounted on a shaft bearing within a vertically divided flow chamber, sometimes called a distributor. The impeller is often plastic and can even be neutrally buoyant in water. There are various designs, but typically, both chambers access a series of radially distributed and angled jets. The lower chamber jets connect to the flowmeter input port and distribute the flow tangentially onto the lower region of the impeller blades, while the upper series, which is angled oppositely, allow the flow to exit. The flow pattern within the flow chamber is thus a vertical spiral and the dynamic pressure drives the impeller to track the flow. This design gives the meters good sensitivity at low flow rates. Due to the distribution principle, the meters are also insensitive to upstream flow condition. Impeller rotation pickups are always mechanical, often magnetically coupled, and frequently also connect with electric contact transmitters. They are primarily used in water measurement, including potable water measurement for domestic and business billing purposes and in conjunction with energy management systems such as hot water building or district heating, and to a much lesser extent in some chemical and pharmaceutical industries for dosing and filling systems involving solvents, refrigerants, acids and alkalis with absolute viscosities less than  $4.5 \text{ mPa s}$ , ( $0.045 \text{ Poise}$ ). Available sizes range from 15 mm to 50 mm. Dynamic ranges lie between 25:1 and 130:1 and flow measurement ranges cover  $0.03$  to  $30 \text{ m}^3 \text{ h}^{-1}$ , ( $0.13$  to  $130 \text{ gpm}$ ). Measurement linearities range between  $\pm 1\%$  to  $\pm 2\%$ , with typical repeatabilities of  $\pm 0.3\%$ . Operating temperatures range from normal to  $90^\circ\text{C}$  ( $200^\circ\text{F}$ ) and maximum operating pressures are available up to  $6.9 \text{ MPa}$  ( $1000 \text{ psi}$ ). A number of potable water measurement systems come with sophisticated telemetry options that allow remote interrogation by radio or telephone. For potable water applications in the U.S., these meters normally comply with the applicable AWWA standard [26], while in Europe EEC, DIN, and other national standards apply.

In the author's opinion, there is also another type of vaned flowmeter that could be classified as a type of multijet turbine. This type comprises an axially mounted, vaned impeller with an upstream element that imparts a helical swirl to the flow. The transducer is typically a small, low-cost, sometimes disposable, plastic component, and is usually designed for liquids (but also to lower accuracies, gases), low-flow rate measurements (down to  $50 \text{ mL min}^{-1}$ ). The dynamic range is high and accuracies range up to  $\pm 0.5\%$ .

Goss [27] describes one particular design in current use. Specialized applications cover the pharmaceutical, medical, and beverage industries.

### **Cylindrical Rotor Flowmeter**

Instead of coupling to a turbulent flow using the fluid dynamic pressure or momentum flux, as in most axial and tangential turbines, a demonstrated research device due to Wadlow et al. [28] provides a linear, volumetric, low gas flow rate measurement using a single, low inertia, smooth cylindrical tangential rotor that couples to a laminar flow via surface friction. The geometry is conceptually that of a single-surfaced rotating vane. A plane Poiseuille flow is created that passes azimuthally over most of the curved rotor surface in a narrow annular passage between the rotor and a concentric housing. The rotor is motor driven via a feedback control loop connected to an error signal producing, differential pressure sensor connected across the gas ports so as to maintain the meter pressure drop equal to zero. Under this condition, the response, as indicated by motor shaft speed, is exactly linear, determined only by geometry and is independent of gas density and viscosity. The demonstration device reported has a 40 mm diameter rotor and 15 mm diameter gas ports. It measures up to a maximum of 25 Lpm bidirectionally, has a linear dynamic range greater than 100:1, is insensitive to upstream flow condition, and has a  $1/e$  step response time of 42 ms, limited only by the external motor torque and combined motor and rotor inertia.

### **Manufacturers**

There is significant and dynamic competition among the numerous manufacturers of the different types of flowmeters described in this section. In all flowmeter types, most manufacturers have exclusive patent rights concerning one or more detailed design aspects that make their products perform differently from those of the competition. Every few years, one or more major turbine flowmeter company can be identified that has changed ownership and name or formed a new partnership. Identifying the competition and selecting the manufacturer are important and sometimes time-consuming parts of the flowmeter selection and specification process. To assist with this, [Table 28.8](#) gives a few selected examples from different manufacturers, of all of the different flowmeter types described in this section. [Table 28.9](#) gives the corresponding contact information for those selected manufacturers, along with the general types offered by each.

### **Conclusion**

However anachronistic intricate mechanical sensors might appear amid current everyday high technology, there are fundamental reasons why axial turbines are likely to experience continued support and development rather than obsolescence, especially for in-line applications requiring in the region of tenth percent volumetric accuracy. Mechanical coupling is the most direct *volume* interaction for a flowing fluid, which is why mechanical meters historically developed first and continue to be the most accurate and reliable types of flowmeter for so many different fluids. Other nonmechanical, perhaps higher technology, or newer approaches thus face high demands for accurate compensation to render such less directly volume-coupled techniques as generally accurate, or more accurate. This is because the error in each corrected factor or assumption in an indirect technique contributes to the overall error. The technology of high-accuracy flowmeters continues to be driven by applications, such as the custody transfer of valuable oil and natural gas, which demand high accuracy and reliability. There is a continuing demand for accurate and reliable water flowmeters. By reason of long proven field experience, turbine and other vane type devices have become one of a few broadly accepted techniques in many major applications such as these where the demands for flow sensors is significant or growing.

**TABLE 28.8** Examples of Turbine and Vaned Flowmeters

Type	Size(s), in.	Description	Example application(s)	Manufacturer	Approx. price range
Axial	0.5	FT 4-8, with SIL smart transmitter	Helicopters — fuel	EG&G Flow Technology	\$2,500
Axial	1	6700 series, type 60	Raw milk, de-ionized water	Flow Automation	\$1,500
Axial	16	Parity series	Custody transfer oil	Fisher-Rosemount Petroleum	\$30,000–\$38,000
Axial dual rotor	12	Auto-Adjust Turbo-Meter	Custody transfer gas	Equimeter	\$42,000
Axial dual rotor	0.25–2	DR Series	Fuel — large jet engine test stands	Exact Flow	\$1,300–\$1,800
Propeller	48	FM182 (150 PSI)	Municipal water	Sparling	\$6,500
Propeller	6	FM102 (150 PSI)	Irrigation	Sparling	\$850
Special tangential	—	Wright Mark 8	Monitoring spirometer	Ferraris Medical	\$800
Axial	—	MS03/MS04 MicroPlus	Diagnostic spirometer	Micro Medical	\$600
Axial	4	WTX802	Chemical dosing for water treatment	SeaMetrics	\$450–\$550
Axial insertion	1.5–10	TX101	Municipal water, water — HVAC	SeaMetrics	\$450
Axial insertion	2+	VTS-300	High pressure steam	Flow Automation	\$2,900
Axial insertion	3+	VL-150-LP	Flare stack control	Flow Automation	\$2,500
Axial insertion dual rotor	2.5–72	F-1200	Water — HVAC	Onicon	\$900
Angular momentum	—	Model 9-217 True Mass Fuel Flowmeter	Large jet aircraft, e.g., Airbus A320, A321	Eldec	Not available
Multijet	1	1720	Domestic water	ABB Kent Messtechnik	\$170
Multijet	1.5	AMD3000	Chemical liquid filling and dosing	Aquametro AG	\$950
Multijet axial	9/32	DFS-2W	Pharmaceutical filling lines, kidney dialysis dialyte, beverage dispensers, OEM	Digiflow Systems	\$42 or less, transducer; \$235 electronics

## References

1. W. F. Z. Lee and H. J. Evans, Density effect and Reynolds number effect on gas turbine flowmeters, *Trans. ASME, J. Basic Eng.*, 87 (4): 1043-1057, 1965.
2. R. E. Thompson and J. Grey, Turbine flowmeter performance model, *Trans. ASME, J. Basic Eng.*, 92(4), 712-723, 1970.
3. M. B. Pate, A. Myklebust, and J. H. Cole, A computer simulation of the turbine flow meter rotor as a drag body, *Proc. Int. Comput. in Eng. Conf. and Exhibit 1984*, Las Vegas: 184-191, New York: ASME, 1984.
4. P. D. Olivier and D. Ruffner, Improved turbine meter accuracy by utilization of dimensionless data, *Proc. 1992 National Conf. Standards Labs. (NCSL) Workshop and Symp.*, Boulder, CO: NCSL, 1992, 595-607.
5. ISA-RP 31.1, *Specification, Installation and Calibration of Turbine Flowmeters*, Research Triangle Park, NC: ISA, 1977.

**TABLE 28.9** Manufacturer Contact Information

Manufacturer	U.S. distributor	Relevant types
EG&G Flow Technology, Inc. 4250E Broadway Road Phoenix, AZ 85040 Tel: (602) 437-1315	Not applicable	Axial turbines — liquid and gas, including 3A sanitary Insertion axial turbines — liquid and gas
Flow Automation, Inc. 9303 W. Sam Houston Pkwy S. Houston, TX 77099 Tel: (713) 272-0404	Not applicable	Insertion axial turbines — liquid and gas Axial turbines — liquid and gas, including 3A sanitary
Fisher-Rosemount Petroleum Highway 301 North P.O. Box 450 Statesboro, GA 30459 Tel: (912) 489-0200	Not applicable	Axial turbines — liquid
Equimeter, Inc. 805 Liberty Blvd. DuBois, PA 15801 Tel: (814) 371-8000	Not applicable	Axial turbines — gas Dual rotor axial turbines — gas
Exact Flow, LLC P.O. Box 14515 Scottsdale, AZ 85267-4545 Tel: (602) 922-7446	Not applicable	Dual rotor axial turbines — liquid
Sparling Instruments Co., Inc. 4097 North Temple City Blvd. P.O. Box 5988 El Monte, CA 91734 Tel: (818) 444-0571	Not applicable	Propeller meters
Ferraris Medical, Ltd Ferraris House Aden Road Enfield Middlesex EN3 7SE U.K. Tel: 44 (0)1818059055	Ferraris Medical, Inc. P.O. Box 344 9681 Wagner Road Holland, NY 14080 (716) 537-2391	Tangential turbine monitoring spirometers
Micro Medical, Ltd. The Admiral's Offices The Chatham Historic Dockyard Chatham, Kent ME4 4TQ U.K. 44 (0)163 843383	Micro Direct, Inc. P.O. Box 239 Auburn, ME 04212 (800) 588-3381	Axial turbine diagnostic spirometers
SeaMetrics Inc. P.O. Box 1589 Kent, WA 98035 Tel: (206) 872-0284	Not applicable	Axial turbines — liquid Insertion axial turbines — liquid Multijet turbines
Onicon, Inc. 2161 Logan St. Clearwater, FL 34625 Tel: (813) 447-6140	Not applicable	Axial turbines — liquid Insertion axial turbines, single and dual rotor — liquid

**TABLE 28.9 (continued)** Manufacturer Contact Information

Manufacturer	U.S. distributor	Relevant types
Eldec Corporation 16700 13 <sup>th</sup> Avenue W. P.O. Box 97027 Lynnwood, WA 98046 Tel: (206) 743-8499	Not applicable	Angular momentum flowmeters
ABB Kent Messtechnik GmbH Otto-Hahn-Strasse 25 D-68623 Lampertheim Germany 49 62069330	ISTEC Corporation 415 Hope Avenue Roselle, NJ 07203 (908) 241-8880	Multijet turbines
Aquametro AG Ringstrasse 75 CH-4106 Therwil 061 725 11 22	ISTEC Corporation 415 Hope Avenue Roselle, NJ 07203 (908) 241-8880	Multijet turbines
Digiflow Systems B.V. Postbus 46 6580 AA Malden The Netherlands 31 243 582929	Digiflow Systems 781 Clifton Blvd. Mansfield, OH 44907 (419) 756-1746	'Multijet' axial turbines — liquid

6. ANSI/ASME MFC-4M-1986 (R1990), *Measurement of Gas Flow by Turbine Meters*, New York: ASME.
7. API MPM, *Measurement of Liquid Hydrocarbons by Turbine Meters*, 3rd ed., Washington, D.C.: API (Amer. Petroleum Inst.), 1995, chap. 5.3.
8. AGA Transmission Meas. Committee Rep. No. 7, *Measurement of fuel gas by turbine meters*, Arlington, VA: AGA (Amer. Gas Assoc.), 1981.
9. Int. Recommendation R32, *Rotary piston gas meters and turbine gas meters*, Paris: OIML (Int. Organization of Legal Metrology), 1989.
10. ISO 9951:1993, *Measurement of gas flow in closed conduits — turbine meters*, Geneva, Switzerland: Int. Organization for Standardization, (also available ANSI), 1993.
11. T. H. J. Van Der Hagen, Proof of principle of a nuclear turbine flowmeter, *Nucl. Technol.*, 102(2), 167-176, 1993.
12. K. Termaat, W. J. Oosterkamp, and W. Nissen, *Nuclear turbine coolant flow meter*, U.S. Patent No. 5,425,064, 1995.
13. AWWA C704-92, *Propeller-type meters for waterworks applications*, Denver, CO: Amer. Water Works Assoc., 1992.
14. ANSI/AWWA C701-88, *Cold water meters — turbine type, for customer service*, Denver, CO: Amer. Water Works Assoc., 1988.
15. B. M. Wright and C. B. McKerrow, Maximum forced expiratory flow rate as a measure of ventilatory capacity, *Br. Med. J.*, 1041-1047, 1959.
16. W. F. Z. Lee, R. V. White, F. M. Sciulli, and A. Charwat, *Self-correcting self-checking turbine meter*, U.S. Patent No. 4,305,281, 1981.
17. W. F. Z. Lee, D. C. Blakeslee, and R. V. White, A self-correcting and self-checking gas turbine meter, *Trans. ASME, J. Fluids Eng.*, 104, 143-149, 1982.
18. D. F. Ruffner, and P. D. Olivier, *Wide range, high accuracy flow meter*, U.S. Patent No. 5,689,071, 1997.
19. D. F. Ruffner, Private communication, 1996.



20. A. Abdul-Razzak, M. Shoukri, and J. S. Chang, Measurement of two-phase refrigerant liquid-vapor mass flow rate. III. Combined turbine and venturi meters and comparison with other methods, *ASHRAE Trans.: Research*, 101(2), 532-538, 1995.
21. W. J. Shim, T. J. Dougherty, and H. Y. Cheh, Turbine meter response in two-phase flows, *Proc. Int. Conf. Nucl. Eng.* — 4, 1 part B: 943-953, New York: ASME, 1996.
22. K. Minemura, K. Egashira, K. Ihara, H. Furuta, and K. Yamamoto, Simultaneous measuring method for both volumetric flow rates of air-water mixture using a turbine flowmeter, *Trans. ASME, J. Energy Resources Technol.*, 118, 29-35, 1996.
23. M. W. Johnson and S. Farroll, Development of a turbine meter for two-phase flow measurement in vertical pipes, *Flow Meas. Instrum.*, 6(4), 279-282, 1995.
24. L. A. Quick, Gas measurement by insertion turbine meter, *Proc. 70th Int. School Hydrocarbon Meas.*, OK, 1995. (Available E. Blanchard, Arrangements Chair, Shreveport, LA, (318) 868-0603.)
25. W. E. Chiles, L. E. Vetsch, and J. V. Peterson, *Shrouded flowmeter turbine and improved fluid flowmeter using the same*, U.S. Patent No. 4,012,957, 1977.
26. ANSI/AWWA C708-91, *Cold-water meters, multi-jet-type*, Denver, CO: Amer. Water Works Assoc., 1991.
27. J. Goss, *Flow meter*, U.S. Patent No. 5,337,615, 1994.
28. D. Wadlow, and L. M. Layden, *Controlled flow volumetric flowmeter*, U.S. Patent No. 5,284,053, 1994.
29. C. R. Sparks, private communication, 1996.

### Further Information

- D. W. Spitzer (ed.), *Flow measurement*, Research Triangle Park, NC: ISA, 1991, is a popular 646 page practical engineering guide of which four chapters concern turbine flowmeters, sanitary flowmeters, insertion flowmeters and custody transfer issues.
- A. J. Nicholl, Factors affecting the performance of turbine meters, *Brown Bov. Rev.*, 64(11), 684-692, 1977, describes some basic design factors not commonly discussed elsewhere.
- J. W. DeFeo, Turbine flowmeters for measuring cryogenic liquids, *Adv. Instrum. Proc.*, 47 pt.1, 465-472, ISA, 1992, provides guidance for a less frequently discussed application in which axial turbines perform well.
- ATS Standardization of spirometry, 1994 Update, *Am. J. Respir. Care Med.*, 152, 1107-1136, 1995, is the latest version of the official U.S. guideline for spirometry generated by the American Thoracic Society.
- M. D. Lebowitz, The use of expiratory flow rate measurements in respiratory disease, *Ped. Pulmonol.*, 11, 166-174, 1991, provides a review of the diagnostic usefulness of PEFr using portable spirometers.
- W. M. Jungowski and M. H. Weiss, Effects of flow pulsation on a single-rotor turbine meter, *Trans. ASME, J. Fluids Eng.*, 118(1), 198-201, 1996.
- C. R. Sparks and R. J. McKee, *Method and apparatus for assessing and quantifying pulsation induced error in gas turbine flow meters*, U.S. Patent No. 5,481,924, 1996, assigned to the Gas Research Institute, Chicago, is a potential solution to the accurate measurement of pulsating gas flows which will require engineering development and a high performance rotation sensor [29].
- K. Ogawa, S. Ito, and C. Kuroda, Laminar-turbulent velocity profile transition for flows in concentric annuli, parallel plates and pipes, *J. Chem. Eng. Japan*, 13(3), 183-188, 1990, provides mathematical descriptions of velocity profiles.
- J. Lui and B. Huan, Turbine meter for the measurement of bulk solids flow rate, *Powder Technol.*, 82, 145-151, 1995, describes theory and experiments relating to a very simple design for a unique application, namely the volumetric measurement of plug flows of sands in a pipe.

## 28.5 Impeller Flowmeters

Harold M. Miller

Impeller flowmeters, sometimes called *paddlewheel* meters, are one of the most commonly used flowmeter variety. The impeller flow sensor is a direct offshoot of the old-fashioned undershot waterwheel. They are a cost-effective alternative to turbine meters, and can be used in applications that are difficult to handle with other types of flow metering instruments. In their mechanical construction, they are usually very simple, with any sophistication residing in the electronics used to detect the rotation rate of the impeller, and in the choice of materials of construction for chemical corrosion attributes of the metered fluids. They are related to turbine meters in that both types use a rotating mechanical element to produce the output signal. They differ in the fact that the impeller meter has its rotary axis transverse to the flow stream, as opposed to the turbine meter axis, which is parallel thereto.

These devices are available in two basic types. The insertion style is the most common. (See [Figures 28.34\(b\)](#) and [28.35](#).) The sensor is directly installed into a hole in a pipe, with saddle or welded fitting installed at the entry to seal the sensor to the pipe. The sensor can also be preinstalled in appropriate Tees in the pipeline. Most suppliers have designs that can be installed in operating pipe systems, with little, if any, loss of the fluid during the installation process. The impeller design is also supplied in in-line (through-flow) sensors for those applications where such use is desirable ([Figure 28.34\(a\)](#)). The in-line meters are commonly of somewhat higher accuracy than the insertion style.

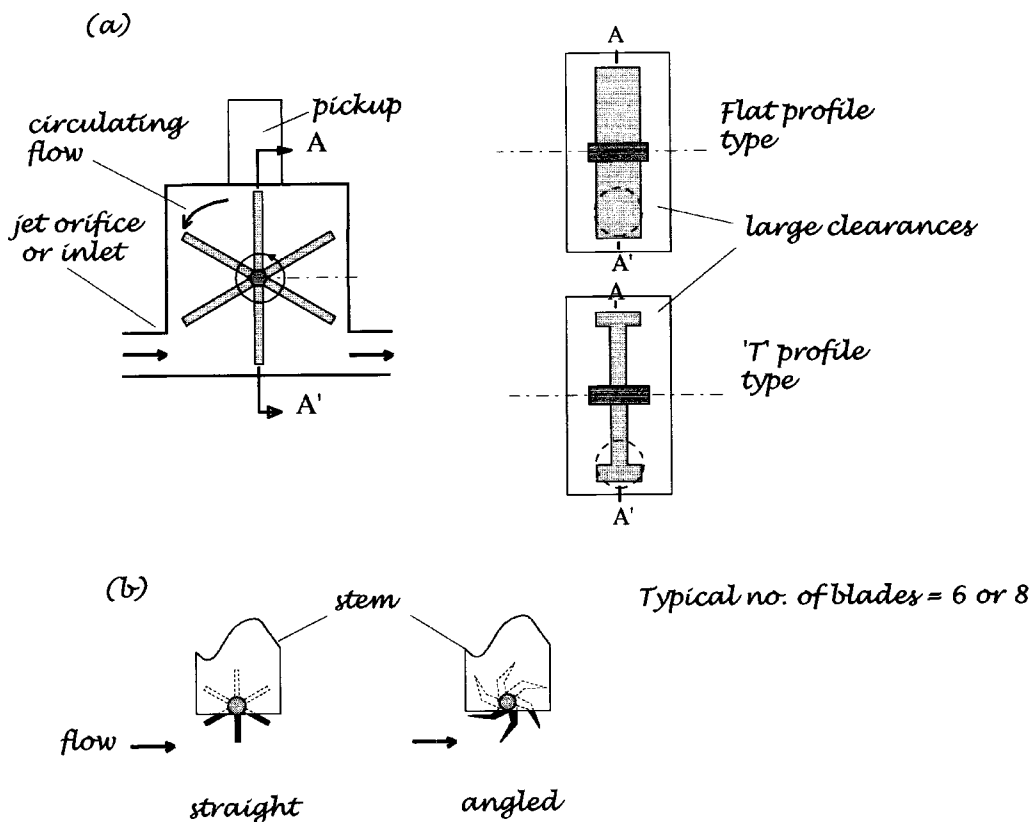


FIGURE 28.34 Impeller flowmeter rotor design variations (a) in-line meters; (b) insertion meters. (Figure courtesy of David Wadlow.)



**FIGURE 28.35** A typical insertion type impeller flow sensor.

In-line meters are *linear, inferential, volumetric* flowmeters for measuring *liquid and gas flows* and are more *sensitive at lower flow rates* compared with, for example, axial turbine flowmeters. (This is of course because the flow blade incidence angle is much greater.) Insertion impeller flowmeters instead measure the flow velocity in a small region within a flow conduit.

Impeller flowmeters are generally suited to much lower flow rate ranges than the same size axial turbines and hence often find applications where axial turbines cannot be used. This, and a tendency for lower cost and high reliability, are key strengths. Competition with in-line axial turbines can only occur in overlapping design flow ranges.

Some in-line meters have interchangeable orifice sizes, allowing the same body to be used over different flow ranges. The orificed in-line meters are typically insensitive to flow condition. Insertion meters are, of course, very sensitive to flow condition if volumetric measurements are inferred. This is an important

distinction and can extend to differences between requirements for specific in-line versions. Installation is important. It affects the user when he or she is designing an installation, selecting a flowmeter, and deciding on how much confidence to place in the measurement reading.

Paddlewheel flowmeters are *never* used in liquid hydrocarbon custody transfer applications. The flow measurement capacity is insufficient to compete in monitoring large volume transfers, and accuracy is not sufficient for valuable fluids.

These meters go by a variety of names, depending on which name the manufacturer selects and also the application. One often-quoted, historical root is also the impulse turbine invented by Pelton in the 19th century and has given rise to the “Pelton wheel turbine” description currently used by some suppliers. A device like this was originally used to drive milling wheels directly about the vertical axis, rather than through a right angle gear as in the “undershot” wheel described. Another common name, besides paddlewheel and impeller-type, based at least on suppliers’ descriptions for the in-line variety, is single-jet tangential, or simply tangential, turbine. The former description distinguishes this design from that of multijet tangential turbine flowmeters and therefore deserves mention. There are thus a confusing variety of names in current use, all relating to essentially the same impeller-like, vaned flowmetering principle:

1. Impeller type: insertion and in-line
2. Paddlewheel type: insertion and in-line
3. Pelton turbine wheel type: in-line
4. Tangential turbine flowmeter: insertion and in-line
5. Single-jet tangential turbine flowmeter: in-line
6. Impulse turbine flowmeter: in-line

Historically, the impeller sensor is based on early electronic speedometers used in pleasure boating. Signet, followed quickly by Data Industrial, moved to modify the basic design of such marine instruments to meet the significantly more demanding service life requirements of industrial flow measurement. The resulting flowmeters, and their descendants, have been widely used since 1975. Significant engineering efforts have resulted in highly reliable instruments used in many extremely demanding applications.

## Sensing Principles

All impeller flow sensors must detect the rotation of the impeller, and in their usual form transmit a pulse train, at a frequency related to the rotational velocity of the impeller. Being essentially a digital output, impeller sensors can typically transmit signals over quite long distances, up to 1 km when so required. Detection principles used include:

1. One or more magnets retained in the impeller or mechanically connected thereto, using the zero crossing of an induced ac field to generate the pulse train.
2. One or more coupling devices contained within the impeller, modulating a transmitted frequency that is processed to produce the pulse train.
3. One or more metallic targets installed within the sensor, sensed by any of the proximity pickup techniques commercially available, to produce output pulses.
4. One or more magnets retained in the impeller, used to switch a Hall effect device, producing the output pulse train.
5. Optical devices, both transmissive and reflective, have been used to sense the passage of the impeller blades to produce the output pulse train.
6. Measurement of the change in electric reactance due to the passage of impeller vanes through the measurement field area, conditioned to produce the output pulse train.

Any given supplier can produce several types of impeller flowmeter, each type using a different detection method depending on market requirements. Since the impeller can operate to rotational velocities of 4000 rpm or higher, output frequencies can be as high as 500 Hz. At low flow rates, the

frequencies can be as low as 0.2 Hz. This factor should be addressed early in the selection procedure because the chosen output device must be capable of the frequency output range of the sensor.

Most sensor manufacturers can either supply or specify an appropriate meter to relate sensor output to flow rate in Engineering units, either U.S. Customary or SI. These meters are usually capable of displaying both flow rate and accumulated flow for the sensor to which they are connected. Additional outputs are available, either stand-alone or in combination with the meter, providing periodic pulse outputs at definable flow increments or analog outputs scaled to flow rate. In addition, certain control functions, alarms, and other special features required by the various markets served are often incorporated in these meters.

## Flow Ranges

The insertion style of impeller meter, even when Tee-installed, is a local sensing device, measuring the flow velocity in only a part of the flow stream. The manufacturer calibrates the meter for average flow across the entire cross-section of the pipe. The paddlewheel location is usually close to the inner diameter of the pipe in a region of flow with a velocity significantly below the average flow velocity in the pipe. Proper calibration practices by the manufacturer make the meters effective at flow rates as low as 10 cm s<sup>-1</sup> average velocity in spite of the low local velocities at the impeller. Generally speaking, flows at Reynolds numbers as low as 5000 can be run with no requirement for special calibration, and frequently lower numbers can be handled with no difficulty. The usual range specification is a flow rate equivalent to 0.3 to 10 m s<sup>-1</sup> average flow velocity. The diversity of products available allows operation to velocities considerably lower than the 0.3 m s<sup>-1</sup> range, indeed to as low as 0.07 m s<sup>-1</sup> in certain specialty impeller flowmeters.

## Installation

**Pipe sizes:** Pipe sizes in which these sensors have been installed run the gamut from small bore tubing to 2.3 m outside diameter. The larger pipe sizes are those that show the greatest installed cost savings over alternative metering systems. The impeller meter, in fact, can be cost-effective in any flowmeter application that is consistent with the accuracy of the instrument, particularly if the application involves pump or valve control.

**Piping system restrictions:** Most suppliers require at least 10 pipe diameter lengths of straight pipe upstream of the installed meter, and 5 downstream. These conditions are required to minimize the asymmetry of the flow stream in the neighborhood of the impeller, in the installed piping, which can be caused by elbows, tees, and valves. More is better; no supplier is likely to complain that there is too great a straight pipe length upstream. Less can adversely affect the calibration of the sensor due to the local variations of velocity resulting from flow disturbances.

**Operating pressure:** Manufacturers' standard offerings are usually consistent with the pressure limitations of the materials of construction of the piping system with plastic piping systems, and are commonly as high as 2.7 MPa with steel or brass piping. Higher pressures are available, but are usually somewhat more expensive. Pressure drop generated by the installed flowmeter is usually low. Manufacturers can usually supply information on the anticipated pressure drop.

**Calibration:** Calibration of the sensors is usually specified by the manufacturer. Some manufacturers provide a calibration factor in terms of gallons per pulse or in pulses per gallon. Others, such as Data Industrial, provide data relating frequency to flow rate in GPM or other volumetric rate units. For insertion-style sensors, any such instrument must be field calibratable to accommodate the variation in the relation of impeller rotational velocity with average flow rate with pipe size variation.

**Accuracy:** Accuracies for in-line impeller flowmeters vary considerably but can be high, ranging from  $\pm 0.2\%$  reading for liquids for one manufacturer to several percent of full scale for several others. The difference between accuracies specified as % full scale and % reading should be particularly noted.

Manufacturers use both, particularly with this class of meter. A  $\pm 1\%$  full-scale device is often far less accurate than, for example, a  $\pm 2\%$  reading device. For example, it is in error by 10% at the minimum of its flow range if the turndown is 10:1, whereas the  $\pm 2\%$  reading device is still only in error by  $\pm 2\%$ .

Output accuracy is usually specified as  $\pm 1\%$  of full rated flow. This specification is broad enough to handle the dimensional and frictional variations in the sensors as manufactured. Some producers will custom-calibrate the sensors to meet special needs, but this task should be performed only when the mating pipe entry and exit can be shipped to, and accommodated by, the manufacturer. Alternatively, the manufacturer can usually provide new calibration values if the meter used is identified, the meter reading is known, and the actual flow is known for at least two points on the flow curve. When calibration in place is required, the anticipated accuracy is in the range of  $\pm 0.5\%$  of full scale or 1% of indicated flow, whichever is greater.

Repeatability of readings is usually on the order of 0.5%. Linearity, except at the extremes of the flow range, is also expected to be no worse than 0.5%, and over the full design range of the meter is normally accurate within the  $\pm 1\%$  of full rated flow.

To achieve the accuracies noted above, careful attention must be paid to proper installation, particularly with regard to insertion depth.

**Design features:** These flow sensors are offered in materials of construction compatible with a broad range of aqueous solutions, of both high and low pH and with deionized water. For this latter service, the history of the sensor, particularly for particle generation, should be reviewed. Flow streams with high concentrations of solids, and particularly of fibrous solids, should be carefully reviewed when the impeller sensor is under consideration. Construction is reasonably forgiving with particulates, but caution in such applications is warranted. Heat transfer fluids are also compatible with sensors from at least two of the suppliers. Basic application limits should be discussed with the supplier, who should have a broad history of successful applications to back up recommendations, as well as sensor materials with test results specific to the measured fluid. So-called “hot tap” or “wet tap” versions are available for installation in operating pipelines and in-line or on-line service. A submersible version capable of metering in flooded well pits for extended periods of time is available from some suppliers. At least two manufacturers provide “intrinsically safe” sensors for application in hazardous environments.

**Areas of application:** Impeller flow sensors are widely used in the following fields with considerable success:

- Agricultural and horticultural irrigation
- Deionized water systems, including silicon wafer fabrication
- Heating, ventilating, and air conditioning, energy management
- Industrial waste treatment
- Industrial filtration systems
- Chemical reagent metering and batching
- Municipal water systems (potable water)

The sensors can be supplied with analog output for control applications, if desired.

Some suppliers have developed specialty impeller meters adapted to provide long life, ruggedness, and maintainability required in more demanding applications. The history of acceptable operation in applications similar to that proposed for the metering system should be reviewed with the supplier. Custodial transfer applications are normally unsuitable for the impeller sensor.

## Manufacturers

The following is a selection of U.S. manufacturers. Their locations and phone numbers are listed in [Table 28.10](#).

**TABLE 28.10** U.S. Manufacturers of Impeller Flowmeters

Manufacturer	City, State	Phone number
Data Industrial Corp.	Mattapoisett, MA	(508) 758-6390
G. Fischer (Signet)	Tustin, CA	(714) 731-8800
SeaMetrics	Kent, WA	(206) 872-0284
Roper Flow Technology, Inc.	Phoenix, AZ	(602) 437-1315
Blancett	Altus, OK	(405) 482-0036
Hoffer Flow Controls, Inc.	Elizabeth City, NC	(800) 628-4584; (919) 331
McMillan Co.	Georgetown, TX	(512) 863-0231
Flowmetrics, Inc.	Canoga Park, CA	(818) 346-4492
Proteus Industries, Inc.	Mountain View, CA	(415) 964-4163

**Data Industrial**

In-line and Insertion Meters: 0.07 to 18 m/s (0.25 to 60 fps) fluid velocity. Available materials to accommodate most industrial fluids. Temperatures from  $-29^{\circ}\text{C}$  to  $152^{\circ}\text{C}$  ( $-20^{\circ}\text{F}$  to  $305^{\circ}\text{F}$ ). Energy monitoring. Digital and/or analog meter outputs. NEMA 4, 4X, and 6P constructions. FM, CSA Approvals.

**G. Fischer (Signet)**

In-line and Insertion Meters: 0.1 to 7 m/s (0.3 to 20 fps) fluid velocity. Available materials to accommodate most industrial fluids. Temperatures to  $149^{\circ}\text{C}$  ( $300^{\circ}\text{F}$ ). Energy monitoring. Digital and/or analog meter outputs. NEMA 4, 4X constructions. FM, CE Approvals.

**SeaMetrics**

In-line meter. Sizes 3/8 in. to 2 in. Plastic, brass. Clean water applications. Flows from 0.05 to 40.0 gpm. Accuracy  $\pm 1\%$  of full scale, (FS). Insertion. Range of IP probes. Plastic, brass, stainless. Sapphire bearings and carbide shafts. Up to  $250^{\circ}\text{F}$ . 0.3 to 30 fps. Accuracy  $\pm 1\%$  to  $\pm 2\%$  FS.

**Roper Flow Technology**

In-line meters: Omniflow<sup>®</sup>, liquids and gases, highly precise, range 7.6 to 5677 mL min<sup>-1</sup> (liquid), 0.0025 to 0.68 Am<sup>3</sup>h<sup>-1</sup> (gases). Cryogenics to  $593^{\circ}\text{C}$ , pressure to 60,000 psi, viscosity compensated.

Optiflo<sup>®</sup>, plastic construction for liquids only with some reduction in performance capabilities.

**Hoffer**

MF Series (Miniflow). High-performance, in-line low flowmeters using a "Pelton rotor" for liquids and gases. Liquid flow ranges from 57 mL min<sup>-1</sup> to 11.5 rpm. Linearity  $\pm 1\%$  reading over 10:1 range. Repeatability  $\pm 0.1\%$  typical. Gas flow ranges depending on density from 0.02 ACFM to 1.0 ACFM. Linearity  $\pm 1.5\%$  reading. Repeatability  $\pm 0.2\%$ . Various bearings available. Ball bearings used for high accuracy applications. UVC curves available. "Smart" transmitter available for temperature-viscosity correction + linearization.

**McMillan**

Low viscosity liquids: In-line meters. Ranges from 13 mL min<sup>-1</sup> to 10 L min<sup>-1</sup>. Accuracies  $\pm 1\%$  to  $\pm 3\%$  full scale. IR rotation sensors. Have a Teflon version for corrosives.

Gases: Teflon version for chlorine, fluorine, etc. Accuracy  $\pm 3\%$  full scale. Ranges: 25 AmL min<sup>-1</sup> to 5 AmL min<sup>-1</sup>.

**Flowmetrics**

Series 600: Stainless steel, in-line tangential turbine for gases and liquids. Ranges: 0.001 to 2.0 GPM liquids; 0.001 to 2.0 ACFM gases. Linearities vary according to range from  $\pm 1\%$  FS to  $\pm 5\%$  FS. Repeatabilities  $\pm 0.05\%$ , traceable NIST.

## Proteus

In-line paddlewheel flowmeters and flow switches — liquids only. Typically used for water cooling lines on electrical or vacuum equipment. Quoted for use with liquids up to 120 cSt. Media include: water, treated water, deionized water, ethylene glycol, light oils, etc. Range 0.08 to 60 gpm. Accuracies vary between models in the  $\pm 3\%$  to  $\pm 4\%$  FS range. Meters bodies can incorporate optional integral temperature and pressure transducers. These meters are also available with a FluidTalk™ computer interface protocol and PC software for constructing embedded control systems for flow, temperature, and pressure.

## References

1. N. P. Cheremisinoff, *Applied Fluid Flow Measurement*, New York: Marcel Dekker, 1979, 106.
2. H. S. Bean (ed.), *Fluid Meters, 6th ed.*, New York: American Society of Mechanical Engineers, 1971, 99.
3. Flow Meter Finder™ Impeller-Type Flow Meters, <http://www.seametrics.com/flowmeter-finder/impeller.htm>.
4. R. Koch and D. Palmer, Revisiting Measurement Technologies, Multijet vs. Positive Displacement Meters in 1996, <http://www.wateronline.com/companies/mastermeterinc/tech.html>.
5. L. C. Kjelstrom, Methods of measuring pumpage through closed conduit irrigation systems, *J. Irrigation Drainage Eng.-ASCE*, 117, 748-757. 1991.

## 28.6 Electromagnetic Flowmeters

---

### *Halit Eren*

*Magnetic flowmeters* have been widely used in industry for many years. Unlike many other types of flowmeters, they offer true noninvasive measurements. They are easy to install and use to the extent that existing pipes in a process can be turned into meters simply by adding external electrodes and suitable magnets. They can measure reverse flows and are insensitive to viscosity, density, and flow disturbances. *Electromagnetic flowmeters* can rapidly respond to flow changes and they are linear devices for a wide range of measurements. In recent years, technological refinements have resulted in much more economical, accurate, and smaller instruments than the previous versions.

As in the case of many electric devices, the underlying principle of the electromagnetic flowmeter is Faraday's law of electromagnetic induction. The induced voltages in an electromagnetic flowmeter are linearly proportional to the mean velocity of liquids or to the volumetric flow rates. As is the case in many applications, if the pipe walls are made from nonconducting elements, then the induced voltage is independent of the properties of the fluid.

The accuracy of these meters can be as low as 0.25% and, in most applications, an accuracy of 1% is used. At worst, 5% accuracy is obtained in some difficult applications where impurities of liquids and the contact resistances of the electrodes are inferior as in the case of low-purity sodium liquid solutions.

### Faraday's Law of Induction

This law states that if a conductor of length  $l$  (m) is moving with a velocity  $v$  ( $\text{m s}^{-1}$ ), perpendicular to a magnetic field of flux density  $B$  (Tesla), then the induced voltage  $e$  across the ends of conductor can be expressed by:

$$e = B l v \quad (28.57)$$

The principle of application of Faraday's law to an electromagnetic flowmeter is given in [Figure 28.36](#). The magnetic field, the direction of the movement of the conductor, and the induced emf are all perpendicular to each other.



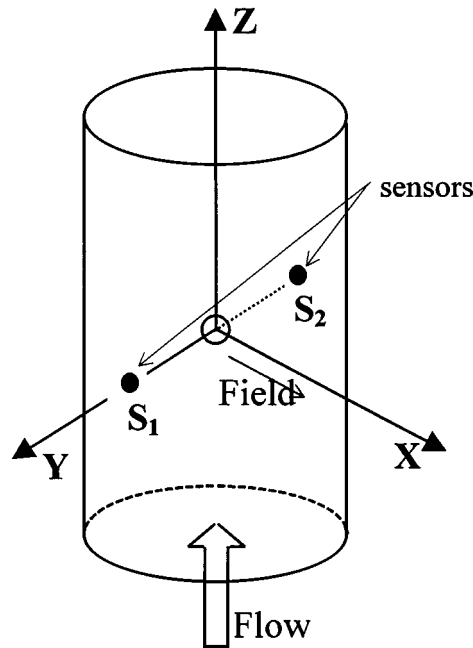


**FIGURE 28.36** Operational principle of electromagnetic flowmeters. Faraday's law states that a voltage is induced in a conductor moving in a magnetic field. In electromagnetic flowmeters, the direction of movement of the conductor, the magnetic field, and the induced emf are perpendicular to each other on  $x$ ,  $y$ , and  $z$  axes. Sensors  $S_1$  and  $S_2$  experience a virtual conductor due to liquid in the pipe.

Figure 28.37 illustrates a simplified electromagnetic flowmeter in greater detail. Externally located electromagnets create a homogeneous magnetic field passing through the pipe and the liquid inside it. When a conducting flowing liquid cuts through the magnetic field, a voltage is generated along the liquid path between two electrodes positioned on the opposite sides of the pipe.

In the case of electromagnetic flowmeters, the conductor is the liquid flowing through the pipe, and the length of the conductor is the distance between the two electrodes, which is equal to the tube diameter. The velocity of the conductor is proportional to the mean flow velocity of the liquid. Hence, the induced voltage becomes:

$$e = B D v \quad (28.58)$$

where  $D$  (m) is the diameter of pipe. If the magnetic field is constant and the diameter of the pipe is fixed, the magnitude of the induced voltage will only be proportional to the velocity of the liquid. If the ends of the conductor, in this case the sensors, are connected to an external circuit, the induced voltage causes a current,  $i$ , to flow, which can be processed suitably as a measure of the flow rate. The resistance of the moving conductor can be represented by  $R$  to give the terminal voltage  $v_T$  of the moving conductor as  $v_T = e - iR$ .

Electromagnetic flowmeters are often calibrated to determine the volumetric flow of the liquid. The volume of liquid flow,  $Q$  ( $L s^{-1}$ ), can be related to the average fluid velocity as:

$$Q = A v \quad (28.59)$$

Writing the area,  $A$  ( $m^2$ ), of the pipe as:

$$A = \pi D^2 / 4 \quad (28.60)$$

gives the induced voltage as a function of the flow rate.

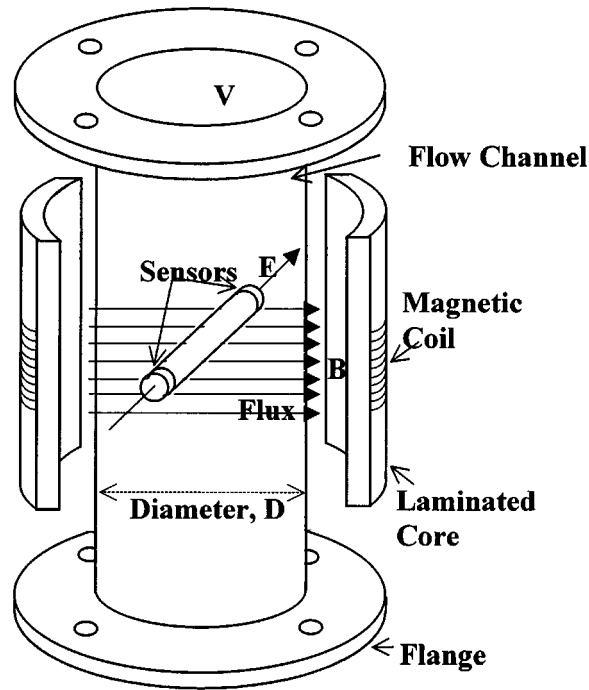


**FIGURE 28.37** Construction of practical flowmeters. External electromagnets create a homogeneous magnetic field that passes through the pipe and the liquid inside. Sensors are located  $90^\circ$  to the magnetic field and the direction of the flow. Sensors are insulated from the pipe walls. Flanges are provided for fixing the flowmeter to external pipes. Usually, manufacturers supply information about the minimum lengths of the straight portions of external pipes.

$$e = \frac{4BQ}{\pi D} \quad (28.61)$$

Equation 28.61 indicates that in a carefully designed flowmeter, if all other parameters are kept constant, then the induced voltage is linearly proportional to the liquid flow only.

Based on Faraday's law of induction, there are many different types of electromagnetic flowmeters available, such as ac, dc, and permanent magnets. The two most commonly used ones are the ac and dc types. This section concentrates mainly on ac and dc type flowmeters.

Although the induced voltage is directly proportional to the mean value of the liquid flow, the main difficulty in the use of electromagnetic flowmeters is that the amplitude of the induced voltage is small relative to extraneous voltages and noise. Noise sources include:

- Stray voltage in the process liquid
- Capacitive coupling between signal and power circuits
- Capacitive coupling in connection leads
- Electromechanical emf induced in the electrodes and the process fluid
- Inductive coupling of the magnets within the flowmeter

### **Construction and Operation of Electromagnetic Flowmeters**

Common to both ac and dc electromagnetic flowmeters, the magnetic coils create a magnetic field that passes through the flow tube and process fluid. As the conductive fluid flows through the flowmeter, a voltage is induced between the electrodes in contact with the process liquid. The electrodes are placed at positions where maximum potential differences occur. The electrodes are electrically isolated from the

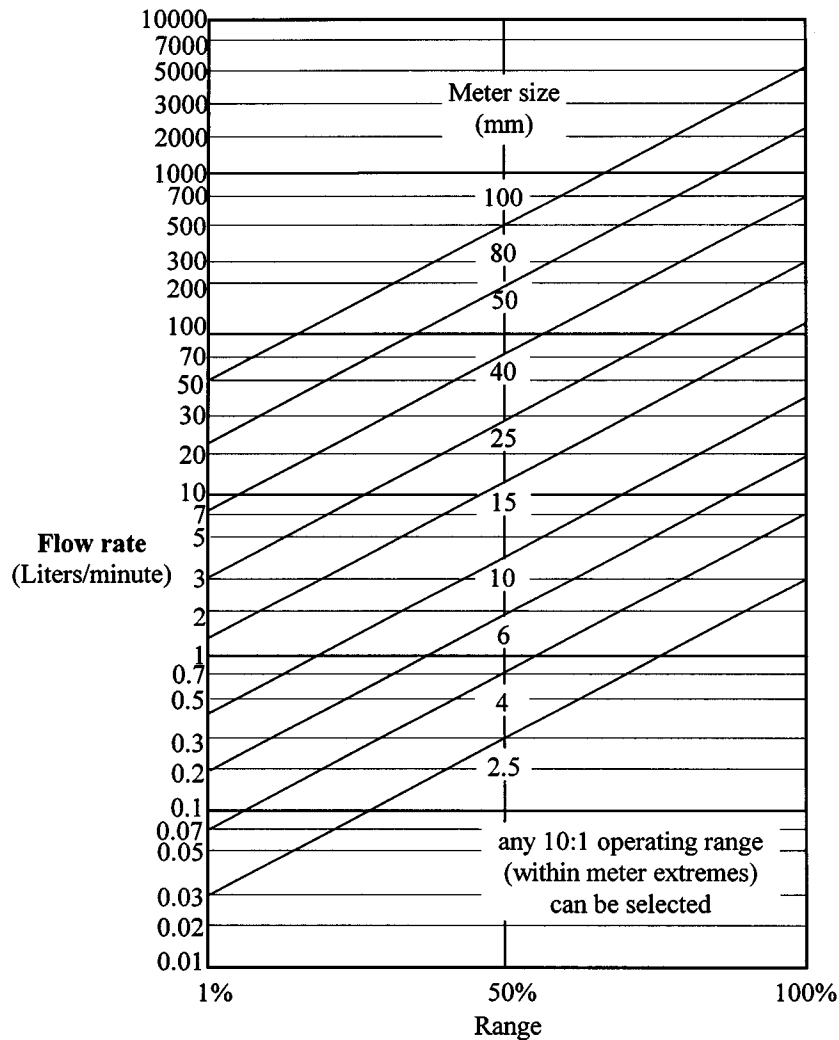


**FIGURE 28.38** Selection of flowmeters. In the selection of a suitable flowmeter for a particular application, care must be exercised in handling the anticipated liquid velocities. The velocity of liquid must be within the linear range of the device. For example, a flowmeter with 100 mm internal diameter can handle flows between 50 L min<sup>-1</sup> to 4000 L min<sup>-1</sup>. An optimum operation will be achieved at a flow rate of 500 L min<sup>-1</sup>.

pipe walls by nonconductive liners to prevent short-circuiting of electrode signals. The liner also serves as protection to the flow tube to eliminate galvanic action and possible corrosion due to metal contacts. Electrodes are held in place by holders that also act as sealing.

Dimensionally, magnetic flowmeters are manufactured from 2 mm to 1.2 m in diameter. In a particular application, the determination of the size of the flowmeter is a matter of selecting the one that can handle the anticipated liquid velocities. The anticipated velocity of the liquid must be within the linear range of the device. As an example of a typical guide for selection, the capacities of various size flowmeters are given in [Figure 28.38](#).

Some electromagnetic flowmeters are made from replaceable flow tubes whereby the field coils are located external to the tubes. In these flowmeters, the flanges are located far apart in order to reduce their adverse effects on the accuracy of measurements; hence, they are relatively larger in dimensions. Whereas in others, the field coils are located closer to the flow tube or even totally integrated together.

In this case, the flanges could be located closer to the magnets and the electrodes, thus giving relatively smaller dimensions. On the other hand, the miniature and electrodeless magnetic flowmeters are so compact in size that face-to-face dimensions are short enough to allow them to be installed between two flanges.

The wetted parts of a magnetic flowmeter include the liners, electrodes, and electrode holders. Many different materials such as rubber, teflon, polyurethane, polyethylene, etc. are used in the construction to suit process corrosivity, abrasiveness, and temperature constraints. The main body of a flowmeter and electrodes can be manufactured from stainless steel, tantalum, titanium, and various other alloys. Liners are selected mainly to withstand the abrasive and corrosive properties of the liquid. The electrodes must be selected such that they cannot be coated with insulating deposits of the process liquid during long periods of operation.

The pipe between the electromagnets of a flowmeter must be made from nonmagnetic materials to allow the field to penetrate the fluid without any distortion. Therefore, the flow tubes are usually constructed of stainless steel or plastics. The use of steel is a better option because it adds strength to the construction. Flanges are protected with appropriate liners and do not make contact with the process fluid.

In some electromagnetic flowmeters, electrodes are cleaned continuously or periodically by ultrasonic or electric means. Ultrasonics are specified for ac and dc type magnetic flowmeters when frequent severe insulating coating is expected on the electrodes that might cause the flowmeter to cease to operate in an anticipated manner.

The operation of a magnetic flowmeter is generally limited by factors such as linear characteristics, pressure ratings of flanges, and temperatures of the process fluids. The maximum temperature limit is largely dependant on the liner material selection and usually is set to around 200°C. For example, ceramic liners can withstand high temperatures, but are subject to cracking in case of sudden changes in temperatures of the process fluid.

During the selection of electromagnetic flowmeters, the velocity constraints should be evaluated carefully to secure accurate performance over the expected range. The full-scale velocity of the flowmeter is typically  $0.3 \text{ m s}^{-1}$  to  $10 \text{ m s}^{-1}$ . Some flowmeters can measure lower velocities with somewhat poorer accuracy. Generally, employment of electromagnetic flowmeters over a velocity of  $5 \text{ m s}^{-1}$  should be considered carefully because erosion of the pipe and damages to liners can be significant.

The accuracy of a conventional magnetic flowmeter is usually expressed as a function of full scale (FS), typically 0.5% to 1% FS. However, dc flowmeters have a well-defined zero due to an automatic zeroing capabilities; therefore, they have a percentage rate of accuracy better than ac types, typically 0.5% to 2%.

## **Types of Electromagnetic Flowmeters**

### **AC Magnetic Flowmeters**

In many commercial electromagnetic flowmeters, an alternating current of 50 Hz to 60 Hz in coils creates the magnetic field to excite the liquid flowing within the pipe. A voltage is induced in the liquid due to Faraday's law of induction, as explained above. A typical value of the induced emf in an ac flowmeter fixed on a 50 mm internal diameter pipe carrying  $500 \text{ L min}^{-1}$  is about 2.5 mV.

Historically, ac magnetic flowmeters were the most commonly used types because they reduced polarization effects at the electrodes. In general, they are less affected by the flow profiles of the liquid inside the pipes. They allow the use of high  $Z_{in}$  amplifiers with low drift and high pass filters to eliminate slow and spurious voltage drifts emanating mainly from thermocouple and galvanic actions. These flowmeters find many applications as diverse as the measurement of blood flow in living specimens. Miniaturized sensors allow measurements on pipes and vessels as small as 2 mm in diameter. In these applications, the excitation frequencies are higher than industrial types, 200 Hz to 1000 Hz.

A major disadvantage of the ac flowmeter is that the powerful ac field induces spurious ac signals in the measurement circuits. This necessitates periodic adjustment of zero output at zero velocity conditions — more frequently than for dc counterparts. Also, in some harsh industrial applications, currents in the magnetic field can vary, due to voltage fluctuations and frequency variations in the power

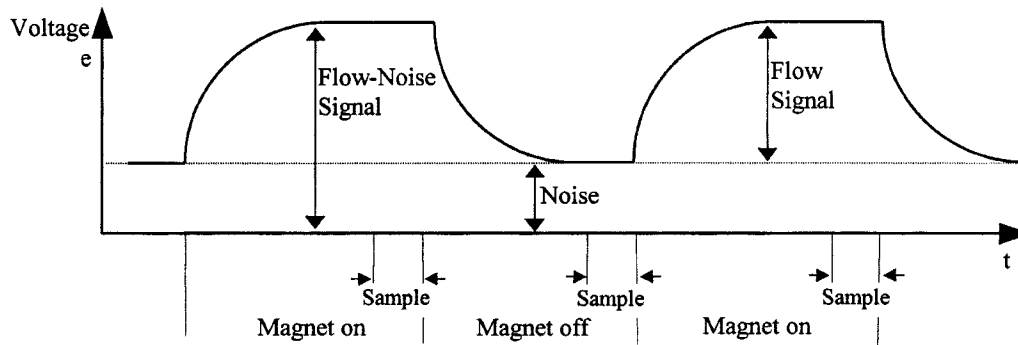


**FIGURE 28.39** The signals observed at the electrodes represent the sum of the induced voltage and the noise. When the current in the magnetic coils is turned off, the signal across the electrodes represents only the noise. Subtracting the measurement of the flowmeter when no current flows through the magnet from the measurement when current flows through the magnet effectively cancels out the effect of noise.

lines. The effect of fluctuations in the magnetic field can be minimized by the use of a reference voltage proportional to the strength of the magnetic field to compensate for these variations. To avoid the effects of noise and fluctuations, special cabling and calibration practices recommended by the manufacturers must be used to ensure accurate operation. Usually, the use of two conduits is required — one for signals and one for power. The cable lengths should also be set to certain levels to minimize noise and sensitivity problems.

Ac flowmeters operating at 50, 60, or 400 Hz are readily available. In general, ac flowmeters can operate from 10 Hz to 5000 Hz. High frequencies are preferred in determining the instantaneous behavior of transients and pulsating flows. Nevertheless, in applications where extremely good conducting fluids and liquid metals are used, the frequency must be kept low to avoid skin effects. On the other hand, if the fluid is a poor conductor, the frequency must not be so high such that dielectric relaxation is not instantaneous.

### Dc Magnetic Flowmeters

Unlike ac magnetic flowmeters, direct current or pulsed magnetic flowmeters excite the flowing liquid with a field operating at 3 Hz to 8 Hz. As the current to the magnet is turned on, a dc voltage is induced at the electrodes. The signals observed at the electrodes represent the sum of the induced voltage and the noise, as illustrated in Figure 28.39. When the current in the magnetic coils is turned off, the signal represents only the noise. Subtracting the measurement of the flowmeter when no current flows through the magnet from the measurement when current flows through the magnet effectively cancels out the effect of noise.

If the magnetic field coils are energized by normal direct current, then several problems can occur: polarization, which is the formation of a layer of gas around the measured electrodes, as well as electrochemical and electromechanical effects. Some of these problems can be overcome by energizing the field coils at higher frequencies or ac. However, higher frequencies and ac generate transformer action in the signal leads and fluid path. Therefore, the coils are excited by dc pulses at low repetition rates to eliminate the transformer action. In some flowmeters, by appropriate sampling and digital signal processing techniques, the zero errors and the noise can be rejected substantially.

The zero compensation inherent in dc magnetic flowmeters eliminates the necessity of zero adjustment. This allows the extraction of flow signals regardless of zero shifts due to spurious noise or electrode coating. Unlike ac flowmeters, a larger insulating electrode coating can be tolerated that could shift the effective conductivity significantly without affecting performance. If the effective conductivity remains high enough, a dc flowmeter will operate satisfactorily. Therefore, dc flowmeters are less susceptible to drifts, electrode coatings, and changes in process conditions in comparison to conventional ac flowmeters.

**TABLE 28.11** List of Manufacturers of Electromagnetic Flowmeters

ABB K-Flow Inc. P.O. Box 849 45 Reese Rd. Millville, NJ 08332 Tel: (800) 294-8116 Fax: (609) 825-1678	Marsh-McBirney, Inc. 4539 Metropolitan Court Frederick, MD 21704 Tel: (301) 879-5599 Fax: (301) 874-2172
Control Warehouse Shores Industrial park Ocala, FL 34472 Tel: (800) 633-0319 Fax: (352) 687-8925	Nusonics Inc. 11391 E. Tecumseh St. Tulsa, OK 74116-1606 Tel: (918) 438-1010 Fax: (918) 438-6420
Davis Instruments 4701 Mount Hope Dr. Baltimore, MD 21215 Tel: (410) 358-3900 Fax: (410) 358-0252	Rosemount Inc. Dept. MCA 15 12001 Technology Dr. Eden Prairie, MN 55344 Tel: (612) 828-3006 Fax: (612) 828-3088
Fischer Porter 50 Northwestern Dr. P.O. Box 1167T Salem, NH 03079-1137 Tel: (603) 893-9181 Fax: (603) 893-7690	Sparling Instruments Co., Inc. 4097 Temple City Blvd. P.O. Box 5988 El Monte, CA 91734-1988 Tel: (800) 423-4539
Johnson Yokogawa Dept. P, Dart Rd. Newman, GA 30265 Tel: (800) 394-9134 Fax: (770) 251-6427	Universal Flow Monitors, Inc. 1751 E. Nine Mile Rd. Hazel Park, MI 48030 Tel: (313) 542-9635 Fax: (313) 398-4274

Dc magnetic flowmeters do not have good response times due to the slow pulsed nature of operations. However, as long as there are not rapid variations in the flow patterns, zero to full-scale response times of a few seconds do not create problems in the majority of applications. Power requirements are also much less as the magnet is energized part of the time. This gives an advantage in power saving of up to 75%.

If the dc current to the magnet is constant, the proportional magnetic field can be kept steady. Therefore, the amplitudes of the dc voltages generated at the electrodes will be linearly proportional to the flow. However, in practice, the current to the magnet varies slightly due to line voltage and frequency variations. As in the case of ac flowmeters, voltage and frequency variations could necessitate the use of a reference voltage. Because the effect of noise can be eliminated more easily, the cabling requirements are not as stringent.

To avoid electrolytic polarization of the electrodes, bipolar pulsed dc flowmeters have been designed. Also, modification of dc flowmeters led to the development of miniature dc magnetic flowmeters with wafer design for a limited range of applications. The wafer design reduces the weights as well as the power requirements.

Table 28.11 provides a listing of several manufacturers of electromagnetic flowmeters.

## Installation and Practical Applications of Electromagnetic Flowmeters

Conventional ac and dc magnetic flowmeters have flanges at the inlet and the outlet that need to be bolted to the flanges of the pipe. Face-to-face dimensions of magnetic flowmeters differ between manufacturers; therefore, once the flowmeter is installed, new piping arrangements could be necessary if a flowmeter is replaced by one from a different manufacturer.

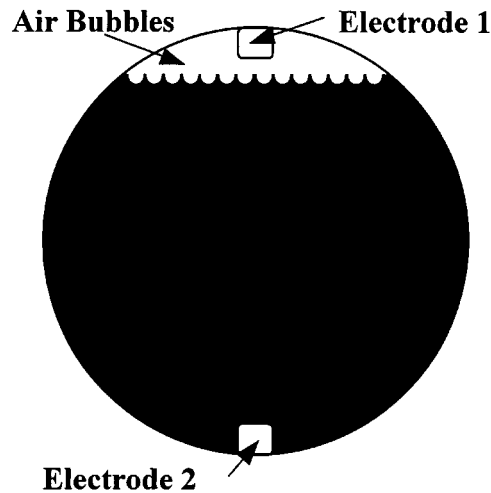


**FIGURE 28.40** The pipes of electromagnetic flowmeters must be full of liquid at all times for accurate measurement. If the liquid does not make full contact with electrodes, the high impedance prevents the current flow; hence, measurements cannot be taken. Also, if the pipe is not full, even if contact is maintained between the liquid and electrodes, the empty portions of the pipe will lead to miscalculated flow rates.

Upstream and downstream straight piping requirements can vary from one flowmeter to another, depending on the manufacturer's specifications. As a rule of thumb, the straight portion of the pipe should be at least  $5D/2D$  from the electrodes and  $5D/5D$  from the face of the flowmeter in upstream and downstream directions, respectively. For good accuracy, one should adhere carefully to the recommendations of manufacturers for piping requirements. In some magnetic flowmeters, coils are used in such a way that the magnetic field is distributed in the coil to minimize the piping effect.

For accurate measurements, magnetic flowmeters must be kept full of liquid at all times. If the liquid does not contact the electrodes, measurements cannot be taken. [Figure 28.40](#) illustrates this point. If the measurements are made in other than vertical flows, the electrodes should be located in horizontal directions to eliminate the possible adverse effect of the air bubbles, because the air bubbles tend to concentrate on the top vertical part of the liquid.

In the selection of magnetic flowmeters, a number of considerations must be taken into account, such as:

- Cost, simplicity, precision, and reproducibility
- Metallurgical aspects
- Velocity profiles and upstream disturbances

Most processes employ circular piping that adds simplicity to the construction of the system. The flowmeters connected to circular pipes give relatively better results compared to rectangular or square-shaped pipes, and velocity profiles of the liquid are not affected by the asymmetry. However, in circular pipes, the fringing of the magnetic field can be significant, making it necessary to employ empirical calibrations.

Selection of materials for constructing the channel of the magnetic flowmeter demands care. If the fluid is nonmetallic, a nonconducting or an insulated channel should be sufficient. In this case, wetted electrodes must be used. Electrodes must be designed to have sufficiently large dimensions to keep the output impedance at acceptable levels. Also, careful handling of electrode signals must be observed because, in many cases, malfunctioning of reference signal electronics is the main cause of flowmeter failure.

Magnetic flowmeters do not require continuous maintenance, except for periodic calibrations. Nevertheless, electrode coating, damage to the liners, and electronic failures can occur. Any modification or repair must be treated carefully because, when installed again, some accuracy can be lost. After each modification or repair, recalibration is usually necessary.

Often, magnetic flowmeter liners are damaged by the presence of debris and solids in the process liquid. Also, the use of incompatible liquid with the liners, wear due to abrasion, excess temperature, and installation and removals can contribute to the damage of liners. The corrosion in the electrodes can also be a contributing factor for the damage. In some cases, magnetic flowmeters can be repaired on-site even if severe damage occurs; in other cases, they must be shipped to the manufacturer for repairs. Usually, manufacturers supply spare parts for electrodes, liners, flow tubes and electronic components.

Calibration of electromagnetic flowmeters is achieved with a magnetic flowmeter calibrator or by electronic means. The magnetic flowmeter calibrators are precision instruments that inject simulated output signals of the primary flowmeter into the transmitter. Effectively, this signal is used to check correct operation of electronic components and make adjustments to the electronic circuits. Alternatively, calibrations can also be made by injecting suitable test signals to discrete electronic components. In some cases, empirical calibrations must be performed at zero flow while the flowmeter is filled with the stationary process liquid.

Application of magnetic flowmeters can only be realized with conductive liquids such as acids, bases, slurries, foods, dyes, polymers, emulsions, and suitable mixtures that have conductivities greater than the minimum conductivity requirements. Generally, magnetic flowmeters are not suitable for liquids containing organic materials and hydrocarbons. As a rule of thumb, magnetic flowmeters can be applied if the process liquids constitute a minimum of about 10% conductive liquid in the mixture.

The lack of any direct Reynolds number constraints and the obstructionless design of magnetic flowmeters make it practical for applications that involve conductive liquids that have high viscosity which could plug other flowmeters. They also measure bidirectional flows.

Despite the contrary belief, magnetic flowmeters demonstrate a certain degree of sensitivity to flow profiles. Another important aspect is the effect of turbulence. Unfortunately, there is very little information available on the behavior of turbulent flows when they are in transverse magnetic fields. [Figure 28.41](#) shows an example of a flow profile in which the velocity profile is perturbed. The fluid is being retarded near the center of the channel, and accelerated at the top and bottom near the electrodes.

An important point in electromagnetic flowmeters is the effect of magneto-hydrodynamics, especially prominent in fluids with magnetic properties. Hydrodynamics is the ability of a magnetic field to modify the flow pattern. In some applications, the velocity perturbation due to the magneto-hydrodynamic effect can be serious enough to influence the accuracy of operations, as in the case of liquid sodium and its solutions.

## Effects of Electric Conductivity of Fluid

For electromagnetic flowmeters to operate accurately, the process liquid must have minimum conductivity of  $1 \mu\text{S cm}^{-1}$  to  $5 \mu\text{S cm}^{-1}$ . Most common applications involve liquids with conductivities greater than  $5 \mu\text{S cm}^{-1}$ . Nevertheless, for accurate operation, the requirement for the minimum conductivity of liquid can be affected by length of leads from sensors to transmitter electronics.

Ac flowmeters are sensitive to the nonconductive coating of the electrodes that may result in calibration shift or complete loss of signals. The dc flowmeters, on the other hand, should not be affected by nonconductive coating to such a great extent, unless the conductivity between electrodes is less than the minimum required value. In some flowmeters, electrodes can be replaced easily; while in others, electrodes can be cleaned by suitable methods. If coating is a continual problem, ultrasonic and other cleaning methods should be considered.

Zero adjustment of ac magnetic flowmeters requires compensation for noise. If the zero adjustment is performed with any fluid other than the process fluid, serious errors can result because of possible



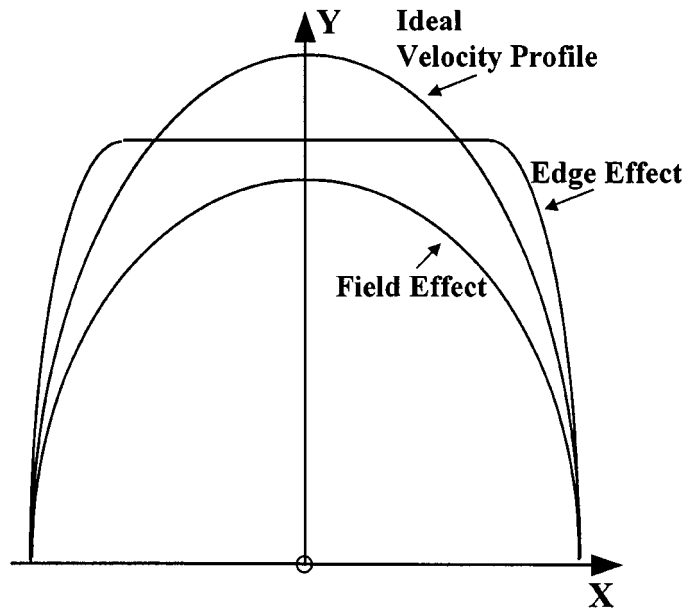


**FIGURE 28.41** Flow profiles in the pipes. Magnetic flowmeters demonstrate a certain degree of sensitivity to flow profiles. The ideal velocity profile can be distorted due to edge effects and also field effects known as magneto-hydrodynamics. In some applications, the velocity perturbation due to the magneto-hydrodynamic effect can be serious enough to severely influence the accuracy of operations.

differences in conductivities. Similarly, if the electrodes are coated with an insulating substance, the effective conductivity of the electrodes can be altered, thereby causing a calibration shift. If the coating changes in time, the flowmeter can continually require calibration for repeatable readings.

The resistance between electrodes can be approximated by  $R = 1/\delta d$ , where  $\delta$  is the fluid conductivity and  $d$  is the electrode diameter. For tap water,  $\delta = 200 \mu\text{S cm}^{-1}$ ; for gasoline,  $\delta = 0.01 \mu\text{S cm}^{-1}$ ; and for alcohol,  $\delta = 0.2 \mu\text{S cm}^{-1}$ . A typical electrode with a 0.74 cm diameter in contact with tap water results in a resistance of 6756  $\Omega$ .

### Signal Pickup and Demodulation Techniques

Magnetic flowmeters are four-wire devices that require an external power source for operations. Particularly in ac magnetic flowmeters, the high-voltage power cables and low-voltage signal cables must run separately, preferably in different conduits; whereas, in dc magnetic flowmeters, the power and signal cables can be run in one conduit. This is because in dc-type magnetic flowmeters, the voltage and the frequency of excitation of the electromagnets are relatively much lower. Some manufacturers supply special cables along with their flowmeters.

In ac flowmeters, the electrode signals can be amplified much more readily compared to their dc counterparts. That is the reason why ac flowmeters have been used successfully to measure very low flow rates, as well as the flow of very weakly conducting fluids. Nevertheless, ac flowmeters tend to be more complicated, bulky, expensive, and they require electromagnets with laminated yokes together with stabilized power supplies. In some magnetic flowmeters, it is feasible to obtain sufficiently large flow signal outputs without the use of a yoke by means of producing a magnetic field by naked coils. In this case, the transformer action to the connecting leads can be reduced considerably.

One of the main drawbacks of ac-type flowmeters is that it is difficult to eliminate the signals due to transformer action from the useful signals. The separation of the two signals is achieved by exploiting the fact that the flow-dependent signal and the transformer signal are in quadrature. That is, the useful signal is proportional to the field strength, and the transformer action is proportional to the time derivative of the field strength. The total voltage  $v_T$  can be expressed as:

$$v_T = v_F + v_t = V_F \sin(\omega t) + V_t \cos(\omega t) \quad (28.62)$$

where  $v_F$  = Induced voltage due to liquid flow  
 $v_t$  = Voltage due to transformer action on wires, etc.

Phase-sensitive demodulation techniques can be employed to eliminate the transformer action voltage. The coil magnetizing current,  $i_m = I_m \sin(\omega t)$ , is sensed and multiplied by the total voltage  $v_T$ , giving:

$$v_T i_m = [V_F \sin(\omega t) + V_t \cos(\omega t)] I_m \sin(\omega t) \quad (28.63)$$

Integration of Equation 28.63 over one period between 0 and  $2\pi$  eliminates the transformer voltage, yielding only the voltage that is proportional to the flow.

$$V_f = V_F I_m \pi \quad (28.64)$$

Where  $V_f$  is the voltage after integration. This voltage is proportional to the induced voltage modified by constants  $I_m$  and  $\pi$ .

In reality, this situation can be much more complicated because of phase shift due to eddy currents in nearby solids and conductors. Other reasons for complexity include: the harmonics because of non-linearity such as hysteresis, and capacitive pickup.

A good electrical grounding of magnetic flowmeters, as illustrated in [Figure 28.42](#), is required to isolate relatively high common mode potential. The sources of ground potential can be in the liquid or in the pipes. In practice, if the pipe is conductive and makes contact with the liquid, the flowmeter should be grounded to the pipe. If the pipe is made from nonconductive materials, the ground rings should be installed to maintain contact with the process liquid.

If the flowmeter is not grounded carefully relative to the potential of the fluid in the pipe, then the flowmeter electrodes could be exposed to excessive common mode voltages that can severely limit the accuracy. In some cases, excessive ground potential can damage the electronics because the least-resistance path to the ground for any stray voltage in the liquid would be via the electrodes.

Some commercial magnetic flowmeters have been developed that can operate on saw-tooth or square waveforms. Universally standardized magnetic flowmeters and generalized calibration procedures still do not exist, and manufacturers use their own particular design of flow channels, electromagnets, coils, and signal processors. Most manufacturers provide their own calibration data.

## Further Information

- J. P. Bentley, *Principles of Measurement Systems*, 2nd ed., New York: Longman Scientific and Technical, 1988.
- E. O. Doebelin, *Measurement Systems: Application and Design*, 4th ed., New York: McGraw-Hill, 1990.
- J. P. Holman, *Experimental Methods for Engineers*, 5th ed., New York: McGraw-Hill, 1989.
- J. A. Shercliff, *Electromagnetic Flow-Measurements*, New York: Cambridge University Press, 1987.
- D. W. Spitzer, *Industrial Flow Measurement*, Research Triangle Park, NC: Instrument Society of America, 1990.

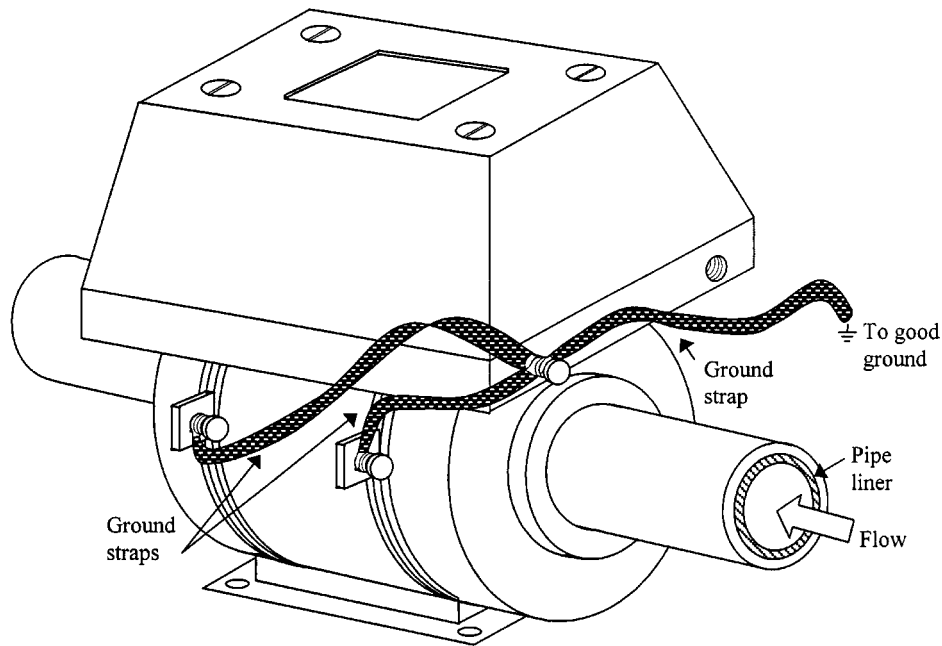


**FIGURE 28.42** Grounding of electromagnetic flowmeters. A good grounding is absolutely essential to isolate noise and high common mode potential. If the pipe is conductive and makes contact with the liquid, the flowmeter should be grounded to the pipe. If the pipe is made from nonconductive materials, ground rings should be installed to maintain contact with the process liquid. Improper grounding results in excessive common mode voltages that can severely limit the accuracy and also damage the processing electronics.

## 28.7 Ultrasonic Flowmeters

*Hans-Peter Vaterlaus, Thomas Hossle, Paolo Giordano, and Christophe Bruttin*

Flow is one of the most important physical parameters measured in industry and water management. There are various kinds of flowmeters available, depending on the requirements defined by the different market segments. For many years, differential pressure types of flowmeters have been the most widely applied flow measuring device for fluid flows in pipes and open channels that require accurate measurement at reasonable cost. In markets like waterpower, water supply, irrigation, etc., however, flow must be measured without any head losses or any pressure drop. This means no moving parts, no secondary devices, nor are any restrictions allowed. Two types of flowmeters presently fulfill this requirement: Electromagnetic and ultrasonic flowmeters. Whereas *ultrasonic flowmeters* can be applied in nearly any kind of flowing liquid, *electromagnetic* flowmeters require a minimum electric conductivity of the liquid for operation. In addition, the cost of ultrasonic flowmeters is nearly independent of pipe diameter, whereas the price of electromagnetic flowmeters increases drastically with pipe diameter.

There are various types of ultrasonic flowmeters in use for discharge measurement: (1) *Transit time*: This is today's state-of-the-art technology and most widely used type, and will be discussed in this chapter section. This type of ultrasonic flowmeter makes use of the difference in the time for a sonic pulse to travel a fixed distance, first against the flow and then in the direction of flow. Transit time flowmeters are sensitive to suspended solids or air bubbles in the fluid. (2) *Doppler*: This type is more popular and less expensive, but is not considered as accurate as the transit time flowmeter. It makes use of the Doppler

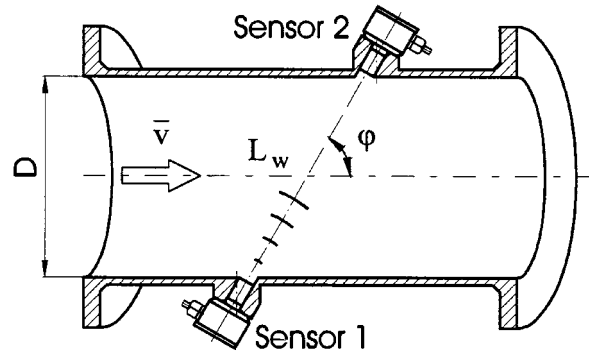


**FIGURE 28.43** Principle of transit time flowmeters. Transmitting an ultrasonic pulse upstream and downstream across the flow: the liquid is moving with velocity  $\bar{v}_a$  and with angle  $\phi$  to the ultrasonic pulse.

frequency shift caused by sound reflected or scattered from suspensions in the flow path and is therefore more complementary than competitive to transit time flowmeters. (3) *Cross-correlation*: Two measuring sections are installed with a certain distance to each other. Both measure the energy absorption of the ultrasonic signal. A cross-correlation calculates the flow velocity. (4) *Phase shift*: The phase position of the transmitting and receiving signal is measured in the direction of the flow and against it. The resulting phase shift angle is directly proportional to the flow velocity. (5) *Drift*: The drift of an ultrasonic signal crossing the flow is measured by signal attenuation.

## Transit Time Flowmeter

### Principle of Operation

The acoustic method of discharge measurement is based on the fact that the propagation velocity of an acoustic wave and the flow velocity are summed vectorially. This type of flowmeter measures the difference in transit times between two ultrasonic pulses transmitted upstream  $t_{21}$  and downstream  $t_{12}$  across the flow, as shown in [Figure 28.43](#). If there are no transverse flow components in the conduit, these two transmit times of acoustic pulses are given by:

$$t_{12} = \frac{L_w}{c + v_a \cos \phi} \quad \text{and} \quad t_{21} = \frac{L_w}{c - v_a \cos \phi} \quad (28.65)$$

where  $L_w$  = Distance in the fluid between the two transducers

$c$  = Speed of sound at the operating conditions

$\phi$  = Angle between the axis of the conduit and the acoustic path

$\bar{v}_a$  = Axial flow velocity averaged along the distance  $L_w$

Since the transducers are generally used both as transmitters and receivers, the difference in travel time can be determined with the same pair of transducers. Thus, the mean axial velocity  $\bar{v}_a$  along the path is given by:

$$\bar{v}_a = \frac{L_w}{2 \cos \phi} \left( \frac{1}{t_{21}} - \frac{1}{t_{12}} \right) = \frac{D}{2 \cos \phi \sin \phi} \left( \frac{1}{t_{21}} - \frac{1}{t_{12}} \right) \quad (28.66)$$

The following example shows the demands on the time measurement technique: assuming a closed conduit with diameter  $D = 150$  mm, angle  $\phi = 60^\circ$ , flow velocity  $\bar{v}_a = 1$  m·s<sup>-1</sup>, and water temperature = 20°C. This results in transmit times of about 116 s and a time difference  $\Delta t$  ( $\Delta t = t_{12} - t_{21}$ ) on the order

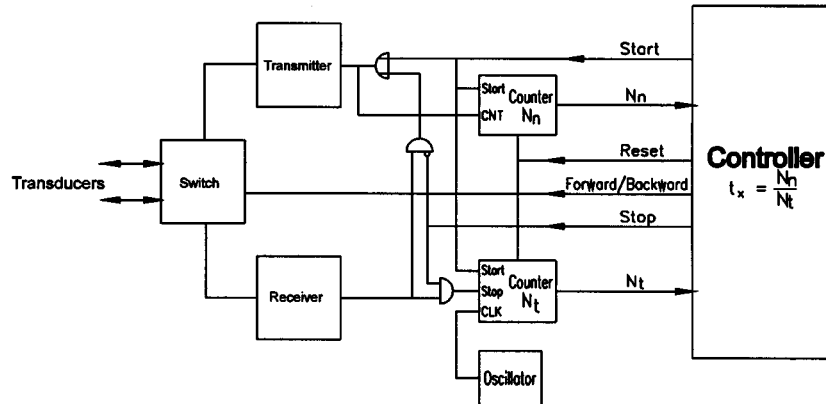


**FIGURE 28.44** Block diagram of a transit time ultrasonic flowmeter using oversampling for higher resolution.

of 78 ns. To achieve an accuracy of 1% of the corresponding full-scale range,  $\Delta t$  has to be measured with a resolution of at least 100 ps ( $1 \times 10^{-10}$  s).

Standard time measurement techniques are not able to meet such requirements so that special techniques must be applied. The advantage of the approach of state-of-the-art real digital measurement is to process the measured value directly by a microcomputer. The most difficult problem is to reach the required resolution and to cope with the jitter of digital logic gates. It is well known in the measurement technique that, if signals are sampled multiple times ( $N_n$ ), the resolution increases with the number of samples (“oversampling”) [1]. This knowledge is not only applied for analog signals but also for transit time signals and is used in today’s technology of flowmeters. The propagation time  $t$  ( $t_{12}$   $t_{21}$ ), depending on the distance the sound pulse has to travel through the fluid, is measured several times. Due to this fact, one obtains the following relation [2]:

$$t = \frac{1}{N_n} \int_0^{\tau} \frac{1}{f} dt \quad (28.67)$$

where  $\tau$  is integration time, and  $f$  is the frequency.

According to the block diagram in Figure 28.44, two counters are used. One counter  $N_t$  is clocked during the measuring period by a stable quartz oscillator; the other one counts the number of samples  $N_n$ . The measurement stops after a certain period of some milliseconds and after having reached an integer value for  $N_n$ . The two counts of  $N_t$  and  $N_n$  are used to calculate propagation time  $t_{12}$  or  $t_{21}$  by dividing  $N_t$  by  $N_n$ . The resolution  $r$  is calculated by:

$$r = \frac{1}{N_n \cdot f} \quad (28.68)$$

Advantages of this measurement method for transit time flowmeters are:

1. The resolution of the velocity measurement is constant (typical value  $0.8 \text{ mm s}^{-1}$ ).
2. The accuracy depends almost only on the stability and the temperature coefficient of the quartz oscillator.
3. Due to the multiple sampling, the jitter of the digital logic is averaged.

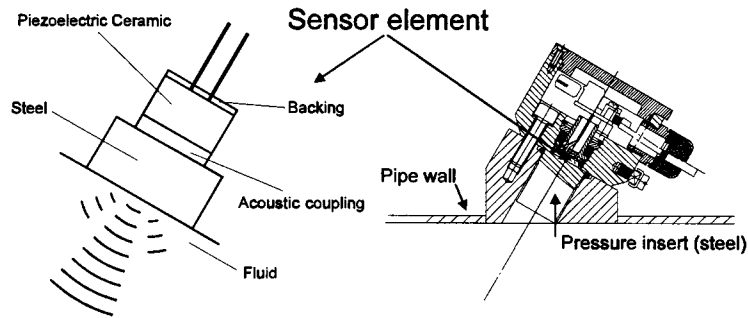


FIGURE 28.45 Ultrasonic transducer in principle and as an example of an existing version. The sensor element can be changed even under pressure.

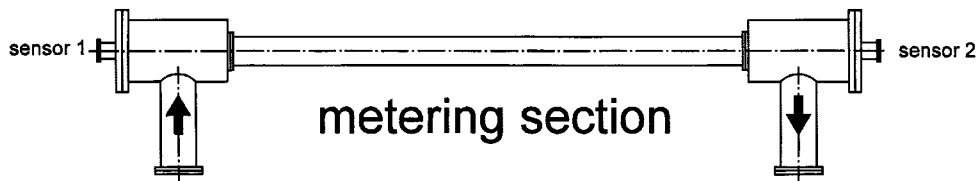


FIGURE 28.46 Axial sensor type. The ultrasonic pulse passes directly down the axis of the pipe.

#### Sensors.

The transducer comprises the piezoelectric element that converts electric to acoustic energy and the basic structure for supporting the piezoceramic and providing electric connections. Transducer design entails choice of the piezoelectric element, determination of suitable dimensions and resonant frequency, and construction to withstand thermal and mechanical stress, see Figure 28.45. Considering the transmission line model [3, 4], the optimal electroacoustic response and the best matching of acoustic impedances  $Z = \rho c$  of the different transducer elements is important. Not only must suitable waveforms to be detected by the electronics be obtained, but also the energy loss must be minimized when crossing several interface boundaries. Because of the wide versatility of pipe sizes and flow conditions, there are a number of different sensor configurations for transit time flowmeters.

#### Axial.

Due to the small differences in small diameter pipes, it is necessary to pass the sonic pulse directly down the axis of the pipe to ensure that there is sufficient path length. Figure 28.46 shows an example of an axial sensor pipe section. The upper pipe size limit for this kind of sensor is about 0.075 m [5].

#### Radial.

Many manufacturers supply complete metering sections with built-in sonic transducers on either side of a spool section. Such sensors, shown in Figure 28.47, are generally called “radial” because of the transducer placement. A lower pipe size limit of radial type sensors is about 100 mm.

#### Field Mounting.

Radial-type sensors are often used to instrument an existing line, where it is desirable to make the installation without cutting out a section of the pipe. To meet this requirement, field-mountable transducers, cemented, drilled, or welded into an existing pipe section, can be used. Metering sections with diameters up to 13 m or more can be achieved in this way.

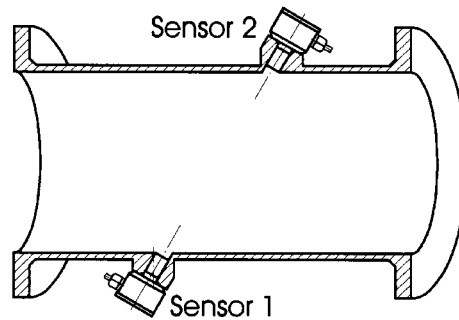


**FIGURE 28.47** Radial sensor type. Manufacturers provide them as complete metering sections or as field-mounting sensors for existing conduits.

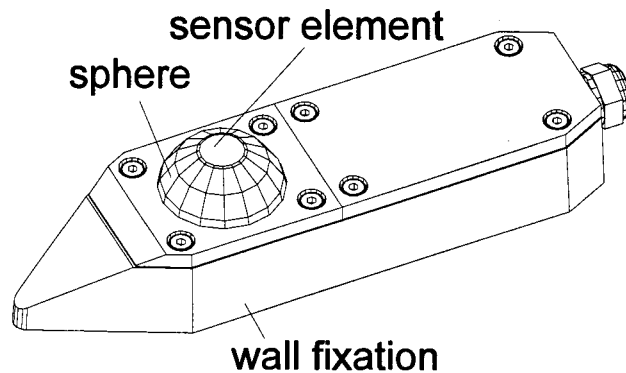


**FIGURE 28.48** Open-channel sensor with sensor element placed on a movable sphere. Alignment of two sensors can be executed by laser equipment.

#### Clamp-on.

If there is a need for an installation where the pipe wall is not penetrated by the transducers, clamp-on systems are the right choice. Achieving a lower accuracy and being somewhat more complex to calibrate, clamp-on systems have their entitlement in applications where an easy movement of the metering section is an important requirement or where an existing process cannot be interrupted. The transducers are mounted on a calibration device and acoustically coupled to the pipe wall with grease and/or epoxy.

#### Open Channels and Special Applications.

In open channels, the transducers are normally mounted on or dug into the channel walls. [Figure 28.48](#) shows an example of an open-channel sensor. The piezoceramic element is placed on a sphere to achieve a wide range of mounting possibilities. Sometimes, existing pipe sections are completely enclosed with rock or concrete. In these cases, the transducers can be fixed in the wall of the conduit. For small diameters, the resulting protrusion of the transducers into the metering section must be taken into account.

#### Measurement of Flow in Closed Conduits.

The most important issue in applying ultrasonic flowmeters is an understanding of the effects of the velocity profile of the flowing fluid within the conduit. The flow profile depends on the fluid, the Reynolds number  $Re$ , the relative roughness and shape of the conduit, upstream and downstream disturbances, and other factors. Transit time flowmeters give an average flow velocity  $v$  along the sonic path. The acoustic flow rate  $Q_{ADM}$  is therefore calculated through  $Q = \bar{v}A$ , with  $\bar{v}$  the area-averaged flow velocity and  $A$  the cross-section of the conduit. In order to obtain the area-averaged flow velocity  $\bar{v}$ , the measured velocity  $\bar{v}_a$  must be corrected by a hydraulic coefficient  $k_h$  that depends on the type of the conduit and

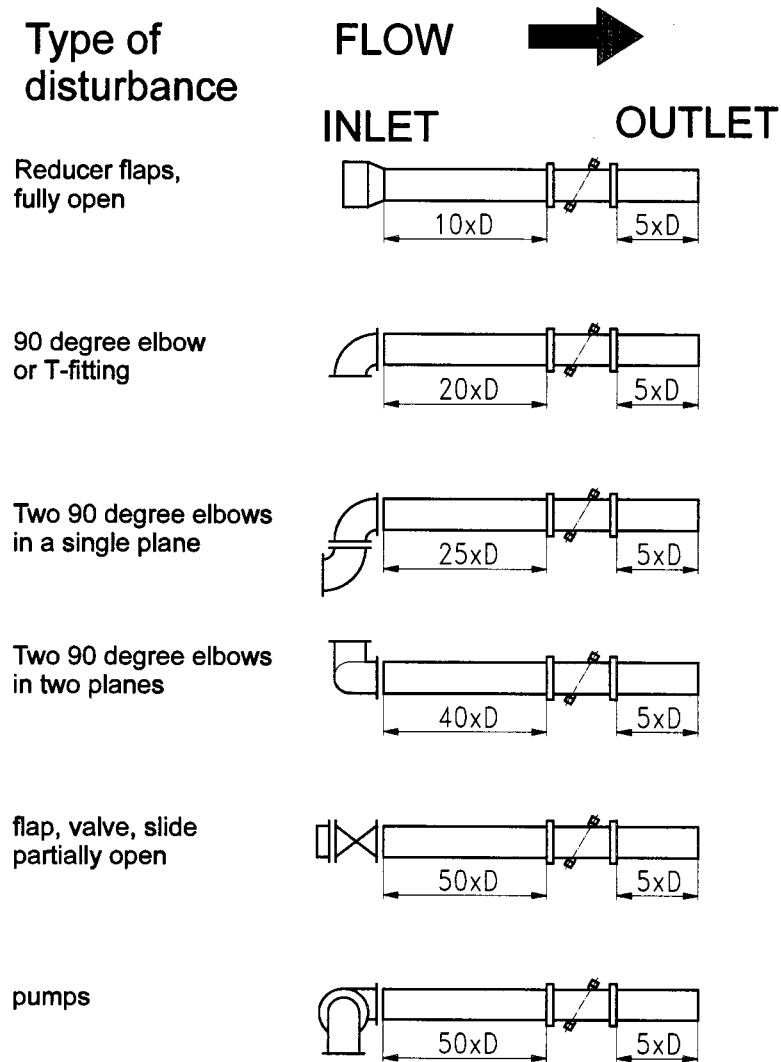


FIGURE 28.49 Minimum straight run requirements for a 1% accuracy of a single-path transit time flowmeter.

the Reynolds number. In order to achieve maximum performance and accuracy of ultrasonic flowmeters, one has to keep to sufficient straight run requirements as shown for some examples in Figure 28.49. By doing so, a typical accuracy of 1% of reading or better can be achieved, even when applying a single-path measurement system. Reduced straight runs lead to reduced accuracy. In some applications, this reduced accuracy is acceptable; if not, a multipath ultrasonic flowmeter must be installed. These flowmeters provide averaging of the various error-producing flow components. Accuracy of 0.5% of reading can be achieved even under nonideal conditions or insufficient straight runs. Figure 28.50 shows four examples of possible sonic path arrangements in a closed conduit.

Single Path with Circular and Rectangular Cross-sections.  
The Reynolds number  $Re$  is given by:

$$Re = \frac{\bar{v} \cdot D}{\nu} \quad (28.69)$$



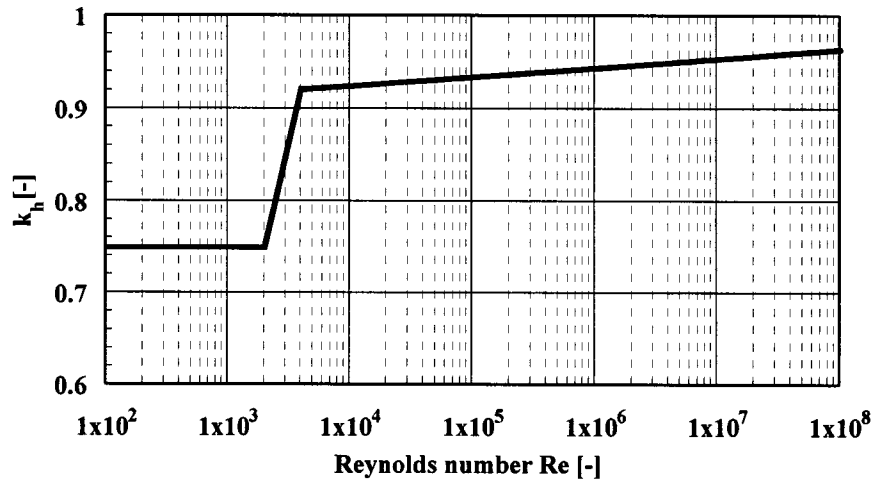


FIGURE 28.50 Dependence of the  $k_h$  factor for single-path measurement on the Reynolds number. Between a Reynolds number of 2000 and 4000, the transitional flow regime occurs.

where  $\bar{v}$  = Mean velocity over the cross section [m·s<sup>-1</sup>]

$D$  = Pipe diameter

$\nu$  = Temperature-dependent cinematic viscosity

In normal piping, a laminar flow exists as long as the Reynolds number is below about 2600. The shape of the velocity profile conforms to a parabola, and the velocity of a point on the profile is given by:

$$v(r) = v_{\max} \left( 1 - \left( \frac{r}{R} \right)^2 \right) \quad (28.70)$$

where  $r$  = Variable radius

$R$  = Pipe radius

Between a Reynolds number  $Re$  of 2600 and 4000, the transitional flow regime with continuous switching between laminar and turbulent velocity profile comes into existence. When the Reynolds number exceeds 4000, the velocity profile enters the turbulent flow regime. Nikuradse [6] showed that the turbulent velocity profile of an axis-symmetrical flow in a closed conduit without swirl and sufficient inlet and outlet sections and smooth walls can be expressed by:

$$v(r) = v_{\max} \left( \frac{R-r}{R} \right)^{\frac{1}{n}} \quad (28.71)$$

where, according to Nikuradse,  $n$  is a Reynolds number-dependent exponent given by:

$$n = \frac{1}{\left( 0.2525 - 0.0229 \times \log(Re) \right)} \quad (28.72)$$

With the definition of a hydraulic corrective coefficient  $k_h$  given by:

$$k_h = \frac{\bar{v}}{v_a} \quad (28.73)$$

where  $\bar{v}$  = Mean velocity over the cross-section  
 $v_a$  = Mean velocity along the sonic path

and integrating over the cross-section according to:

$$k_h = \frac{\frac{1}{A} \int_0^R \int_0^{2\pi} v(r) r dr d\theta}{\frac{1}{2R} \int_{-R}^R v(r) dr} \quad (28.74)$$

one obtains for laminar flow a hydraulic corrective coefficient of  $k_h = 0.75$ .

In the turbulent flow regime, according to Nikuradse [6], the hydraulic corrective coefficient  $k_h$ , dependent on the Reynolds number  $Re$ , can be expressed by:

$$k_h = \frac{1}{1.125 - 0.011 \times \log(Re)} \quad (28.75)$$

for a circular cross-section, and

$$k_h = 0.79 + 0.02 \times \log(Re) \quad (28.76)$$

for a rectangular cross-section.

In hydropower applications, the Reynolds number  $Re$  generally exceeds the value of 4000. Figure 28.50 shows the dependence of the  $k_h$  factor in closed conduits with circular cross-section on the Reynolds number. The Reynolds number not only changes its value as a function of the flow velocity  $v$  for a given diameter  $D$ , but is also strongly dependent on the temperature-dependent cinematic viscosity  $\nu(T)$ . Not taking into account for correct value of  $Re$  can easily lead to errors of the  $k_h$  factor and thus to the flow-rate  $Q$  on the order of 2% to 3%. Modern transit time meters with microprocessors update the  $k_h$  factor at a rate of 4 times a second and by measuring the temperature  $T$  of the fluid at the same rate. A correct  $k_h$  factor is obtained and hence a temperature and Reynolds number-compensated flow rate  $Q$ .

Multipath Integration in Circular Cross-sections.

In reality, however, the straight run requirements as defined in Figure 28.49 cannot always be kept. In addition, cross flow errors occur when nonaxial components of velocity in a pipe alter the transit times of a pulse between the sensors. Nonaxial velocities are caused by such disturbances in closed conduits as bends, asymmetric intake flows, and discontinuities in the pipe wall or pumps. It has become accepted practice to eliminate the sensitivity of an acoustic flowmeter to velocity distributions by increasing the number of acoustic paths  $n$ . Additional paths not only decrease substantially the velocity distribution error, but also reduce the numerical integration error as well as errors due to path misalignment. This suggests that for accurate measurements for which a few tenths of a percent error are significant, the cost of installing more sensors for a four-path arrangement according to Figure 28.51 can be justified. In a

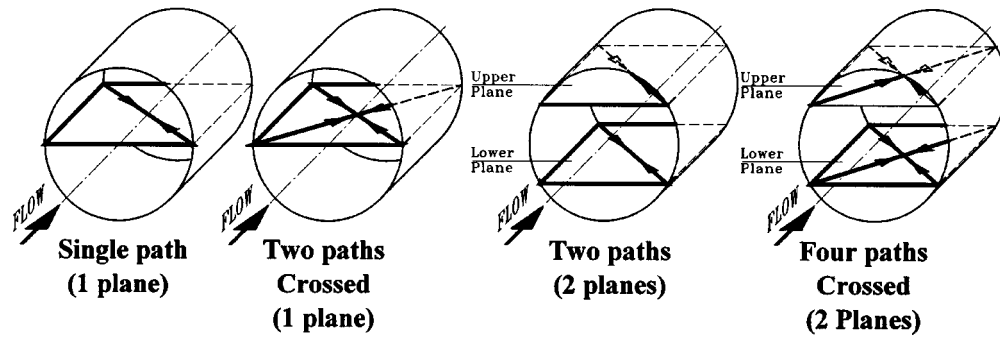


FIGURE 28.51 Possible sonic path arrangements for transit time flowmeters in closed conduits. Using multiple paths leads to reduced straight run requirements.

multipath measurement system, according to the integration method described by IEC 41, Appendix J1 [7], the flowrate  $Q_{ADM}$  can be expressed by:

$$Q_{ADM} = k \frac{D}{2} \sum_{i=1}^n \bar{v}_{ai} W_i L_{wi} \sin \varphi_i \quad (28.77)$$

where  $\bar{v}_{ai}$  = Velocities along the acoustic path  $i$   
 $W_i$  = Corresponding weighting factor  
 $L_{wi}$  = Corresponding path length  
 $\varphi_i$  = Corresponding path angle

The method described in IEC 41 needs a very accurate transducer positioning due to the fact that the weighting factors  $W_i$  obtained by mathematical analysis are only valid when the sensors are positioned at the correct locations. Misalignment of the acoustic paths in conjunction with fixed weights can lead to considerable errors.

### Measurement of Flow in Open Channels

Open-channel flow measurement is used in many applications, including water supply networks, hydrography, allocation of water for irrigation and agricultural purposes, sewage treatment plants, etc. Discharge measurements in rivers and open channels are often computed by means of a rating curve, used to convert records of water level readings into flow rates. The rating curve is developed using a set of discharge measurements and water level in the stream, and must be checked periodically to ensure that the level-discharge relationship has remained constant; many phenomena can cause the rating curve to change so that the same recorded water level produces a different discharge. This is the case of open channels under changeable hydraulic conditions due, for example, to backwater effects, gates, and where an univocal stage-discharge relationship does not exist. In this context, acoustic flowmeter application is extremely interesting and is currently experiencing wide success in water management. In fact, while different flow rate values can correspond to a given water level in relation to the hydraulic characteristics, there is always an univocal relationship between the acoustic wave propagation velocity in a flowing fluid and the flowing fluid itself.

By means of the ultrasonic technique, discharge through open channels can be determined using single- and multipath technology. In a single-path configuration, particular attention must be paid to define the vertical velocity distribution (Figure 28.52) in order to achieve a good level of accuracy by a single “line” velocity reading  $\bar{v}_{az}$  at the distance  $z$  above the bottom. On the other hand, in a multipath configuration, the mean line velocity profile is well described. In this case, special attention must be paid to the integration method used to determine the flow rate from the acoustic path readings.

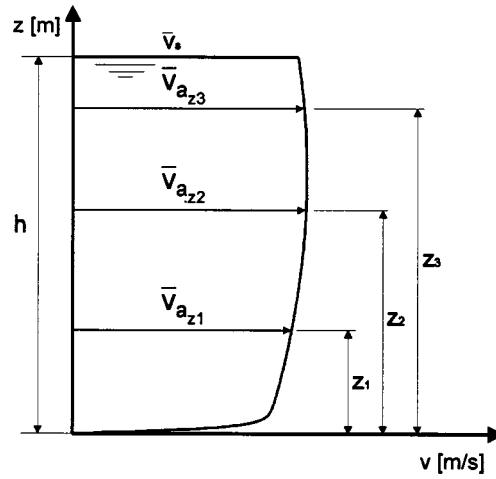


FIGURE 28.52 Open channel: possible vertical velocity distribution.

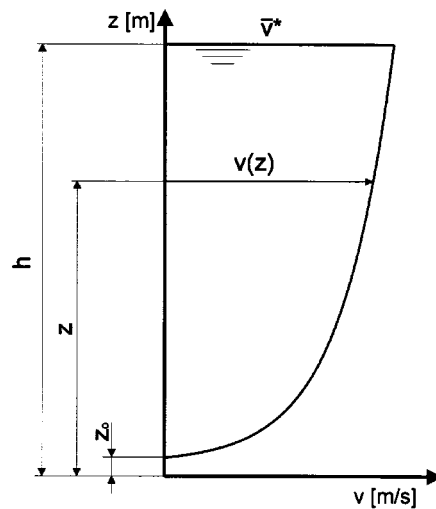


FIGURE 28.53 Logarithmic law describing open-channel velocity profile.

#### Single Path.

In single-path measurements, using the area-velocity method, the flow rate  $Q$  is calculated through  $Q = \bar{v}A$  with  $\bar{v}$  ( $\text{m s}^{-1}$ ) the area-averaged flow velocity and  $A$  the cross-section. To obtain the velocity average  $\bar{v}$  over the entire cross-section, the mean path velocity  $\bar{v}_{az}$ , measured by the acoustic flowmeter at a given depth  $z$ , must be corrected by a dimensionless hydraulic corrective coefficient  $k_h$  according to the relation  $\bar{v} = k_h \bar{v}_{az}$ . In general, the coefficient  $k_h$  reflects the influence of the horizontal and vertical velocity profile. It mainly depends on the water level, on the cross-section shape, and on the boundary roughness. The mean vertical velocity profile can be described by the well-known logarithmic law (Figure 28.53) given by [8].

$$\bar{v}(z) = \left( \frac{\bar{v}^*}{k} \right) \ln \frac{z}{z_0} \quad (28.78)$$

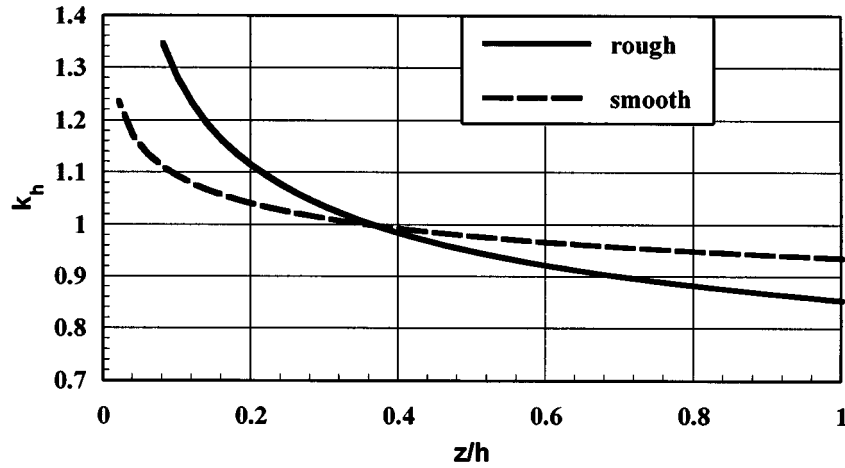


FIGURE 28.54 Logarithmic  $k_h$  factor in open channels for two different roughnesses  $k_s$ .

where  $\bar{v}(z)$  = Mean flow velocity at a distance  $z$  above the bottom

$k$  = Von Kàrmàn's turbulence constant

$z$  = Distance above the bottom

$\bar{v}^*$  = Shear velocity

$z_0$  = Constant of integration, dependent on the boundary roughness

When the boundary surface is hydraulically rough,  $z_0$  has been found to depend solely on the roughness height  $k_s$  according to the relation  $z_0 = k_s/30$ . Integrating Equation 28.78 over the total water height  $h$  and substituting for  $\bar{v}$ , the following equation is obtained:

$$k_h = \frac{\ln\left(\frac{h}{k_s}\right) - 1}{\ln\frac{z}{k_s}} \quad (28.79)$$

assuming  $z_0$  negligible with respect to  $h$ .

In Figure 28.54, the logarithmic  $k_h$  factor is represented for two different bottom roughness. However, in many practical applications, it is often difficult to define correct values for  $k_s$ . For this reason, another  $k_h$  model has been developed on the basis of the power law [9, 10]. In this formula, the exponent  $1/m$  is not constant anymore, but depends on the roughness and the hydraulic radius to take into account the influence of the channel shape. The mean vertical velocity profile  $\bar{v}(z)$ , according to the power law, can be expressed by the following formula (Figure 28.55):

$$\bar{v}(z) = \bar{v}_s \left(\frac{z}{h}\right)^{\frac{1}{m}} \quad (28.80)$$

where  $h$  = Current water level

$\bar{v}$  = Mean line velocity at the free surface (maximum value)

$1/m$  = Exponent

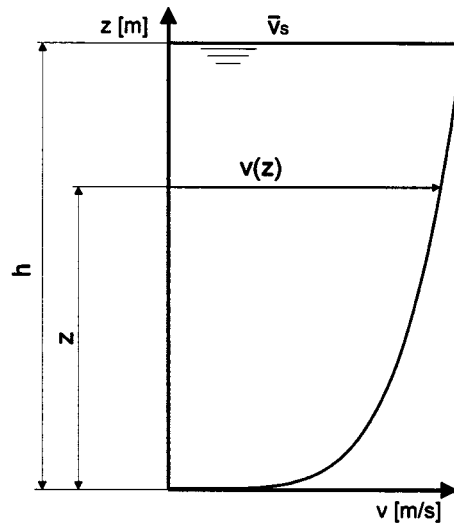


FIGURE 28.55 Power law describing open-channel velocity profile.

From the integration of Equation 28.80 over the total water depth, one obtains the following expression for the  $k_h$  factor:

$$k_h = \frac{m}{m+1} \left( \frac{h}{z} \right)^{\frac{1}{m}} \quad (28.81)$$

The value of  $m$ , depending on the roughness, can be expressed using the a dimensional friction factor  $f$  of the Darcy–Weisbach formula [8], according to:

$$m = k \sqrt{\frac{8}{f}} \quad (28.82)$$

where  $k$  = Von Kàrmàn constant, varying from 0.2 to 0.4

$k$  depends on the suspended load (low values for high turbidity), or can be expressed using the Manning formula by the relation [11]:

$$m = \left( \frac{k}{\sqrt{g}} \right) \frac{R_h^{\frac{1}{6}}}{n} \quad (28.83)$$

where  $g$  = Gravity acceleration  
 $n$  = Manning's roughness coefficient  
 $R_h$  = Hydraulic radius

In Figure 28.56, the corrective factor is represented for smooth and rough surfaces. By means of this relation, an easier field application has been obtained due to wide familiarity with the Manning formula in open-channel flow computation because of its simplicity of form, high versatility, and satisfactory results.

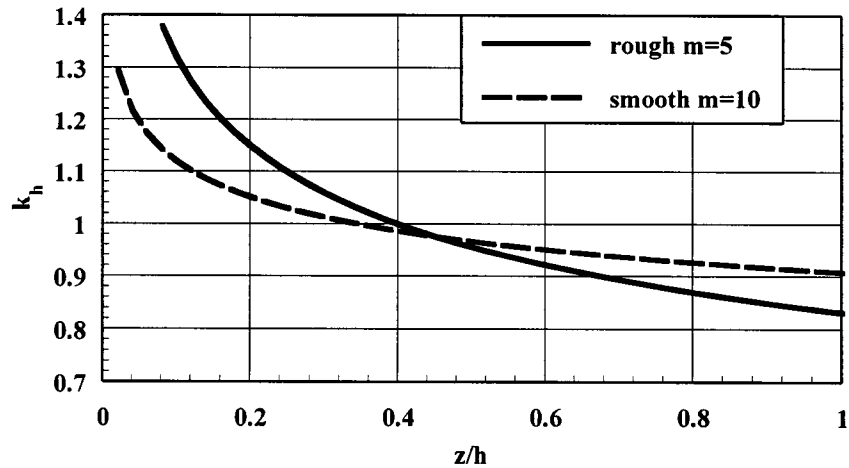


FIGURE 28.56 Power law  $k_h$  factor in open channels for two different roughnesses.

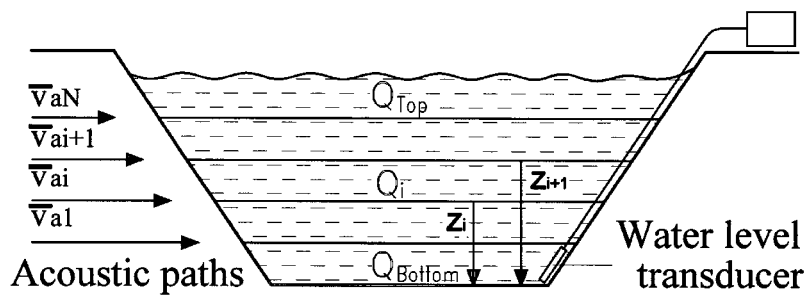


FIGURE 28.57 Multipath measurement in open channels by the mean section method. The flow velocity is measured by several levels.

#### Multipath.

The foregoing equations for the mean vertical velocity profile in open channels predict that the maximum mean velocity occurs at the free surface. Field and laboratory measurements, however, demonstrate that the maximum mean velocity occurs below the free surface, strongly depending on the ratio  $B/h$ , with  $B$  being the channel width. These observations show that a one-dimensional velocity distribution law cannot always completely describe flow profiles in open channels. Therefore, to reduce uncertainties in velocity profile description and to achieve high accuracies even under unfavorable hydraulic conditions, a multipath configuration must be used.

In multipath measurement, using the “mean section method,” the flow velocity is measured at several levels between the free surface and the channel bottom (Figure 28.57). The total discharge  $Q_{ADM}$  is performed by the relation [12]:

$$Q_{ADM} = Q_b + Q_t + \sum_{i=1}^n \left( \frac{\bar{v}_{ai} + \bar{v}_{ai+1}}{2} \left[ A(z_{i+1}) - A(z_i) \right] \right) \quad (28.84)$$

where  $Q_b$  = Flow rate in the bottom section with the bottom velocity obtained from the lowest path velocity by correction for bottom friction

$Q_t$  = Flow rate at the highest active section with velocity  $v_{top}$ , interpolated from the velocity profile

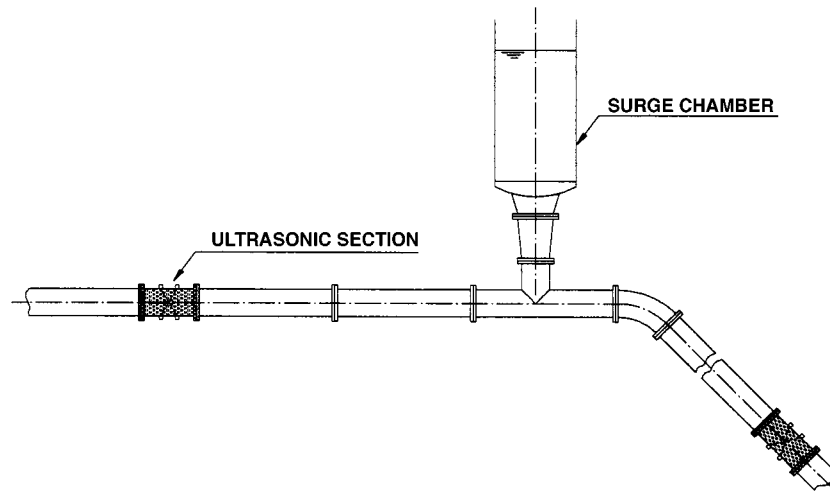


**FIGURE 28.58** Penstock leak detection by transit time flowmeter. The penstock contains a surge chamber that causes mass oscillation in case of load changes of the turbine.

$\bar{v}_{ai}$  = Mean velocity along the  $i$ th acoustic path  
 $A(z_i)$  = Cross-section below the  $i$ th path

Modern microprocessor-controlled ultrasonic flowmeters can cope with either single-path or multi-path measurement in open channels, using the logarithmic or the power law for single-path measurement. In addition, up-to-date completely modular systems are able to use the major part of the equipment for measuring both in open channels and closed conduits.

#### **Application: Penstock Leak Detection with Surge Chambers**

Penstock leak detection is a typical acoustic flowmeter application [13]. It is used for immediate recognition of pipe rupture and leak losses in penstocks. Two flowmeters are installed at opposite ends of the penstock: one for measuring  $Q_{up}$  as near as possible to the intake, the other for measuring  $Q_{down}$  at the powerhouse entrance. In this description, the upstream flow is compared to the downstream flow and the flow difference.  $\Delta Q = Q_{up} - Q_{down}$  is calculated and supervised. If the difference  $\Delta Q$  exceeds a given threshold, the system enunciates alarms or valve closure contacts.

In hydropower applications another problem arises due to the presence of surge chambers (Figure 28.58). This hydraulic structure causes mass oscillations due to load changes of the turbine. Up to now, if there was a surge tank in a penstock, one had two possibilities. On the one hand, one could divide the penstock into two parts: one before the surge chamber, one after it, and protect them separately. This solution is expensive and very often impractical because the surge chamber is built into the rock and inaccessible. On the other hand, one could develop something like a “leak detection algorithm,” which includes the oscillatory behavior of a penstock. Such a system, however, needs extensive field tests and the knowledge for exact settings of resonant frequency, damping factor, and thresholds. The latest technology in ultrasonic flowmeters, combined with accurate water level sensors, can offer a solution to this problem. By applying the formula:

$$\Delta Q = Q_{up} - Q_{down} - \frac{\Delta V_{chamber}}{\Delta t} \quad (28.85)$$

changes of the volume of the surge chamber due to mass oscillations are taken into account, leading to a better and more realistic behavior of penstock leak detection in the presence of surge tanks.



**TABLE 28.12** Companies Manufacturing and Distributing Ultrasonic Transit Time Flowmeters

Rittmeyer AG P.O. Box 2143 CH-6302 Zug Switzerland Tel: (+4141)-767-1000 Fax: (+4141)-767-1075 instrumentation@rittmeyer.ch http://www.rittmeyer.com/	Accusonic Division, ORE International, Inc. P.O. Box 709 Falmouth, MA 02541 Tel: (508) 548-5800 http://www.ore.com/
Krohne Messtechnik GmbH&Co.KG Postfach 10 08 62 Ludwig-Krohne-Strasse 5 4100 Duisburg 1 Germany http://www.krohne.com/	Fuji Electric Co., Ltd. 12-1 Yurakucho 1-chome Chiyoda-ku Tokyo 100, Japan Tel: Tokyo 211-7111
Danfoss A/S DK-6430 Nordborg Denmark Tel: (+45) 74 88 22 22	Crouzet SA Division "Aérospatial" 25, rue Jules-Védrines 26027 Valence Cedex, France Tel: 75 79 85 11
Panametrics, Inc. 221 Crescent Street Waltham, MA 02254 Tel: (617) 899-2719 http://www.panametrics.com/	Nusonics Inc. 11391 E. Tecumseh St. Tulsa, OK 74116-1602 Tel: (918) 438-1010
	Ultraflux le technoparc 17, rue Charles Edouard Jeanneret 78306 Poissy Cedex, France Tel: 33(1)39 79 26 40

### Instrumentation and Manufacturers/Distributors

Table 28.12 gives an overview of some companies manufacturing and distributing transit time flowmeters. Prices of transit time flowmeters have a very wide range due to the wide versatility of different applications and are therefore difficult to list accurately. Generally, ultrasonic flowmeters are seldom sold as a "pre-packed" instrument. For this reason, the price for a metering section, including installation, varies from a few \$1000 to nearly \$100,000.

### References

1. M. Barmettler and P. Gruber, Anwendung von Oversampling-Verfahren zur Erhöhung der Auflösung digital erfasster Signale, *Technisches Messen*, Oldenbourg Verlag, 1992.
2. D. Hoppe, Kombinierte Zählung und Abstandsbestimmung von Impulssignalen, *Technisches Messen*, Oldenbourg Verlag, 10, 1991.
3. R. Krimholtz, D. Leedom, and G. Matthaei, New equivalent circuits for elementary piezoelectric transducers, *Electronics Lett.*, 6, 398, 1970.
4. P. D. Edmonds, *Methods of Experimental Physics, Ultrasonics*, New York: Academic Press, 1981.
5. D. W. Spitzer, *Flow Measurement, Practical Guides for Measurement and Control*, Research Triangle Park, NC: Instrument Society of America, 1991.
6. J. Nikuradse, Gesetzmässigkeiten der turbulenten Strömung in glatten Röhren, *VDI Verlag GmbH*, 1932.
7. F. L. Brand, Akustische Verfahren zur Durchflussmessung, *Messen, Prüfen Automatisieren*, April 1987.
8. *International Standard IEC 41*, 3rd ed., 1991.
9. R. H. French, *Open Channel Hydraulics*, New York: McGraw-Hill, 1985, 30.

10. Chen-Iung Chen, *J. Hydraulic Eng.*, 379, 117, 1990.
11. M. F. Karim and J. F. Kennedy, *J. Hydraulic Eng.*, 162, 113, 1987.
12. G. Grego, M. Baldin, et al., *Application of an Acoustic Flowmeter for Discharge Measurement in the Po*.
13. G. Grego and M. Baldin, *Energia Elettrica*, 1, 52, 72, 1995.
14. H. P. Vaterlaus and H. Gabler, A new intelligent ultrasonic flowmeter for hydropower applications, *Int. Water Power & Dam Construction*, 1994.

## 28.8 Vortex Shedding Flowmeters

---

*Wade M. Mattar and James H. Vignos*

The *vortex shedding flowmeter* first emerged 25 to 30 years ago and has steadily grown in acceptance since then to be a major flow measurement technique. Its appeal is due, in part, to the fact that it has no moving parts yet produces a frequency output that varies linearly with flow rate over a wide range of Reynolds numbers. The vortex meter has a very simple construction, provides accuracy (1% or better) comparable to higher priced and/or more maintenance-intensive techniques, and works equally well on liquids and gases. In addition, it is powered primarily by the fluid and lends itself more readily than other linear flow devices to two-wire operation. Comparing the vortex shedding flowmeter to an orifice plate, the former has higher accuracy and rangeability, does not require complex pressure impulse lines, is less sensitive to wear and, for volumetric flow measurement, does not require the need to compensate for fluid density.

Industrial vortex shedding flowmeters are normally available in pipe sizes ranging from 15 mm to 300 mm (1/2 in. to 12 in.), with some manufacturers offering sizes up to 400 mm (16 in.). Flow ranges covered depend on fluid properties and meter design. Typical ranges for a 15 mm meter are:

- Water at 21°C (70°F); 0.06 to 2.2 L s<sup>-1</sup> (1 to 35 gallons per minute)
- Air at 16°C (60°F) and 101 kPa (14.7 psia); 1.1 to 15.7 L s<sup>-1</sup> (140 to 2000 cubic feet per hour)
- Dry saturated steam at 689 kPa (100 psig); 4.5 to 225 kg h<sup>-1</sup> (10 to 500 pounds per hour)

Typical ranges for a 300 mm (12 in.) meter are:

- Water at 21°C (70°F); 5.4 to 5400 L s<sup>-1</sup> (85 to 8500 gallons per minute)
- Air at 16°C (60°F) and 101 kPa (14.7 psia); 157 to 12500 L s<sup>-1</sup> (20,000 to 1,600,000 cubic feet per hour)
- Dry saturated steam at 689 kPa (100 psig); 1240 to 124000 kg h<sup>-1</sup> (2750 to 275,000 pounds per hour)

Temperature capability ranges from cryogenic temperatures up to 427°C (800°F). Pressure capability as high as 20.7 MPa (3000 psig) is available.

### Principle of Operation

Probably the first time, ages ago, that anyone placed a blunt obstacle in a flowing fluid, he or she observed the whirlpools or vortices that naturally form and shed downstream. In everyday life, examples of vortex shedding are numerous. The undulation of a flag is due to vortex shedding from the pole, and the singing of telephone wires in a strong wind is due to shedding from the wires. Analysis by Theodore von Karman in 1911 described the stability criterion for the array of shed vortices. Consequently, when a stable array of vortices form downstream from an obstacle, it is often referred to as the von Karman vortex street (Figure 28.59).

Very early on, it was noted that, for a large class of obstacles, as the velocity increased, the number of vortices shed in a given time (or frequency of vortex shedding) increased in direct proportion to the velocity. The dimensionless Strouhal number, *St*, is used to describe the relationship between vortex shedding frequency and fluid velocity and is given by:

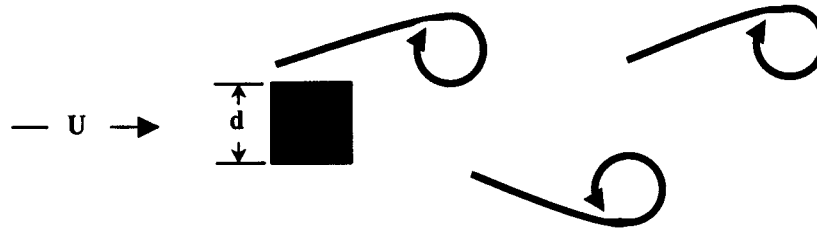


FIGURE 28.59 Von Karman vortex street.

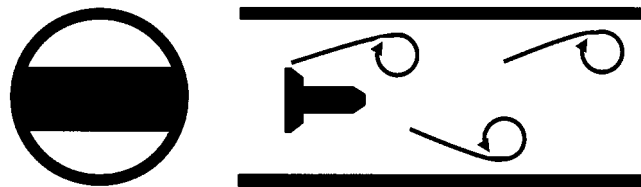


FIGURE 28.60 Vortex shedding in a pipe.

$$St = \frac{f \times d}{U} \quad (28.86)$$

where  $f$  = Vortex shedding frequency  
 $d$  = Width of shedding body  
 $U$  = Fluid velocity

Alternatively,

$$U = \frac{f \times d}{St} \quad (28.87)$$

Although early studies were conducted in unconfined flow, it was later observed that vortex shedding also occurred in confined flow, such as exists in a pipe (see Figure 28.60). For this case, the average fluid velocity,  $\bar{U}$ , and the meter Strouhal number,  $St'$ , replace the fluid velocity and Strouhal number, respectively, in Equation 28.87 to give:

$$\bar{U} = \frac{f \times d}{St'} \quad (28.88)$$

Since the cross-sectional area,  $A$ , of the pipe is fixed, it is possible to define a flowmeter  $K$  factor,  $K$ , that relates the volumetric flow rate ( $Q$ ) to the vortex shedding frequency. Given that:

$$Q = A \times \bar{U} \quad (28.89)$$

From Equation 28.88, one obtains:

$$Q = \left( \frac{A \times d}{St'} \right) \times f \quad (28.90)$$

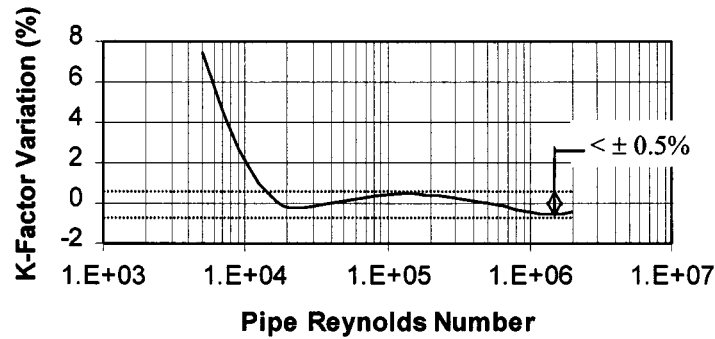


FIGURE 28.61 Typical  $K$  factor curve.

Defining:

$$K = \frac{St'}{(A \times d)} \quad (28.91)$$

results in:

$$Q = \frac{f}{K} \quad (28.92)$$

Vortex shedding frequencies range from less than 1 Hz to greater than 3000 Hz, the former being for large meters at low velocities and the latter for small meters at high velocities.

For a vortex shedding flowmeter, an obstacle is chosen that will produce a constant  $K$  factor over a wide range of pipe Reynolds numbers. Thus, simply counting the vortices that are shed in a given amount of time and dividing by the  $K$  factor will give a measurement of the total volume of fluid that has passed through the meter. A typical  $K$  factor vs. Reynolds number curve is shown in Figure 28.61.

The variation in  $K$  factor over a specified Reynolds number range is sometimes referred to as *linearity*. For the example in Figure 28.61, it can be seen that between Reynolds numbers from 15,000 to 2,000,000, the  $K$  factor is the most linear. This is referred to as the *linear range* of the shedder. The wider the linear range a shedder exhibits, the more suitable the device is as a flowmeter.

At Reynolds numbers below the linear range, linearization is possible but flowmeter uncertainty can increase.

## Calculation of Mass Flow and Standard Volume

Although the vortex flowmeter is a volumetric flowmeter, it is often combined with additional measurements to calculate or infer mass flow or standard volume.

To determine mass flow,  $\dot{M}$ :

$$\dot{M} = \rho_f \times Q = \rho_f \times \frac{f}{K} \quad (28.93)$$

where  $\rho_f$  = Fluid density at flowing conditions.

It is often desirable to know what the volumetric flow rate would be at standard process conditions with respect to pressure and temperature. This is referred to as *standard volume*. In different parts of the world and for different industries, the standard temperature and pressure can be different. The fluid density at standard conditions is referred to as the *base density*,  $\rho_b$ .

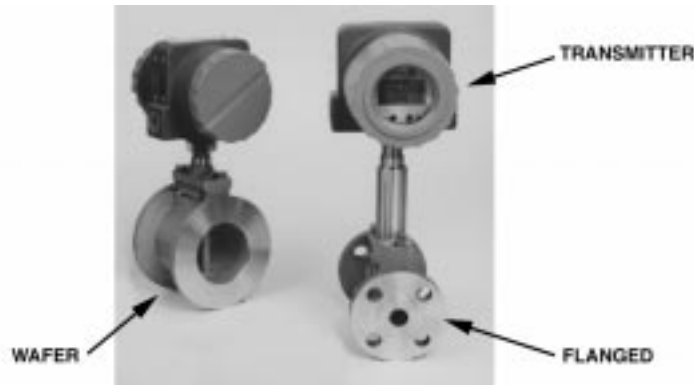


FIGURE 28.62 Vortex flowmeter construction.



FIGURE 28.63 Shedder cross-sections.

To calculate *standard volume*,  $Q_v$ :

$$Q_v = \left( \frac{\rho_f}{\rho_b} \right) \times \frac{f}{K} \quad (28.94)$$

## Flowmeter Construction

The vortex shedding flowmeter can be described as having two major components: the *flow tube* and the *transmitter*. Both are described below.

### Flow Tube

The flow tube is composed of three functional parts: the flowmeter *body*, which contains the fluid and acts as a housing for the hydraulic components; the *shedder*, which generates the vortices when the fluid passes by; and the *sensor(s)*, which by some transducing means detects the vortices and produces a usable electric signal.

#### Flowmeter Body.

The pressure-containing portion of the vortex flowmeter, sometimes referred to as the *flowmeter body*, is available in two forms: wafer or flanged (see [Figure 28.62](#)). The wafer design, which is sandwiched between flanges of adjacent pipe, is generally lower in cost than the flanged design, but often its use is limited by piping codes.

#### Shedder.

The *shedder* spans the flowmeter body along the diameter and has a constant cross-section along its length. Typical cross-sections are shown in [Figure 28.63](#).

#### Sensors.

When shedding is present, both the pressure and velocity fields in the vicinity of the shedder will oscillate at the vortex shedding frequency. *Pressure or velocity sensors* are used to transform the oscillating fields to an electric signal, current or voltage, from which the vortex shedding frequency can be extracted.

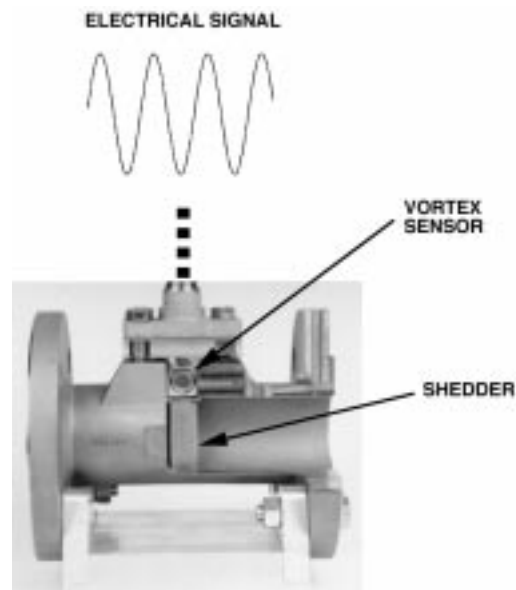


FIGURE 28.64 Example of vortex sensor.

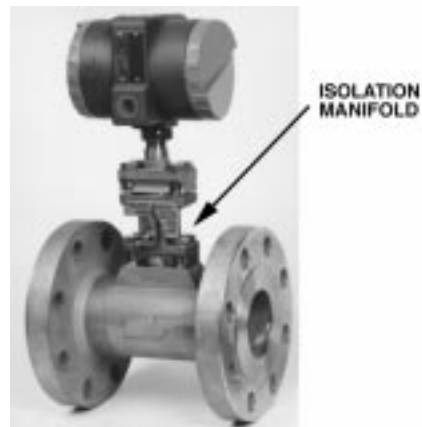


FIGURE 28.65 Isolation manifold for sensor replacement.

Figure 28.64 shows an example of a piezoelectric differential pressure sensor located in the upper portion of the shedder, which converts the oscillating differential pressure that exists between the two sides of the shedder into an electric signal. Some other sensing means utilized to detect vortex shedding are capacitive, thermal, and ultrasonic. Often times the flowmeter electronics are mounted remotely from the flow tube. This might require a local preamplifier to power the sensor or boost its signal strength.

Since the sensor is the most likely mechanical component in a vortex flowmeter to fail, most designs have a provision for replacement of the sensors. In some cases, they can be replaced without removing the flowmeter from the pipeline. An example of an isolation manifold for sensor replacement under process conditions is shown in Figure 28.65.

### Transmitter

Vortex flowmeter *transmitters* can be classified into two broad groups: analog and intelligent (or smart). Communication with the analog transmitter is carried out via local manual means, including switches

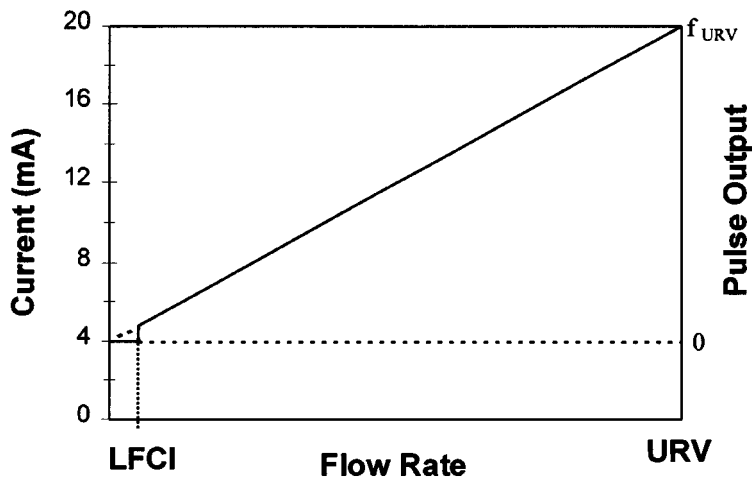


FIGURE 28.66 4 mA to 20 mA and pulse outputs.

and jumper wires. Communication with the newer intelligent device is carried out via digital electronic techniques. Both types of transmitters are two-wire devices. One of the more important features of the intelligent transmitter is that it allows application-specific information to be loaded into the transmitter. This information is then used internally to automatically tailor the transmitter to the application, including calibration of the 4 mA to 20 mA output. Before describing these devices, it is useful to consider the three most common forms of flow measurement signals provided by vortex transmitters.

#### Measurement Output Signals.

The three most common ways for a transmitter to communicate measurement information to the outside world are 4 mA to 20 mA, digital, and pulse signals.

The *4 mA to 20 mA signal* is the dc current flowing in the power leads to the transmitter. This current is directly proportional to the vortex shedding frequency and, hence, is also linear with flow (see Figure 28.66). 4 mA corresponds to zero flow and 20 mA to the maximum flow rate, i.e., the upper range value (URV) of the meter. A frequency-to-analog converter in the analog meter and a digital-to-analog converter in the intelligent meter produce this output.

The *digital signal* is a digitized numeric value of the measured flow rate in engineering units transmitted over the two wires powering the meter.

The *pulse signal* is a squared-up version of the raw vortex signal coming from the sensor (see Figure 28.67), and is accessible via a pair of electric terminals inside the transmitter housing. The frequency of the pulse signal is either identical to the vortex shedding frequency (raw pulse) or some multiple thereof (scaled pulse). As discussed in the Principle of Operation section, in either case, the frequency of the pulse signal is linearly proportional to flow rate, going from zero to the frequency at the URV,  $f_{URV}$  (see Figure 28.66).

As shown in Figure 28.66, at a low but nonzero flow rate, the frequency and mA signals drop to 0 Hz and 4 mA, respectively. The flow rate at which this abrupt change takes place is normally referred to as the low flow cut-in, LFCI, or cut-off. The reason for this forced zero is to avoid erroneous flow measurements at low flow, which result from process noise, including hydrodynamic fluctuations, mechanical vibration, and electrical interference. The digital signal also drops to zero below the LFCI flow rate.

#### Analog Transmitter.

Originally, *analog transmitters* were constructed entirely of analog electronic components. Today, they are built around a combination of analog and digital electronic components. In either case, the measurement output is in the form of a raw pulse and/or a 4 mA to 20 mA signal. Depending on the particular

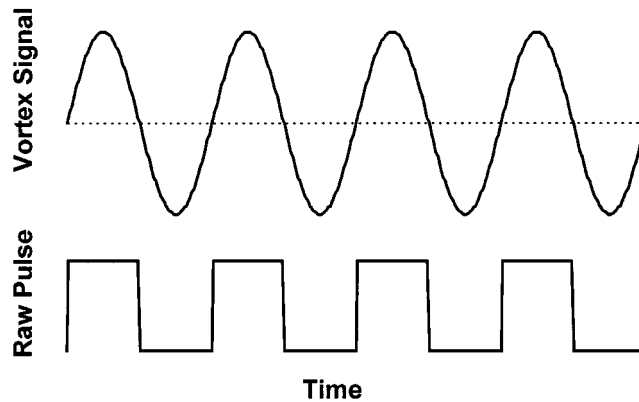


FIGURE 28.67 Raw pulse output.

transmitter, one or more of the following functions are available for tailoring the device via mechanical means to the specific application.

1. Signal output selection: If the transmitter provides both raw pulse and 4 mA to 20 mA signals, but not simultaneously, a means is available for selecting the one desired.
2. 4 mA to 20 mA calibration: Use of this signal requires that 20 mA correspond to the desired URV. This is accomplished by inputting, via a signal or pulse generator, a periodic signal whose frequency corresponds to the upper range frequency (URF), and adjusting the output current until it reads 20 mA. The URF, which is the frequency corresponding to the vortex shedding frequency at the desired URV, is calculated using the equation  $URF = K \times URV$ .

In order to achieve the accuracy specified by the manufacturer, the  $K$  used in the above calculation must be corrected for process temperature and piping effects according to the manufacturer's instructions. The temperature effect is a result of thermal expansion of the flow tube, and is described by:

$$\Delta K(\%) = -300 \times \alpha \times (T - T_0) \quad (28.95)$$

where  $\alpha$  is the thermal expansion coefficient of the flow tube material, and  $T_0$  is the fluid temperature at which the meter was calibrated. If the shedder and meter body materials are different,  $\alpha$  must be replaced by  $(2\alpha_1 + \alpha_2)/3$ , where  $\alpha_1$  is the thermal expansion coefficient of the meter body material and  $\alpha_2$  that of the shedder.

Piping disturbances also affect the  $K$  factor because they alter the flow profile within the flow tube. This will be discussed in more detail in the section entitled "Adjacent Piping."

3. LFCI: For optimum measurement performance, the low flow cut-in should be set to fit the specific application. The goal is to set it as low as possible, while at the same time avoiding an erroneous flow measurement output.
4. Filter settings: To reduce noise present on the signal from the sensor, electronic filters are built into the transmitter. Normally, means are provided for adjusting these filters, that is, setting the frequencies at which they become active. By attenuating frequencies outside the range of the vortex shedding frequency, which varies from one application to another, better measurement performance is achieved.

Intelligent Transmitters.

*Intelligent transmitters*, which are microprocessor-based digital electronic devices, have measurement outputs that usually include two or more of the following: raw pulse, scaled pulse, 4 mA to 20 mA and



digital. With regard to the digital output, there is at present no single, universally accepted protocol for digital communication; however, a number of proprietary and nonproprietary protocols exist.

The presence of a microprocessor in the intelligent transmitter allows for improved functionality and features compared to the analog transmitter, including:

- Elimination of the need for 4 mA to 20 mA calibration
- Automatic setting of low flow cut-in
- Automatic setting of filters
- Adaptive filtering (active filters that track the vortex frequency)
- Digital signal conditioning
- $K$  factor correction for temperature and piping disturbances
- Correction for nonlinearity of  $K$  factor curve, including the pronounced nonlinearity at low Reynolds numbers (see [Figure 28.61](#))
- Integral flow totalization
- Digital measurement output in desired engineering units

Configuring — that is, tailoring the transmitter to a specific application — is carried out by one or more of the following digital communicators:

- Local configurator: a configurator, built into a transmitter, that has a display and keypad
- Hand-held terminal: a palm-size digital device programmed for configuration purposes
- PC configurator: a personal computer containing configuration software
- System configurator: a digital measurement and control system with imbedded configuration software

Using one of these configurators, the dataset of parameters that defines the configuration can be modified to fit the application in question. The details of this dataset vary, depending on the specific transmitter; however, the general categories of information listed below apply.

- Flowtube parameters (e.g., tube bore,  $K$  factor, serial no.)
- User identification parameters (e.g., tag no., location)
- Transmitter options (e.g., measurement units, function selections)
- Process fluid parameters (e.g., fluid density and viscosity, process temperature)
- Application parameters (e.g.,  $K$  factor corrections, URV, LFCI level)
- Output options (e.g., measurement output modes, damping, fail-safe state)

## Application Considerations

### Meter Selection

From a safety viewpoint, it is essential that the vortex flowmeter satisfy the appropriate electrical safety requirements and be compatible with the process, that is, be able to withstand the temperature, pressure, and chemical nature of the process fluid. From a mechanical viewpoint, it must have the proper end connections and, if required for critical applications, have a sensor that can be replaced without shutting down the process. Meter size and measurement output signal type are also very important selection factors.

Size.

Contrary to what one might expect, the required *meter size* is not always the same as the nominal size of the piping in which it is to be installed. In some applications, selecting the size based on adjacent piping will not allow the low end of the required flow range to be measured. The appropriate criteria for selecting meter size is that the meter provides a reliable and accurate measurement over the entire required flow range. This could dictate a meter size that is less than the adjacent piping.

Pressure drop is a competing sizing criteria to that described above. This drop is given by:

$$\Delta P = C \times \rho_f \times Q^2 / D^4 \quad (28.96)$$

where  $C$  is a constant dependent on meter design, and  $D$  is the bore diameter of the flow tube. The tendency is to pick a flow tube with the same nominal diameter as the adjacent piping to eliminate the extra pressure drop introduced by a smaller-sized meter. However, in the majority of cases, this added drop is of little consequence.

The meter manufacturer can provide the needed information for making the proper selection. In some cases, sizing programs from manufacturers are available on the Internet in either an interactive or downloadable form.

#### Measurement Output Options.

As mentioned previously, three types of *measurement outputs* are in current use: a 4 mA to 20 mA analog signal, a pulse train, and a digital signal. Some vortex meters will provide all three of these outputs, but not always simultaneously. It is essential that the meter has the output(s) required by the application.

### Meter Installation

The performance specifications of a vortex flowmeter are normally established under the following conditions: (1) the flow tube is installed in a pipeline running full with a single-phase fluid; (2) the piping adjacent to the flow tube consists of straight sections of specified schedule pipe (normally Schedule 40), typically a minimum of 30 PD (pipe diameters) in length upstream and 5 PD downstream of the flow tube with no flow-disturbing elements located within these sections; and (3) the meter is located in a vibration free and electrical interference free environment. As a consequence, certain constraints are placed on where and how the meter is installed in process piping if published performance specifications are to be achieved. These constraints are discussed below. Because meters from different suppliers differ in their sensitivity to the above influences, the statements made are of a qualitative nature. The specific manufacturer should be consulted for more quantitative information.

#### Location.

The flowmeter should be located in a place where vibration and electrical interference levels are low. Both of these influences can decrease the signal-to-noise ratio at the input to the transmitter. This reduction can degrade the ability of the meter to measure low flows.

The meter should not be installed in a vertical line in which the fluid is flowing down because there is a good possibility that the pipe will not be full.

#### Adjacent Piping.

Recommended practice is to mount the flowmeter in the process piping according to the manufacturer's stated upstream and downstream minimum straight-length piping requirements. These are typically 15 to 30 PD and 5 PD, respectively. Piping elements such as elbows or reducers upstream of the meter normally affect its  $K$  factor, but not its linearity. This allows a bias correction to be applied to the  $K$  factor. Many manufacturers provide bias factors for common upstream piping arrangements. Some who offer intelligent flowmeters make the corrections internally once the user has selected the appropriate configuration from a picklist. For piping elements and arrangements where the bias correction is not available, an *in situ* calibration should be run if the manufacturer's specified uncertainty is to be achieved. If this is not possible, calibration in a test facility with an identical configuration should be run.

The same situation as above applies if the pipe schedule adjacent to the meter differs from that under which the meter was calibrated.

To avoid disturbance to the flow, flange gaskets should never protrude into the process fluid.

The following recommendations apply if a control valve is to be situated near a vortex flowmeter. In liquid applications, the control valve should be located a minimum of 5 PD downstream of the flowmeter. This not only prevents disturbance to the flow profile in the flow tube, but also aids in preventing flashing and cavitation (see below). In gas applications, the control valve should be installed upstream of the meter, typically a minimum of 30 PD upstream of the meter to ensure an undisturbed flow profile. Having the pressure drop across the valve upstream of the meter results in a decreased density and subsequent increased velocity at the flowmeter. This helps in achieving good measurements at low flows.

For condensable gases, such as steam, it also helps to reduce the amount of condensate that might otherwise be present at the flowmeter.

#### Orientation.

In general, meter orientation is not an issue for vortex flowmeters, particularly for vertical pipe installations. However, for meters having electronics at the flow tube, it is recommended in high-temperature horizontal pipe applications that the flow tube be oriented with the electronics beneath the meter. Although vortex flowmeters are not recommended for multiphase applications, they do operate with somewhat degraded performance with dirty fluids (i.e., small amounts of gas bubbles in liquid, solid particles in liquid, or liquid droplets in gas). The degree of degradation in horizontal pipe applications depends to some extent on the specific meter design. Orienting the flow tube according to manufacturer's recommendations for the dirty fluid in question can help to alleviate this problem.

#### Pressure and Temperature Taps.

The placement of pressure and temperature taps for determining gas densities, if required, is also an important consideration. Recommendations for location of these taps vary, depending on the manufacturer. The temperature probe is inserted typically 6 PD downstream of the flow tube. This prevents any flow disturbance in the meter, and at the same time gets the probe as close to the meter as possible. The pressure tap is made typically 4 PD downstream of the meter. Although a pressure tap does not significantly affect the flow, its placement is critical for achieving an accurate density measurement.

#### Process Conditions.

Flashing and cavitation can occur in a liquid application just downstream of the shedder if the pressure drop across the meter results in the downstream pressure being below the vapor pressure of the liquid. These phenomena lead to undefined measurement errors and possibly to structural damage, and hence should be avoided. This is usually accomplished by increasing the inlet pressure or inserting a back-pressure valve downstream of the meter. To avoid flashing and cavitation, the downstream pressure after recovery (approximately 5 PD downstream) must be equal to or greater than  $P_{\text{dmin}}$ , where:

$$P_{\text{dmin}} = c_1 \times \Delta P + c_2 \times P_{\text{vap}} \quad (28.97)$$

where  $P_{\text{dmin}}$  = Minimum absolute downstream pressure after recovery

$P_{\text{vap}}$  = Vapor pressure of the liquid at the flowing temperature

$\Delta P$  = Overall pressure drop

$c_1, c_2$  = Empirical constants for a specific meter (normally available from the meter manufacturer)

Pulsating flow can also, in some circumstances, lead to measurement errors. It is best to avoid placing the meter in process lines where noticeable pulsation exists.

### Meter Configuration

It is important when installing an analog or intelligent vortex flowmeter that it be configured for the specific application (see section above on Flowmeter construction). This is often done by the supplier prior to shipping if the user supplies the relevant information at the time the order is placed. If this is not the case, the user must carry out the configuration procedures provided by the manufacturer.

### Recent Developments

Recent efforts have been made to make the vortex flowmeter into a real-time mass flow measurement device. As was demonstrated in the "Principle of Operation" section, the output of the meter, based on the frequency of vortex shedding, is related to actual volumetric flow (see Equation 28.92). In intelligent transmitters, the flowing density (the density at flowing conditions) and the base density can be entered into the transmitter's database. Based on these values, mass flow or standard volumetric flow can be computed (see Equations 28.93 and 28.94). This procedure is valid if the flowing density does not vary

in time. If this is not the case, an on-line, real-time measure of the density must be provided. Two different approaches have been used. One (multisensor) employs sensors in addition to the vortex sensor; the other (single sensor) relies on additional information being extracted from the vortex shedding signal.

### Multisensor

In this method, temperature and pressure measurements are made in addition to the vortex frequency. This approach is similar to that used in orifice-d/p mass flowmetering, in which case temperature and pressure ports are located in the pipe normally downstream of the orifice plate. However, for the multisensor vortex, the temperature and pressure sensors are incorporated into the flowmeter rather than located in the adjacent piping. Using these two additional measurements, the flowing density is calculated from the equation of state for the process fluid.

### Single Sensor

This approach takes advantage of the fact that, in principle, for a force- or pressure-based vortex shedding sensor, the amplitude of the vortex shedding signal is directly proportional to the density times the square of the fluid velocity; that is:

$$\text{Signal amplitude} \propto \rho_f \times U^2 \quad (28.98)$$

The fluid velocity can be determined from the vortex frequency; that is:

$$\text{Frequency} \propto U \quad (28.99)$$

Hence,

$$\frac{\text{Signal amplitude}}{\text{Frequency}} \propto \rho_f \times U \propto \text{Mass flow} \quad (28.100)$$

This approach, in principle, is independent of the process fluid, and requires no additional sensors.

### Further Information

- R. W. Miller, *Flow Measurement Engineering Handbook*, 3rd ed., New York: McGraw-Hill, 1996, chap. 14.
- W. C. Gotthardt, Oscillatory flowmeters, in *Practical Guides for Measurement and Control: Flow Measurement*, D. W. Spitzer (ed.), Research Triangle Park, NC: Instrument Society of America, 1991, chap. 12.
- J. P. DeCarlo, *Fundamentals of Flow Measurement*, Research Triangle Park, NC: Instrument Society of America, 1984, chap. 8.
- ASME MFC-6M, Measurement of Fluid Flow in Closed Conduits Using Vortex Flowmeters, American Society of Mechanical Engineers, 1998.

## 28.9 Thermal Mass Flow Sensors

---

### *Nam-Trung Nguyen*

This chapter section deals with thermal mass flowmeters. The obvious question that arises is, what is actually meant by mass flow and thermal mass flowmeter? To answer this question, one should first understand what is the flow and what is the physical quantity measured by the meter. The flow can be understood here by the motion of a continuum (fluid) in a closed structure (channel, orifice), and is the

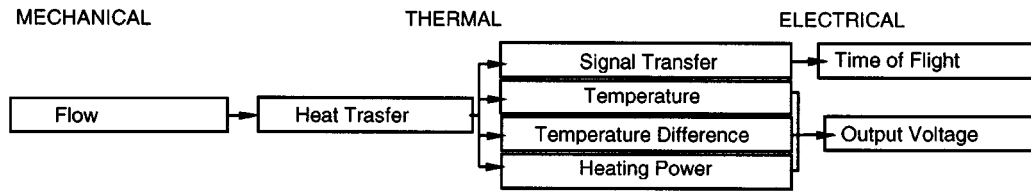


FIGURE 28.68 The three signal domains and the signal transfer process of a thermal flow sensor.

measured object. The associated physical quantity measured by the meter is the mass flux that flows through a unit cross-section. The equation for the volume flow rate  $\Phi_v$  is given by:

$$\Phi_v = dV/dt = vA \quad (28.101)$$

where  $V$  = Volume through in the time  $t$

$v$  = Average velocity over the cross-section area  $A$  of the channel

With the relation between volume  $V$ , mass  $M$ , and the density of fluid  $\rho$ :

$$V = M/\rho \quad (28.102)$$

the mass flow rate  $\Phi_m$  can be derived by using Equations 28.101 and 28.102 to obtain:

$$\Phi_m = (\Phi_v \rho) + \left( V \frac{d\rho}{dt} \right) \quad (28.103)$$

For time invariable fluid density, one obtains:

$$\Phi_m = \Phi_v \rho = Av\rho \quad (28.104)$$

A thermal mass flow sensor will generally output a signal related to the mass flux:

$$\phi_m = \Phi_m / A = v\rho \quad (28.105)$$

and convert the mechanical variable (mass flow) via a thermal variable (heat transfer) into an electrical signal (current or voltage) that can be processed by, for example, a microcontroller. Figure 28.68 illustrates this working principle. The working range for any mass flux sensor is somewhat dependent on the fluid properties, such as thermal conductivity, specific heat, and density, but not on the physical state (gas or liquid) of the fluid.

## Principles of Conventional Thermal Mass Flowmeters

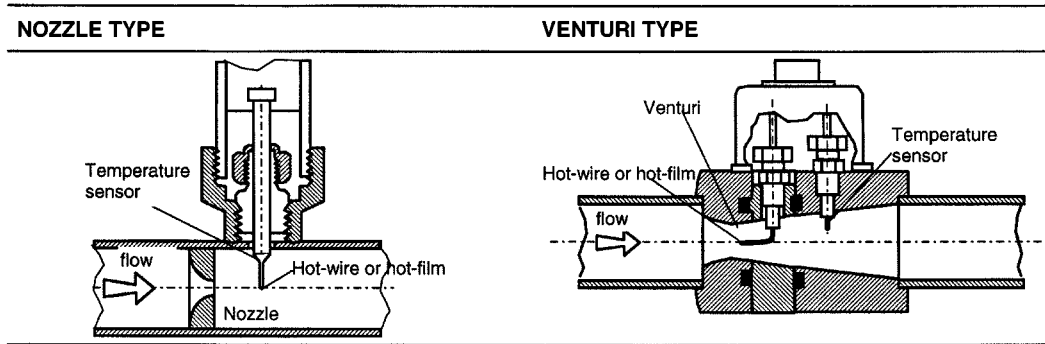
With two heater control modes and two evaluation modes, there are six operational modes shown in Table 28.13 and three types of thermal mass flowmeters:

- Thermal mass flowmeters that measure the effect of the flowing fluid on a hot body (increase of heating power with constant heater temperature, decrease of heater temperature with constant heating power). They are usually called hot-wire, hot-film sensors, or hot-element sensors.
- Thermal mass flowmeters that measure the displacement of temperature profile around the heater, which is modulated by the fluid flow. These are called calorimetric sensors.
- Thermal mass flowmeters that measure the passage time of a heat pulse over a known distance. They are usually called time-of-flight sensors.

**TABLE 28.13** Operational Modes of Thermal Mass Flow Sensors

Heater controls	Constant heating power		Constant heater temperature	
Evaluation	Heater temperature	Temperature difference	Heating power	Temperature difference
Operational Modes	Hot-wire and hot-film type	Calorimetric type	Hot-wire and hot-film type	Calorimetric type
	Time-of-flight type		Time-of-flight type	

**TABLE 28.14** Typical Arrangements of Flow Channel



### Hot-Wire and Hot-Film Sensors

The dependence of the heat loss between a fine wire as well as a thin film and the surrounding fluid has traditionally been the most accepted method for measuring a fluid flow: the hot-wire method. The hot-film method uses film sensors for detecting the flow. The basic elements of this sensor type are discussed.

*Flow channel:* In contrast to the thermal anemometer described in Chapter 29 for point measurement, thermal mass flow sensors of the hot-wire and hot-film type have a flow channel defining the mass flow. Table 28.14 shows two typical arrangements.

*Sensor element:* Hot-wire sensors are fabricated from platinum, platinum-coated tungsten, or a platinum-iridium alloy. Since the wire sensor is extremely fragile, hot-wire sensors are usually used only for clean air or gas applications. On the other hand, hot-film sensors are extremely rugged; therefore, they can be used in both liquid and contaminated-gas environments. In the hot-film sensor, the high-purity platinum film is bonded to the rod. The thin film is protected by a thin coating of alumina if the sensor will be used in a gas, or of quartz if the sensor will be used in a liquid. The alumina coatings have a high abrasion resistance and high thermal conductivity. Quartz coatings are less porous and can be used in heavier layers for electrical insulation. Typical hot-wire and hot-film sensors are shown in Table 28.15.

The sensor element, whether it is a wire or a film, should be a resistor that has a resistance with a high temperature coefficient  $\alpha$ . For most sensor materials, the temperature dependence can simply be expressed by a first-order function:

$$R = R_r \left[ 1 + \alpha (T - T_r) \right] \quad (28.106)$$

where  $R$  = Resistance at operating temperature  $T$

$R_r$  = Resistance at reference temperature  $T_r$

$\alpha$  = Temperature coefficient

For research applications, cylindrical sensors are most common, either a fine wire (typical diameters from 1 to 15  $\mu\text{m}$ ) or a cylindrical film (typical diameters from 25 to 150  $\mu\text{m}$ ). Industrial sensors are often a resistance wire wrapped around a ceramic substrate that has typical diameters from 0.02 mm to 2 mm. Table 28.16 shows some typical parameters of industrial hot-wire and hot-film sensors.

**TABLE 28.15** Typical Hot-Wire and Hot-Film Sensors (1, hot-wire; 2, sensor supports; 3, electric leads; 4, hot-film; 5, contact caps; 6, quartz rod)

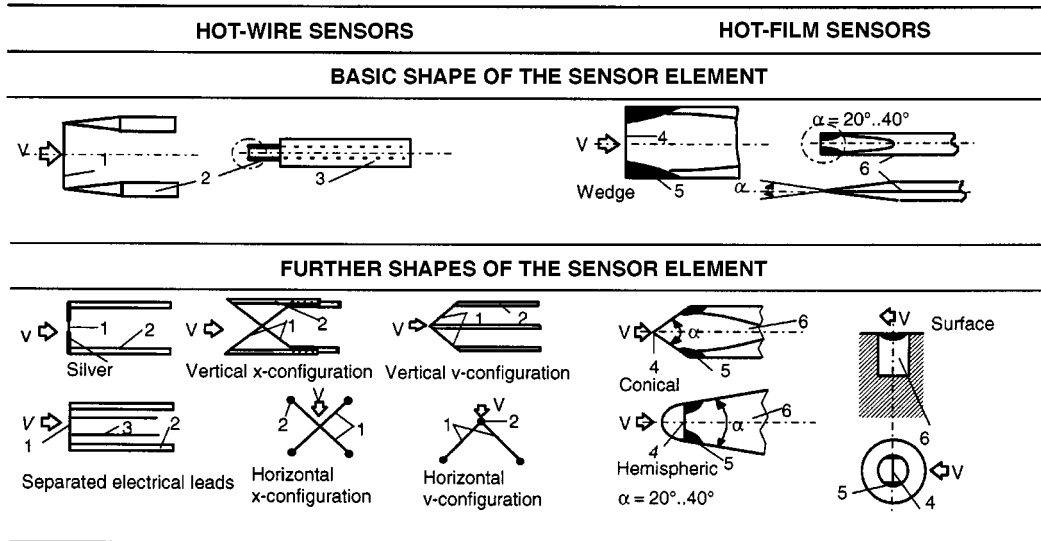


**TABLE 28.16** Typical Parameters of Hot-Wire and Hot-Film Sensors [3]

Parameter	Hot-wire	Hot-film
Sensor element	Platinum hot-wire (diameter 70 $\mu\text{m}$ )	Platinum hot-film (alumina coated)
Operational mode	Constant heater temperature in air	
Working temperature range	-30 to 200°C	
Characteristics	Nonlinear	
Accuracy in %	$\pm 4$	$\pm 2$
Time response in ms	$< 5$	12
Sensitivity in $\text{mV kg}^{-1} \text{h}^{-1}$	1	5

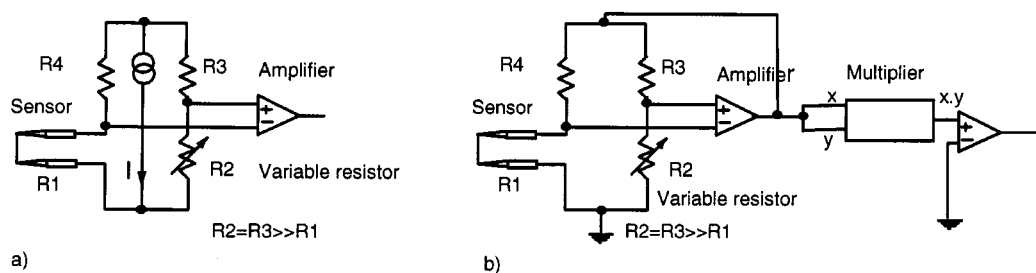


**FIGURE 28.69** Control and evaluation circuit of heat-wire and heat-film sensors: (a) constant-current bridge; (b) constant-temperature bridge.

*Control and evaluation circuit:* The constant-current and constant-temperature bridge are conventional circuits for control and evaluation of heat-wire or heat-film sensors.

A constant-current Wheatstone bridge with a hot-wire sensor is shown schematically in [Figure 28.69\(a\)](#). In this circuit, resistors  $R_3$  and  $R_4$  are much larger than sensor resistor  $R_1$ . Therefore, current through  $R_1$  is essentially independent of changes in the sensor resistor  $R_1$ . Any flow in the channel cools the hot wire, decreases its resistance as given by Equation 28.106, and unbalances the bridge. The

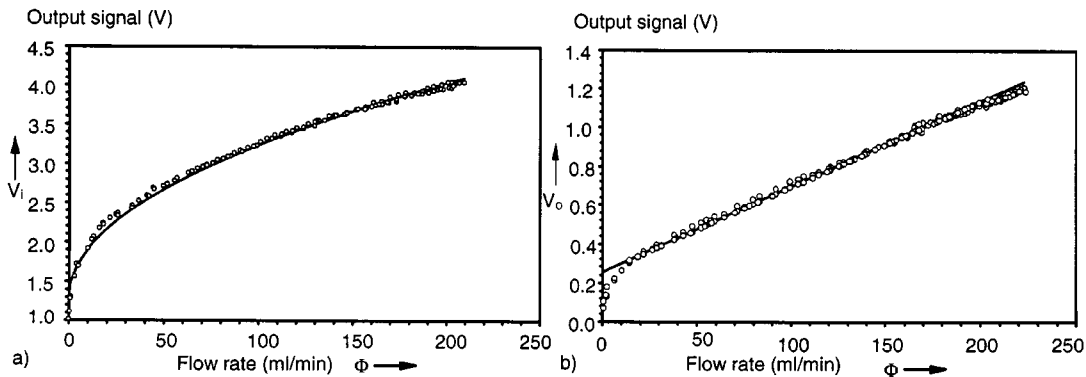


FIGURE 28.70 Sensor characteristics of the constant-temperature mode before (a) and after (b) linearization.

TABLE 28.17 Typical Calorimetric Sensors

INTRUSIVE TYPE		NON-INTRUSIVE TYPE	
Upstream sensor	Downstream sensor	Upstream sensor	Downstream sensor
Heater		Heater	

unbalanced bridge produces an output voltage  $V_o$ , which is related to the mass flow. Because the output voltage  $V_o$  from the bridge is small, it must be amplified before it is recorded. The value of the thermal coefficient  $\alpha$  for  $R_1$  and  $R_2$  should be equal in order to eliminate signal errors due to changes in ambient temperature. Similarly, thermal coefficients for  $R_3$  and  $R_4$  should also be equal.

The constant-temperature Wheatstone bridge is shown in Figure 28.69(b). The bridge is balanced under no-flow conditions with the variable resistor  $R_2$ . The flow cools the hot wire, and its resistance decreases and unbalances the bridge. A differential amplifier balances the bridge with the feedback voltage. The output signal can be linearized before recording.

Because the output signal has a square-root-like characteristic, the linearizer can be realized easily using a multiplier (i.e., AD534 of Analog Devices) with two equal input signals (a squarer). Figure 28.70 illustrates the results. With this method, there is linearization error in the low flow range.

### Calorimetric Sensors

The displacement of the temperature profile caused by the fluid flow around a heating element can be used for measuring very small mass flow. Depending on the location of the heating and sensing elements, there are two types of calorimetric sensors: the intrusive sensors that lie in the fluid, and the nonintrusive sensors that are located outside the flow. Table 28.17 illustrates the two typical calorimetric sensors.

The intrusive type has many limitations. The heater and the temperature sensors must protrude into the fluid. Therefore, corrosion and erosion damage these elements easily. Furthermore, the integrity of the piping is sacrificed by the protrusions into the flow, thus increasing the danger of leakage.

In the nonintrusive sensor type, the heater and the temperature sensors essentially surround the flow by being located on the outside of the tube that contains the flow. The major advantage of this sensor type is the fact that no sensor is exposed to the flowing fluid, which can be very corrosive. This technique is generally applied to flows in the range of  $1 \text{ mL min}^{-1}$  to  $500 \text{ L min}^{-1}$ . The larger flows are measured using the bypass arrangement. Figure 28.71(a) shows the measured shift of the temperature distribution around the heater. The asymmetry of the temperature profile increases with flow. The measurement



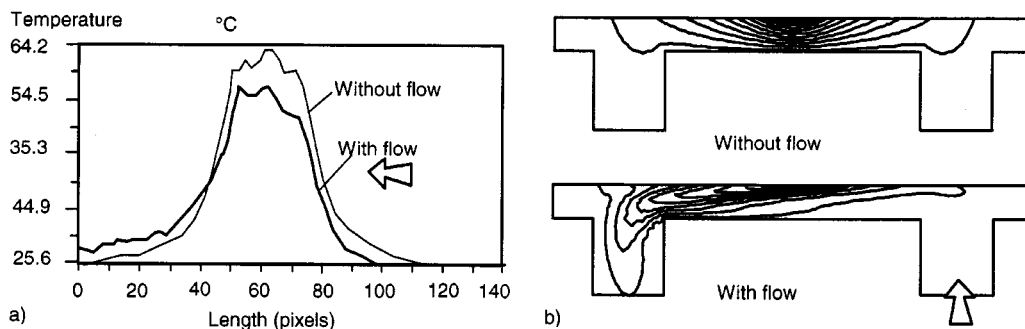


FIGURE 28.71 Temperature distribution around the heater: (a) measurement (b) numerical simulation.

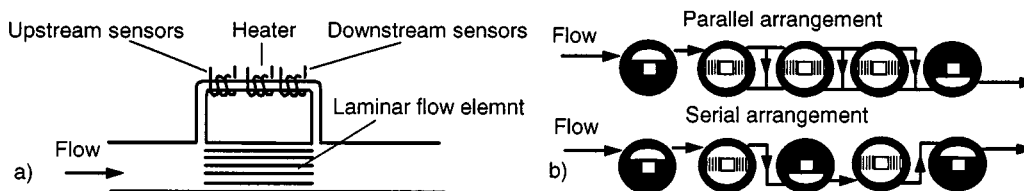


FIGURE 28.72 Bypass arrangement for large flow range: (a) principle (b) a solution for the laminar flow element [4].

TABLE 28.18 Typical Parameters of Calorimetric Sensors [4]

Parameter	Gases	Liquids
Working temperature	0°C to 70°C	0°C to 70°C
Accuracy in %	±1%	±1%
Linearity	±0.2%	±0.2%
Flow range 1:50	min. 5 mL min <sup>-1</sup> max. 100 L min <sup>-1</sup>	min. 5 g h <sup>-1</sup> max. 1000 g h <sup>-1</sup>

was carried out using a thermography system [10]. To understand the working principle, the effect of fluid mechanics and heat transfer should be reviewed. The mathematical theory for this problem is discussed later in this chapter. Figure 28.71(b) illustrates the influence of the flow over the temperature distribution.

Because the calorimetric mass flow sensors are sensitive in low-flow ranges, bypass designs have been introduced in order to make the sensors suitable for the measurement of larger flow ranges. The sensor element is a small capillary tube (usually less than 3 mm in diameter). They ensure laminar flow over the full measurement range. The laminar flow elements are located parallel to the sensor element as a bypass (Figure 28.72(a)). They are usually a small tube bundle, a stack of disks with etched capillary channels [4] (Figure 28.72(b)), or a machined annular channel.

Table 28.18 shows typical parameters of calorimetric flow sensors. Compared to the hot-wire or hot-film sensors, this sensor type has good linearity and is only limited by signal noise at low flows and saturation at high flows. While the linear range may exceed a 100:1 ratio, the measurable range may be as large as 10,000:1 [21]. The small size of the capillary sensor tube is advantageous in minimizing the electric power requirement and also in increasing the time of response. Because of the small size of the tube, it necessitates the use of upstream filters to protect against plugging of dust particles. With the bypass arrangement, a relatively wide flow range is possible.

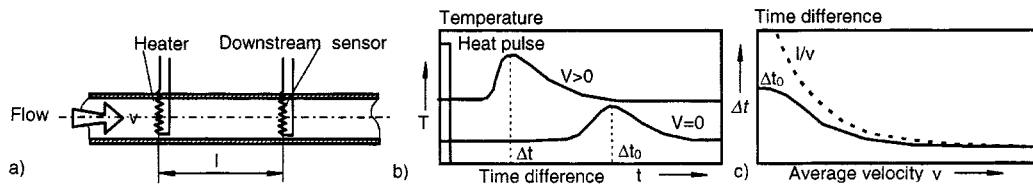


FIGURE 28.73 Time-of-flight sensors: (a) principle; (b) temperature at downstream sensor; (c) sensor characteristic.

### Time-of-Flight Sensors

The time-of-flight sensor consists of a heater and one or more temperature sensors downstream, Figure 28.73(a). The heater is activated by a current pulse. The transport of the generated heat is a combination of diffusion and forced convection. The resulting temperature field can be detected by temperature sensors located downstream. The detected temperature output signal of the temperature sensor is a function of time and flow velocity. The sensor output is the time difference between the starting point of the generated heat pulse and the point in time at which a maximum temperature at the downstream sensor is reached, Figure 28.73(b). At the relatively low flow rates, the time difference depends mainly on the diffusivity of the fluid medium. At relatively high flow rates, the time difference tends to relate to the ratio of the heater–sensor distance and the average flow velocity [5].

Because of the arrangement shown in Figure 28.73(a), the time-of-flight sensors have the same limitations as the intrusive type of calorimetric sensors: corrosion, erosion, and leakage. Since the signal processing needs a while to measure the time difference, this sensor type is not suitable for dynamic measurement. The advantage of this type of volumetric flow sensor is the independence of fluid properties as well as fluid temperature in the higher flow range. The influence of fluid properties on the mass flow sensor output is described in [21], as well as an approach to compensate for changes in these properties, which is valid for both hot-element and calorimetric sensors.

### Mass and Heat Transfer

The most important signal of the transfer process shown in Figure 28.68 is the thermal signal. There are different kinds of thermal signals: temperature, heat, heat capacity, and thermal resistance. In the following, the transfer of heat and the interaction between heat and temperature will be explained by three mean heat transfer processes: conduction, convection, and radiation. The first two processes can be described by the general equation of a transfer process. The transfer variables in the equation can be the momentum (momentum equation), the temperature (energy equation), or the mass (mass equation).

A transfer process consists of four elements: accumulation, conduction, induction, and convection. The *accumulation process* describes the time dependence of the transfer variable. The *conduction* presents the molecular transfer. The *convection* is the result of the interaction between the flow field and the field of the transfer variable. The *induction* describes the influence of external fields and sources.

#### Conduction

When there is a temperature gradient in a substance, the heat will flow from the hotter to the colder region, and this heat flow  $q$  (in  $\text{W m}^{-2}$ ) will be directly proportional to the value of the temperature gradient:

$$q = -\lambda \frac{dT}{dx} \quad (28.107)$$

where  $T$  is the temperature. The above expression is called the Fourier's law of heat conduction and defines the material constant  $\lambda$  (in  $\text{W K}^{-1} \text{m}^{-1}$ ), the thermal conductivity. Figure 28.74 shows the order of the thermal conductivity  $\lambda$  of different materials.

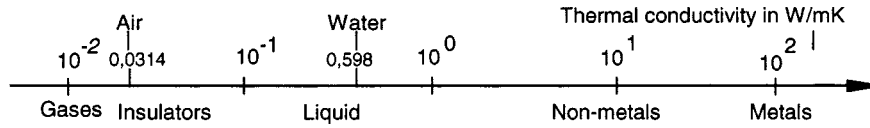


FIGURE 28.74 The order of thermal conductivity of different materials.

The differential form of the heat-conduction equation is a special case of the energy equation (see next subsection on convection). The transfer equation only consists of the accumulative, conductive, and inductive terms:

$$\frac{\partial T}{\partial t} = \frac{\lambda}{\rho c} \left( \frac{\partial^2 T}{\partial x^2} + \frac{\partial^2 T}{\partial y^2} + \frac{\partial^2 T}{\partial z^2} \right) + \frac{q'}{\rho c} \quad (28.108)$$

where  $\rho$  is the density,  $c$  is the specific heat at constant pressure and  $q'$  (in  $\text{W m}^{-3}$ ) is the amount of heat (in joules) per unit of volume and time that can be generated inside the material itself, either through the action of a separate heat source, or through a change in phase of matter.

In the steady state without internal heat sources, the equation of conduction reduces to:

$$\frac{\partial^2 T}{\partial x^2} + \frac{\partial^2 T}{\partial y^2} + \frac{\partial^2 T}{\partial z^2} = 0 \quad (28.109)$$

### Convection

In general, there are two kinds of convection: forced convection and natural convection. The first one is caused by a fluid flow, the other one by itself because of the temperature dependency of fluid density and the buoyancy forces. To describe convection, three conservation equations are required:

- Conservation of mass: continuity equation

$$\frac{\partial \rho}{\partial t} + \nabla(\rho v) = 0 \quad (28.110)$$

- Conservation of momentum: Navier–Stokes equation

$$\frac{\rho \partial v}{\partial t} + v \nabla v = -\nabla p + \eta \nabla^2 v + \rho g \quad (28.111)$$

- Conservation of energy: energy equation

$$\frac{\partial T}{\partial t} + v \nabla T = \left( \frac{\lambda}{\rho c} \right) \nabla^2 T + \frac{q'}{\rho c} \quad (28.112)$$

where  $\eta$  is the dynamic viscosity of the fluid. The temperature field and the heat power can be found by solving these three equations. For designing and understanding the thermal flow sensor, the convective heat transfer can be expressed in the simplest form:

$$Q = \varepsilon A \Delta T \quad (28.113)$$

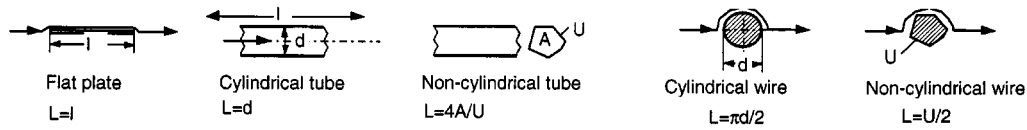


FIGURE 28.75 Definition of the characteristic length of different objects [6].

where  $Q$  (in W) = heat transfer rate (or the heat power)

$\varepsilon$  = heat transfer coefficient between the heated surface  $A$  and the fluid

$\Delta T$  = temperature difference between the heated body and ambient

The dimensionless Nusselt number describes the heat transfer. The relationship between the heat transfer coefficient  $\varepsilon$  and the Nusselt number  $Nu$  can be expressed as follows:

$$\varepsilon = Nu \frac{\lambda}{L} \quad (28.114)$$

where  $L$  is the characteristic length (the length  $L$  of a flat plate, the hydraulic diameter  $D_h$  of a tube, and the half of the perimeter of a wire, Figure 28.75). The hydraulic diameter  $D_h$  can be calculated using the wetted perimeter  $U$  and the cross-sectional area  $A$  of the tube:

$$D_h = \frac{4A}{U} \quad (28.115)$$

The relevant dimensionless number which describes the flow is the Reynolds number  $Re$ :

$$Re = \frac{vL}{\nu} \quad (28.116)$$

where  $v$  is the average flow velocity and  $\nu$  the kinematic viscosity of the fluid, which is defined by the density  $\rho$  and the dynamic viscosity  $\eta$ :

$$\nu = \frac{\eta}{\rho} \quad (28.117)$$

Table 28.19 shows a collection of formulae for calculating the Nusselt number. The fluid properties (kinematic viscosity  $\nu$  and Prandtl number  $Pr$ ) should be chosen at the average temperature  $T_{av}$  between the heater temperature  $T + \Delta T$  and the fluid temperature  $T$ :

$$T_{av} = T + \frac{\Delta T}{2} \quad (2.118)$$

In the case of natural convection, the Nusselt number depends on the Grashof number  $Gr$ , which describes the influence of buoyancy forces:

$$Gr = \frac{g\beta L^3 \Delta T}{\nu^2} \quad (28.119)$$

**TABLE 28.19** Nusselt Number (Nu) of Forced Convection [6]

Object	$Nu_{\text{lam}}$ for laminar regime	$Nu_{\text{turb}}$ for turbulent regime	Average Nusselt number Nu
Flat plate	$Nu_{\text{lam}} = 0.664 \sqrt{\text{Re}} \sqrt{\text{Pr}}$ <p>Re &lt; 10<sup>5</sup>; 0.6 &lt; Pr &lt; 2000</p>	$Nu_{\text{turb}} = \frac{0.037 \text{Re}^{0.8} \text{Pr}}{1 + 2.443 \text{Re}^{-0.1} (\text{Pr}^{2/3} - 1)}$ <p>5 · 10<sup>5</sup> &lt; Re &lt; 10<sup>7</sup>; 0.6 &lt; Pr &lt; 2000</p>	$Nu = \sqrt{Nu_{\text{lam}}^2 + Nu_{\text{turb}}^2}$ <p>10 &lt; Re &lt; 10<sup>7</sup>; 0.6 &lt; Pr &lt; 2000</p>
Cylindrical tube	$Nu_{\text{lam}} = 3.65 + \frac{0.19 (\text{Re Pr } d/l)^{0.8}}{1 + 0.117 (\text{Re Pr } d/l)^{0.467}}$ <p>Re &lt; 2300; 0.1 &lt; (Re Pr d/l) &lt; 10<sup>4</sup></p>	$Nu_{\text{turb}} = \frac{\xi/8 (\text{Re} - 1000) \text{Pr}}{1 + 12.7 \sqrt{\xi/8} (\text{Pr}^{2/3} - 1)} \left[ 1 + \left( \frac{d}{l} \right)^{2/3} \right]$ <p>where  <math>\xi = (1.28 \log_{10} \text{Re} - 1.64)^{-2}</math></p> <p>Thermal entrance, fully developed flow,                  2300 &lt; Re &lt; 10<sup>4</sup></p> $Nu_{\text{turb}} = \sqrt[3]{3.66^3 + 1.61^3 \text{Re Pr } d/l}$ <p>Thermal entrance, developing flow,                  2300 &lt; Re &lt; 10<sup>6</sup></p>	
Short cylindrical tube 0.1 < d/l < 1	$Nu_{\text{lam}} = 0.664^3 \sqrt{\text{Pr}} \sqrt{\text{Re } d/l}$ <p>Re &lt; 2300; 0.1 &lt; (Re Pr d/l) &lt; 10<sup>4</sup></p>		
Wire	$Nu_{\text{lam}} = 0.664 \sqrt{\text{Re}} \sqrt{\text{Pr}}$ <p>10 &lt; Re &lt; 10<sup>7</sup>; 0.6 &lt; Pr &lt; 1000</p>	$Nu_{\text{turb}} = \frac{0.037 \text{Re}^{0.8} \text{Pr}}{1 + 2.443 \text{Re}^{-0.1} (\text{Pr}^{2/3} - 1)}$	$Nu = 0.3 + \sqrt{Nu_{\text{lam}}^2 + Nu_{\text{turb}}^2}$

**TABLE 28.20** The Average Nusselt Number of Free Convection in Some Special Cases

Cases	Equation	Ref.
Vertical flat plate or wire	$Nu = 0.55(Gr Pr)^{1/4}$	[7]
Horizontal flat plate	For the upper surface: $Nu = 0.76(Gr Pr)^{1/4}$ For the lower surface: $Nu = 0.38(Gr Pr)^{1/4}$	[8]

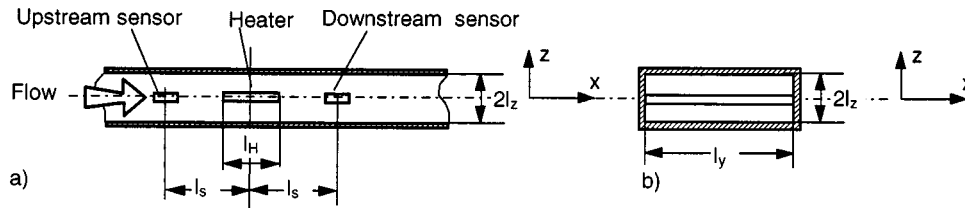


**FIGURE 28.76** Analytical model for the intrusive type of calorimetric sensors: (a) length cut, (b) cross-section.

where  $g$  is the acceleration due to the gravity ( $9.81 \text{ m s}^{-2}$ ),  $\beta$  the thermal expansion coefficient of the fluid, and  $\Delta T$  is the temperature difference between the hot fluid and the ambient. The average Nusselt number can be calculated for a laminar flow ( $10^4 < GrPr < 10^8$ ) in Table 28.20.

### Radiation

A body can either emit or absorb thermal radiation. Radiation is not important for the operational principle of thermal mass flow because of its relatively low magnitude.

Following, the physical and mathematical backgrounds of these three sensor types are discussed in detail. The working principle and the influence of fluid properties on the sensor signal can be determined using these mathematical models. However, the mathematical models only describe the relationship between thermal variables (heat power, temperature) and the average velocity. Further relationships between mass flow, mass flux, thermal, and electrical variables can be derived using Equations 28.101 to 28.106.

## Analytical Models for Calorimetric Flowmeters

### Model for the Intrusive Type of Calorimetric Sensors

In a quasi-static situation, the incoming heat at a certain point in the fluid must be equal to the outgoing heat. The heat is transported either by conduction in the fluid and/or supporting beams, or by convection through the thermal mass of the fluid. Ultimately, the heat is transported to the walls of the tube; see Figure 28.76 and Table 28.18. A heat balance equation results in a differential equation for  $T$  in  $x$ . The temperature profile in the  $y$  and  $z$  directions is assumed to be constant and linear, respectively [9].

Referring to Figure 28.76 and using  $A$  as the cross-section area of the flow channel ( $A = l_y 2l_z$ ),  $\rho$  as the fluid density,  $c$  as the fluid heat capacity (at constant pressure),  $v$  as the average fluid velocity, and  $\lambda$  as the fluid thermal conductivity, one finds that:

$$\frac{\partial^2 T}{\partial x^2} - v \left( \frac{\rho c}{\lambda} \right) \frac{\partial T}{\partial x} - \left( \frac{T}{l_z^2} \right) = 0 \quad (28.120)$$

or

$$\frac{\partial^2 T}{\partial x^2} - \left(\frac{\nu}{a}\right) \frac{\partial T}{\partial x} - \frac{T}{l_z^2} = 0 \quad (28.121)$$

where  $a = \lambda/\rho c$  is the thermal diffusivity of the fluid. Equation 28.121 is linear in  $T$ . Solving the differential equation using a heater length  $l_H$ , a heater power  $Q$ , and the boundary condition:

$$\lim_{x \rightarrow \pm\infty} T(x) = 0 \quad (28.122)$$

the following temperature distribution results:

$$x < \frac{-l_H}{2} \quad \text{for} \quad T(x) = T_0 \exp\left[\gamma_1 \left(x + \frac{l_H}{2}\right)\right] \quad (28.123)$$

$$\frac{l_H}{2} < x < \frac{l_H}{2} \quad \text{for} \quad T(x) = T_0 \quad (28.124)$$

$$x > \frac{l_H}{2} \quad \text{for} \quad T(x) = T_0 \exp\left[\gamma_2 \left(x - \frac{l_H}{2}\right)\right] \quad (28.125)$$

where

$$\gamma_{1,2} = \frac{\left(\nu \pm \sqrt{\nu^2 + 2a^2/l_z^2}\right)}{(2a)} \quad (28.126)$$

$$T_0 = \frac{P}{\left[\left(\frac{2\lambda l_y l_H}{l_z}\right) + A\lambda(\gamma_1 - \gamma_2)\right]} \quad (28.127)$$

The temperature difference between the two sides, upstream (at  $x = l_s$ ) and downstream (at  $x = -l_s$ ) can be then calculated as:

$$\Delta T(\nu) = T_0 \left\{ \exp\left[\gamma_2 \left(\frac{l_s - l_H}{2}\right)\right] - \exp\left[\gamma_1 \left(\frac{-l_s + l_H}{2}\right)\right] \right\} \quad (28.128)$$

### Model for the Nonintrusive Type of Calorimetric Sensors

A simple, one-dimensional model is used to show the working principle of the nonintrusive type with capillary-tube and heater wire winding around it. Geometric parameters and assumptions are given in [Figure 28.77](#). Because of the symmetry, only half of the capillary-tube will be considered for the calculation model. The conservation of thermal energy in a lumped element ([Figure 28.77\(c\)](#)) can be given in the following equation:

$$Q_{\text{cond},x,\text{fluid}} + Q_{\text{conv},x,\text{fluid}} + Q_{\text{cond},x,\text{wall}} = Q_{\text{cond},y,\text{fluid}} \quad (28.129)$$

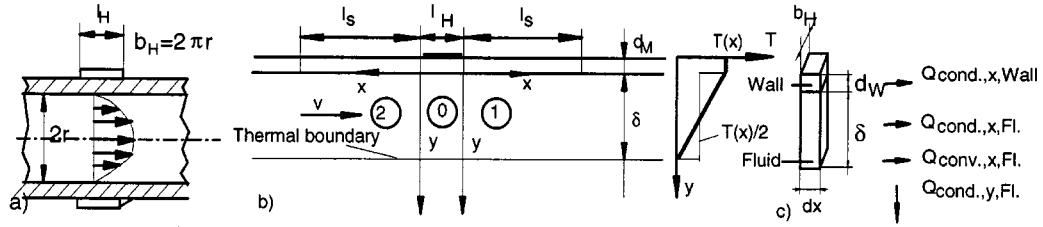


FIGURE 28.77 Analytical model for the nonintrusive type of calorimetric sensors: (a) heater and channel geometry, (b) model geometry, and (c) model of a lumped element.

The indices define the conduction or convection in the  $x$ - or  $y$ -axis in the fluid as well as in the heated wall. Defining the temperature along the  $x$ -axis as  $T(x)$ , the average flow velocity as  $v$ , the thermal conductivities of wall material as  $\lambda_w$  and of fluid as  $\lambda$ , the thermal diffusivity of fluid  $a = \lambda/(\rho c)$ , and the thickness of the average thermal boundary layer as  $\delta$  one finds the heat balance equation:

$$\left[ \frac{1}{2} + \left( \frac{\lambda_w d_w}{\lambda \delta} \right) \right] \frac{\partial^2 T}{\partial x^2} - \frac{v}{2a} \frac{\partial T}{\partial x} - \frac{T(x)}{\delta^2} = 0 \quad (28.130)$$

The thickness of the average thermal boundary layer  $\delta$  depends on the flow velocity [15]. For gases with a small Prandtl number ( $Pr < 1$ ) or liquids with a low Reynolds number, one can assume that:

$$\delta = r \quad (28.131)$$

After solving Equation 28.130 in the local coordinate systems 1 and 2 (Figure 28.77(b)), one obtains the temperature difference  $\Delta T(v)$  between the temperature sensors:

$$\Delta T(v) = \vartheta_0 \left[ \exp(\gamma_2 l_s) - \exp(\gamma_1 l_s) \right] \quad (28.132)$$

with:

$$\gamma_{1,2} = \frac{\left( v \pm \sqrt{v^2 + 16a^2 \kappa / \delta^2} \right)}{4a\kappa} \quad (28.133)$$

The dimensionless factor:

$$\kappa = \frac{1}{2} + \frac{(\lambda_w d_w)}{(\lambda \delta)} \quad (28.134)$$

describes the influence of the wall on the heat balance. If the wall is neglected, we get  $\kappa = 1/2$  as in the similar case of Equation 28.121. The heater temperature  $T_0$  can be calculated for the constant heat power  $Q$ :

$$T_0 = \frac{Q}{\left\{ 2\pi r \lambda \left[ \frac{l_H}{\delta} + \sqrt{\frac{(v^2 \delta^2)}{(4a^2) + 4\kappa}} \right] \right\}} \quad (28.135)$$



### Model for the Time-of-Flight Type

The transport of the heat generated in a line source through a fluid is governed by the energy equation (112). The analytical solution of this differential equation for a pulse signal with input strength  $q'_0$  ( $\text{W m}^{-1}$ ) is given in [11] as:

$$T(x, y, t) = \left( \frac{q'_0}{4\pi\lambda t} \right) \exp \left\{ - \left[ \frac{(x-vt)^2 + y^2}{4at} \right] \right\} \quad (28.136)$$

where  $a$  denotes the thermal diffusivity. By measuring the top time  $\tau$  at which the signal passes the detection element ( $y = 0$ ), in other words differential Equation 28.136 with respect to time, one can obtain the basic equation for the so-called “time-of-flight” of the heat pulse:

$$v = \frac{x}{t} \quad (28.137)$$

For Equation 28.136 to be valid, the term  $4at$  must be much smaller than the heater-sensor distance  $x$ . This assumes that forced convection by the flow is dominating over the diffusive component. In other words, Equation 28.136 is true at high flow velocities. When the diffusive effect is taken into account, the time-of-flight is given by:

$$\Delta t = \tau = \frac{\left[ -2a + (4a^2 + v^2 x^2)^{1/2} \right]}{v^2} \quad v \neq 0 \quad (28.138)$$

$$\tau = \frac{x^2}{4a} \quad v = 0 \quad (28.139)$$

### Principles of Microflow Sensors

In research papers, the first reference to thermal mass flow sensor normally cited is that of King in 1914. Since then, microsystems technology has been developed. The development of thermal flow sensor can be realized in micron-size using the three current technologies: bulk micromachining, surface micromachining, epimicromachining and LIGA-techniques (LIGA: German description of “Lithographie, Galvanoformung, Abformung”). These fabrication techniques (except LIGA) are compatible with conventional microelectronic processing technology. Thermal flow sensors developed using these technologies will be called “microflow sensors” in this section. The operational modes are similar to the conventional thermal flow sensor. In Table 28.21, the microflow sensors are classified after their transducing principle. With these new sensors, very small flows in the nanoliter and microliter range can be measured. Table 28.22 shows some realized examples of microflow sensors.

### Smart Thermal Flow Sensors and Advanced Evaluation Circuits

Conventional sensors usually have separate electronics, which causes high cost and prevents large serial production. An integrated smart thermal flow sensor is defined as a chip that contains one or more sensors, signal conditioning, A/D conversion, and a bus output [15]. Therefore, there is a need for advanced evaluation methods that convert the thermal signal directly into a frequency and duty-cycle output.

**TABLE 28.21** The Transducing Principle of Microflow Sensors

Transducing principle	Realization	Application
Thermoresistive	Metal film (platinum), polycrystalline silicon, single crystalline silicon or metal alloys.	Measurement of temperature, temperature difference, and heat power
Thermoelectric	<i>p</i> Si-Al (bipolar-technology), polySi-Al (CMOS-technology) or <i>p</i> PolySi- <i>n</i> PolySi thermopiles	Measurement of temperature and temperature difference
Thermoelectronic	Transistors, diodes	Measurement of temperature and temperature difference
Pyroelectric	Pyroelectric materials (LiTaO <sub>3</sub> ) with metal or silicon resistors as heater and electrodes	Measurement of heat power
Frequency analog	SAW oscillators	Measurement of temperature

### The Duty-Cycle Modulation for the Hot-Wire Sensors

The constant heater temperature can be controlled by modulation of the amplitude of the heat voltage (conventional principle) or by modulation of the duty-cycle. The heater is activated when the output signal is high. This heater controlling output goes low when the temperature level  $T_0 + \Delta T$  is reached. During low output, the heating temperature decreases to the temperature level  $T_0 + \Delta T$ , where the output goes high again and restarts the heating cycle. The temperature level is determined by a reference resistor and a variable resistor. An increase in the flow rate increases the convective cooling of the heater, and it needs a longer time to reach the temperature level. That results in the higher output time  $t_H$ . Figure 28.78 shows the working principle of the duty-cycle modulation, where  $t_d$  is the time delay in the switching action. Defining the maximum heating power as  $Q_{\max}$  (the output signal is always high), one obtains the relation:

$$Q = Q_{\max} \left( \frac{t_H}{t_{\text{total}}} \right) \quad (28.140)$$

### The Electrical Sigma-Delta Modulation for Calorimetric Sensors

Conventional signal conditioning circuits use an analog-to-digital converter (ADC) to get digital sensor readout, which can be regarded as an amplifier or a voltmeter. They read the information signal from the sensor, but do not interact with the sensor. In contrast, sigma-delta converters are a part of the sensor function since they act as a feedback amplifier for the sensor output. Hence, sigma-delta conversion normally results in a much more robust sensor signal than is provided by conventional ADCs. Following, the principle of sigma-delta conversion applied to calorimetric flow sensors is explained.

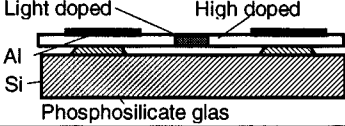
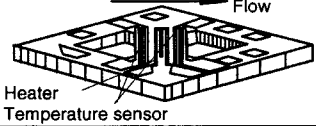
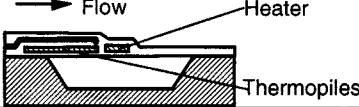
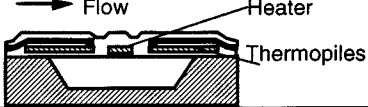
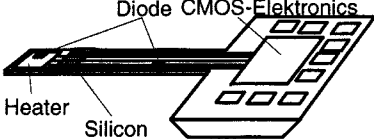
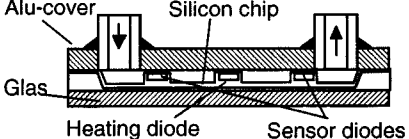
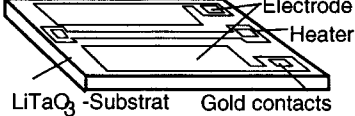
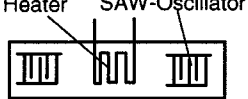
The transistors  $T_1$  and  $T_2$  represent two switchers that feed the constant current  $I_0$  into the  $RC$  network. It is assumed in this example that the temperature on the resistor  $R_{s2}$  is higher than the temperature on  $R_{s1}$ . Therefore, the resistance of  $R_{s2}$  is larger than  $R_{s1}$ . It results in a larger time constant for the charging of  $C_2$ . With the help of the comparators and the D-flip-flop, the constant current  $I_0$  can be switched on and off. The switching signals  $f1$  and  $f2$  have, in the same time period, different pulse numbers  $N + S$  and  $N$ :

$$\frac{R_{s2}}{R_{s1}} = \frac{(N + S)}{N} = 1 + \frac{\Delta R}{R_{s1}} \quad (28.141)$$

Thus:

$$\frac{\Delta R}{R_{s1}} = \frac{S}{N} \quad (28.142)$$

TABLE 28.22 Examples of Microthermal Mass Flow Sensors

TRANSDUCING PRINCIPLE	HOT-WIRE OR HOT-FILM	CALORIMETRIC
Thermoresistive [13, 14]		
Thermoelectric [15,16]		
Thermoelectronic [17, 18]		
Pyroelectric [19]		
Frequency analog [20]		

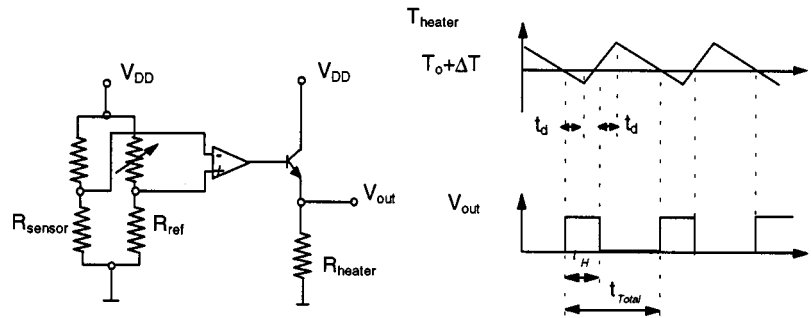


**FIGURE 28.78** The duty-cycle modulation for hot wire sensors: (a) basic circuit; (b) the heater temperature detected by  $R_{\text{sensor}}$  and the output voltage  $V_{\text{out}}$  vs. the time.

with:

$$R_{s1} = \frac{(V_{\text{ref}} N)}{(I_0 G)} \quad (28.143)$$

The resistance difference as well as the temperature difference can be calculated:

$$\Delta R = \frac{(S V_{\text{ref}})}{G I_0} \quad (28.144)$$

The counting and recording of  $S$  and  $G$  are shown in [Figure 28.79](#).

### The Thermal Sigma–Delta Modulation

The principle of thermal sigma–delta modulation is based on the conventional electrical sigma–delta: the thermal sigma–delta converter uses a thermal integrator (thermal  $R/C$ -network) instead of an electric integrator (electric  $R/C$ -network). [Figure 28.80](#) shows the principle of thermal sigma–delta modulation. The comparator output modulates the flip-flop. The flip-flop synchronizes the heating signal by its clock. Therefore, the heating periods are chopped into further small pulses that depend on the clock frequency. The heater is actuated step-by-step until the comparator switches again, and one obtains a frequency analog output at the flip-flop [22].

## Calibration Conditions

### Calibration of Hot-Wire and Hot-Film Sensors

The hot-wire and hot-film sensors are based on the point velocity measurement (see [Table 28.14](#)). Therefore, the measurement results depend on the velocity distribution inside the flow channel. Achieving a high signal-to-noise ratio can thus require spatial arrays of hot-wire and hot-film sensors that give more information about the velocity field and thus more accurate results of the mass flow in channel. With the use of a nozzle, a Venturi, or a flow conditioner, the flow profile is preconditioned, which leads to an acceptable accuracy.

### Temperature Dependence of Fluid Properties

Most fluid properties depend on the working temperature. The heat transfer process depends on the fluid properties. The measurement of fluid temperature (see [Table 28.14](#)) keeps the heater on a constant

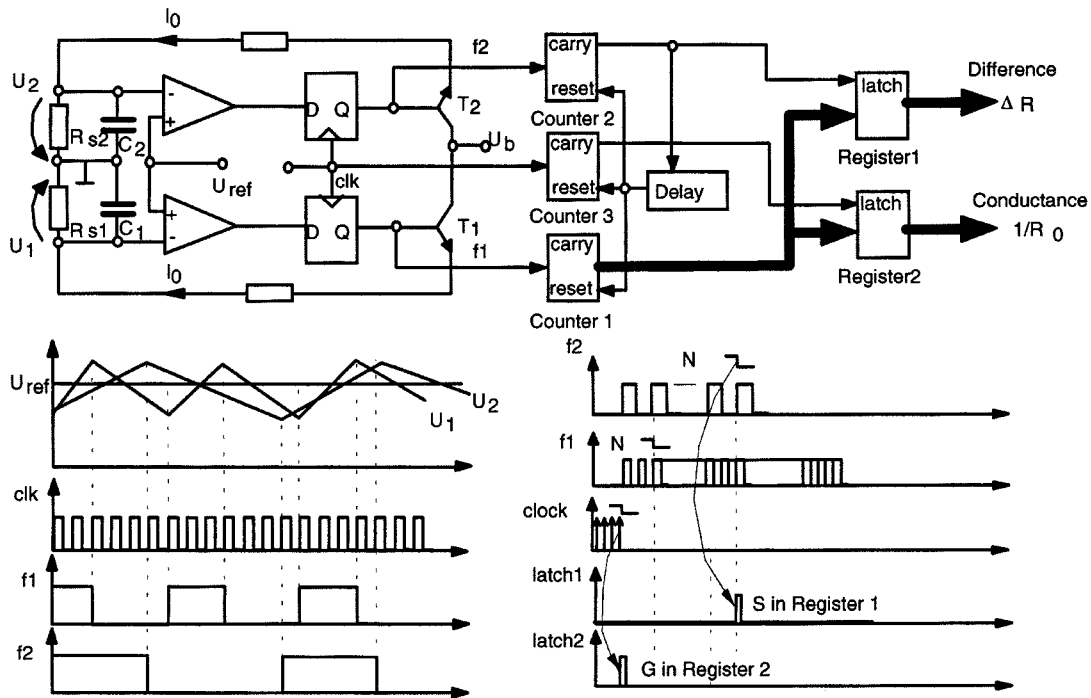


FIGURE 28.79 Sigma-delta conversion for calorimetric sensors.

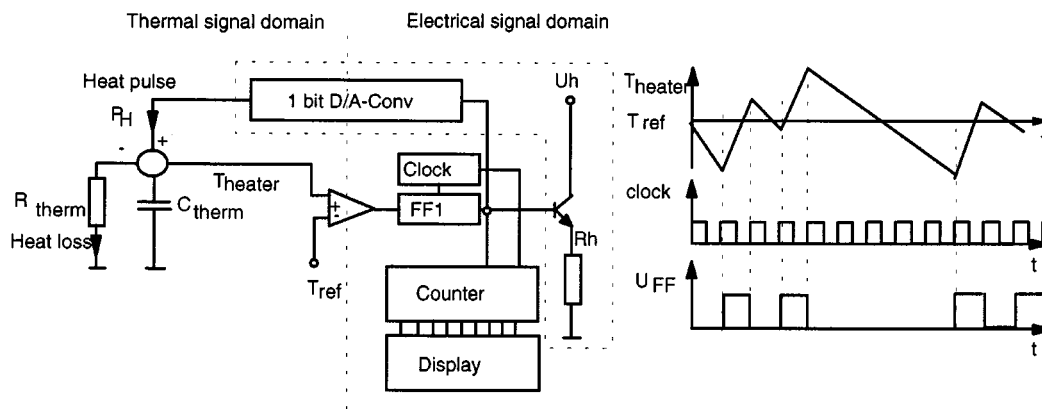


FIGURE 28.80 Principle of thermal sigma-delta modulation.

temperature difference to the fluid and can also be used for compensation of variations in temperature. For these reasons, accurate thermal mass flow sensors require both flow calibration and calibration for temperature compensation. Furthermore, the influence of temperature and/or fluid composition can be derived utilizing the relationships developed in the sections on modeling (Equations 28.120–28.135).

### Instrumentation and Components

Table 28.23 lists some companies that manufacture and market thermal mass flowmeters.

**TABLE 28.23** Manufactures of Thermal Mass Flow Sensors

Manufacturers	Data	Approximate price
KOBOLD Instruments Inc. 1801 Parkway View Drive Pittsburg, PA 15205	Calorimetric type: MAS-Series; air; min. range 0–10 mL min; max. range 0–40 L min. T max. 50°C; max. pressure 10 bar; accuracy $\pm 2\%$	~ US\$850
	Hot wire type: ANE-Series; air; range 0–20 m/s; working temperature 20–70°C	~ US\$1200
HÖNTZSCH GmbH Box 1324, Robert-Bosch Str. 8 D-7050 Waiblingen, Germany	Hot wire type: range 0.05–20 m/s	
	BRONKHORST HI-TEC Nijverheidstraat 1A 7261 AK Ruurlo, Netherlands	Calorimetric type: gases and liquids; min. range (gas) 0–5 mL min; max. range (liquid) 0–1000 ml/min; max. pressure 400 bar
HONEYWELL, MicroSwitch, Freeport, IL	Calorimetric type: Gases; range 0–1000 ml/min; max. pressure 1.75 bar	
SIERRA INSTRUMENTS INC. 5 Harris Ct., Bldg. L Monterey, CA 93924	Calorimetric type: all gases from 1 ml/min–10,000 l/min; –40–100°C; 30 bar max.; 1% accuracy	~ US\$400–1200
	Hot-wire type in stainless-steel sheath: gases from 0–100 m/s; –40–400°C; 100 bar max.; 2% accuracy	~ US\$60–2000
BROOKS INSTRUMENT DIVISION Emerson Electric Co. 407 W. Vine Street Hatfield, PA 19440	Calorimetric type: all gases from 1 ml/min to 10,000 l/min; –40–100°C; 100 bar max.; 1% accuracy	~ US\$400–1200

## References

1. Béla G. Lipták, *Flow Measurement*, Radnor, PA: Chilton Book, 1993.
2. H. Strickert, *Hitzdraht und Hitzfilmanemometrie* (Hot-wire and hot-film anemometry), Berlin: Verlag Technik, 1974.
3. G. Schnell, *Sensoren in der Automatisierungstechnik* (Sensors in the automation techniques), Braunschweig: Verlag Vieweg, 1993.
4. *Mass Flow and Pressure Meters/Controllers*, The Netherlands: Bronkhorst Hi-Tec B. V., 1994.
5. T. S. J. Lammerink, F. Dijkstra, Z. Houkes, and J. van Kuijk, Intelligent gas-mixture flow sensor, *Sensors and Actuators A*, 46/47, 380–384, 1995.
6. VDI-Wärmeatlas, VDI-Verlag, 1994.
7. H. Schlichting, *Boundary Layer Theory*, 7th ed., New York: McGraw-Hill, 1979.
8. A. J. Chapman, *Heat Transfer*, 4th ed., New York: Macmillan, 1984.
9. T. S. J. Lammerink, Niels R. Tas, Miko Elwenspoek, and J. H. J. Fluitman, Micro-liquid flow sensor, *Sensors and Actuators A*, 37/38, 45–50, 1993.
10. N.T. Nguyen and W. Dötzel, A novel method for designing multi-range electrocaloric mass flow sensors: asymmetrical locating with heater- and sensor arrays, *Sensors and Actuators A*, 62, 506–512, 1997.
11. J. van Kuijk, T. S. T. Lammerink, H.-E. de Bree, M. Elwenspoek, and J. H. J. Fluitman, Multi-parameter detection in fluid flows, *Sensors and Actuators A*, 46/47, 380–384, 1995.
12. S. M. Sze, *Semiconductor Sensors*, New York: John Wiley & Sons, 1994.
13. You-Chong Tai and Richard S. Muller, Lightly-doped polysilicon bridge as a flow meter, *Sensors and Actuators A*, 15, 63–75, 1988.
14. R. G. Johnson and R. E. Higashi, A highly sensitive silicon chip microtransducer for air flow and differential pressure sensing applications, *Sensors and Actuators A*, 11, 63–67, 1987.
15. H. J. Verhoeven and J. H. Huijsing, An integrated gas flow sensor with high sensitivity, low response time and pulse-rate output, *Sensors and Actuators A*, 41/42, 217–220, 1994.

16. F. Mayer, G. Salis, J. Funk, O. Paul, and H. Baltes, Scaling of thermal CMOS gas flow microsensors experiment and simulation, *MEMS '96*, San Diego, 1996, 116-121.
17. Göran Stemme, A CMOS integrated silicon gas-flow sensor with pulse-modulated output, *Sensors and Actuators A*, 14, 293-303, 1988.
18. Canqian Yang and Heinrik Soeberg, Monolithic flow sensor for measuring millilitre per minute liquid flow, *Sensors and Actuators A*, 33, 143-153, 1992.
19. Dun Yu, H. Y. Hsieh, and J. N. Zemel, Microchannel pyroelectric anemometer, *Sensors and Actuators A*, 39, 29-35, 1993.
20. S. G. Joshi, Flow sensors based on surface acoustic waves, *Sensors and Actuators A*, 44, 63-72, 1994.
21. U. Bonne, Fully compensated flow microsensor for electronic gas metering, *Proc. Int. Gas Research Conf.*, 16-19 Nov. '92, Orlando, FL, 3, 859, 1992.
22. J. H. Huijsing, F. R. Riedijk, and G. van der Horn, Developments in integrated smart sensors, *Proc. of Transducer 93*, Yokohama, Japan, 1993, 320-326.

## 28.10 Coriolis Effect Mass Flowmeters

---

*Jesse Yoder*

Coriolis flowmeters were developed in the 1980s to fill the need for a flowmeter that measures mass directly, as opposed to those that measure velocity or volume. Because they are independent of changing fluid parameters, Coriolis meters have found wide application. Many velocity and volumetric meters are affected by changes in fluid pressure, temperature, viscosity, and density. Coriolis meters, on the other hand, are virtually unaffected by these types of changes. By measuring mass directly as it passes through the meter, Coriolis meters make a highly accurate measurement that is virtually independent of changing process conditions. As a result, Coriolis meters can be used on a variety of process fluids without recalibration and without compensating for parameters specific to a particular type of fluid. Coriolis flowmeters are named after Gaspard G. Coriolis (1792–1843), a French civil engineer and physicist for whom the Coriolis force is named.

Coriolis meters have become widely used in industrial environments because they have the highest accuracy of all types of flowmeters. They measure mass directly, rather than inferentially. Coriolis meters do not have moving parts like turbine and positive displacement meters, which have parts that are subject to wear. Maintenance requirements for Coriolis meters are low, and they do not require frequent calibration. Wetted parts can be made from a variety of materials to make these meters adaptable to many types of fluids. Coriolis meters can handle corrosive fluids and fluids that contain solids or particulate matter. While these meters were used mainly for liquids when they were first introduced, they have recently become adaptable for gas applications.

### Theory of Operation

Coriolis meters typically consist of one or two vibrating tubes with an inlet and an outlet. While some are U-shaped, most Coriolis meters have some type of complex geometric shape that is proprietary to the manufacturer. Fluid enters the meter in the inlet, and mass flow is determined based on the action of the fluid on the vibrating tubes. [Figure 28.81](#) shows flow tube response to Coriolis acceleration.

Common to Coriolis meters is a central point that serves as the axis of rotation. This point is also the peak amplitude of vibration. What is distinctive about this point is that fluid behaves differently, depending on which side of the axis of rotation, or point of peak amplitude, it is on. As fluid flows toward this central point, the fluid takes on acceleration due to the vibration of the tube. As the fluid flows away from the amplitude of peak vibration, it decelerates as it moves toward the tube outlet. On the inlet side of the tube, the accelerating force of the flowing fluid causes the tube to lag behind its no-flow position. On the outlet side of the tube, the decelerating force of the flowing fluid causes the tube to lead ahead of its no-flow position. As a result of these forces, the tube takes on a twisting motion as it passes through

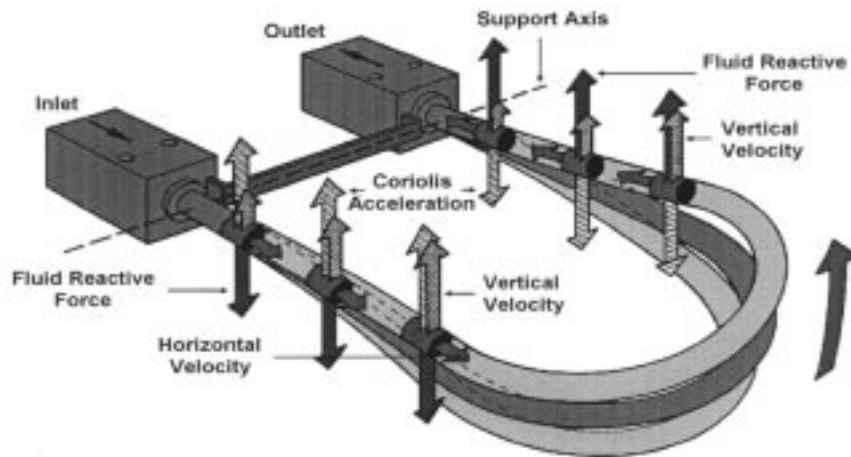


FIGURE 28.81 Flow tube response to Coriolis acceleration.

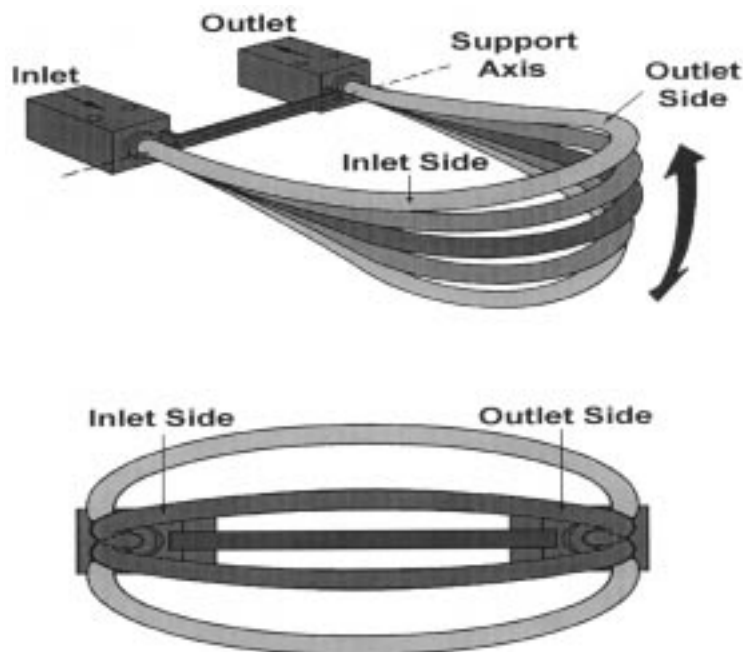


FIGURE 28.82 Two views of an oscillating flow tube with no flow.

each vibrational cycle; the amount of twist is directly proportional to the mass flow through the tube. [Figure 28.82](#) shows the Coriolis flow tube in a no flow situation, and [Figure 28.83](#) shows Coriolis tube response to flow.

The Coriolis tube (or tubes, for multitube devices) is vibrated through the use of electromagnetic devices. The tube has a drive assembly, and has a predictable vibratory profile in the no-flow position. As flow occurs and the tube twists in response to the flow, it departs from this predictable profile. The degree of tube twisting is sensed by the Coriolis meter's detector system. At any point on the tube, tube motion represents a sine wave. As mass flow occurs, there is a phase shift between the inlet side and the outlet side. This is shown in [Figure 28.84](#).



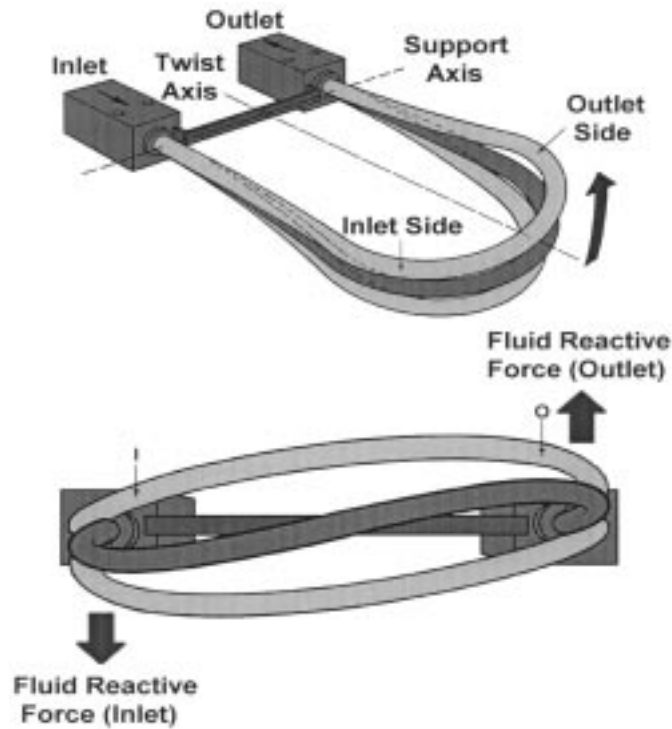


FIGURE 28.83 Two views of an oscillating flow tube in response to flow.

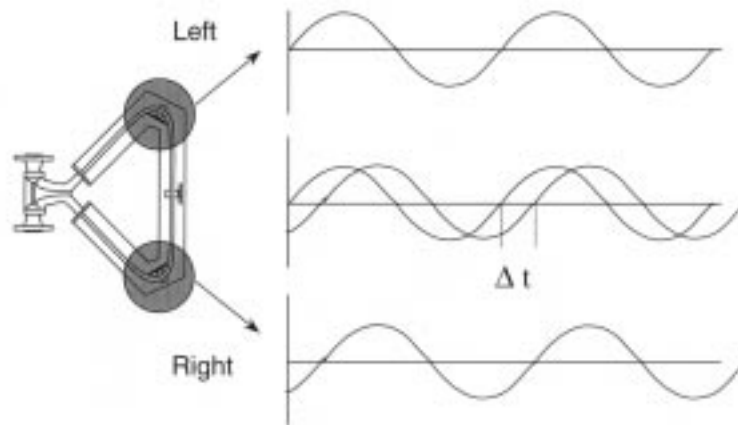


FIGURE 28.84 Phase shift between inlet side and outlet side.

The Coriolis force induced by flow is described by an equation that is equivalent to Newton's second law for rotational motion. This equation is as follows:

$$F = 2m\omega\bar{v} \quad (28.145)$$

In Equation 28.145,  $F$  is force,  $m$  is the mass to be applied to a known point at a distance  $L$  from the axis 0-0,  $\omega$  is a vector representing angular motion, and  $\bar{v}$  is a vector that represents average velocity.

## Construction

The internal part of the Coriolis tube is the only part of the meter that is wetted. A typical material of construction is stainless steel. Other corrosion-resistant metals such as Hastelloy are used for tube construction. Some meters are lined with Teflon.

Some designs have thin-wall as well as standard tubes. A thin-wall design makes the meter more useful for gas and low-velocity liquid applications, where the amount of twist by the tube is reduced. It is important to be aware of the extent to which the fluid degrades or attacks the tube wall or lining. If the fluid eats away at the wall, this can reduce the accuracy of the meter.

## Advantages

The most significant advantage of Coriolis meters is high accuracy under wide flow ranges and conditions. Because Coriolis meters measure mass flow directly, they have fewer sources of errors. Coriolis meters have a high turndown, which makes them applicable over a wide flow range. This gives them a strong advantage over orifice plate meters, which typically have low turndown. Coriolis meters are also insensitive to swirl effects, making flow conditioning unnecessary. Flow conditioners are placed upstream from some flowmeters to reduce swirl and turbulence for flowmeters whose accuracy or reliability is affected by these factors.

Coriolis meters have a low cost of ownership. Unlike turbine and positive displacement meters, Coriolis meters have no moving parts to wear down over time. The only motion is due to the vibration of the tube, and the motion of the fluid flowing inside the tube. Because Coriolis flowmeters are designed not to be affected by fluid parameters such as viscosity, pressure, temperature, and density, they do not have to be recalibrated for different fluids. Installation is simpler than installation for many other flowmeters, especially orifice plate meters, because Coriolis meters have fewer components.

Coriolis meters can measure more than one process variable. Besides mass flow, they can also measure density, temperature, and viscosity. This makes them especially valuable in process applications where information about these variables reduces costs. It also makes it unnecessary to have a separate instrument to measure these additional variables.

## Disadvantages

The chief disadvantage of Coriolis meters is their initial cost. While some small meters have prices as low as \$4000, the base price for most Coriolis meters is \$6000 and up. The cost of Coriolis meters rises significantly as line sizes increase. The physical size of Coriolis meters increases substantially with the increase in line size, making 150 mm (6 in.) the upper line size limit on Coriolis meters today. The large size of some Coriolis meters makes them difficult to handle, and can also make installation difficult in some cases.

The lack of an established body of knowledge about Coriolis meters is a substantial disadvantage. Because Coriolis meters were recently invented, not nearly as much data are available about them as are for differential pressure-based flowmeters. This has made it difficult for Coriolis meters to gain approvals from industry associations such as the American Petroleum Institute. This will change with time, as more manufacturers enter the market and users build up a larger base of experience.

## Applications

Coriolis meters have no Reynolds number constraints, and can be applied to almost any liquid or gas flowing at a sufficient mass flow to affect vibration of the flowmeter. Typical liquid applications include foods, slurries, harsh chemicals, and blending systems. The versatility of Coriolis meters in handling multiple fluids makes them very useful for plants where the flow of multiple fluid types must be measured.

There are an increasing number of gas applications for Coriolis meters. While gas applications are still very much in the minority, the use of this meter to measure gas is likely to increase as more is learned about its use for this purpose.

## A Look Ahead

There are some important areas of research for Coriolis meters. While most Coriolis meters have been bent, several manufacturers have recently introduced straight-tube designs. Manufacturers will continue to fine-tune the single-tube vs. double-tube design, and to work on tube geometry. As noted above, the use of Coriolis meters for gas and also for steam applications is another area for future development.

## References

- E. O. Doebelin, *Measurement Systems: Application and Design*, 4th ed., New York: McGraw Hill, 1990, 603–605.
- R. S. Figliola and D. E. Beasley, *Theory and Design for Mechanical Measurements*, 2nd ed., New York: John Wiley & Sons, 1995, 475–478.
- K. O. Plache, Coriolis/Gyroscopic Flowmeter, *Mechanical Engineering*, MicroMotion Inc., Boulder, CO, March 1979, 36–41.
- L. Smith and J. R. Ruesch, *Flow Measurement*, D. W. Spitzer (ed.), Research Triangle Park, NC: Instrument Society of America, 1996, 221–247.

## 28.11 Drag Force Flowmeters

---

*Rekha Philip-Chandy, Roger Morgan, and Patricia J. Scully*

In a *target flowmeter* a solid object known as a *drag element* is exposed to the flow of fluid that is to be measured. The force exerted by the fluid on the drag element is measured and converted to a value for speed of flow.

The flow-sensing element has no rotating parts, and this makes the instrument suitable for conditions where abrasion, contamination, or corrosion make more conventional instruments unsuitable. An important application of such flowmeters involves environmental monitoring in areas such as meteorology, hydrology, and maritime studies to measure speeds of air or water flow and turbulence close to the surface. In these applications, the fluid flows are sporadic and multidirectional.

A further advantage of the instrument is that it can be made to generate a measurement of flow *direction* in two dimensions, or even in three dimensions, as well as of flow speed. To implement this feature, the drag element must be symmetrical in the appropriate number of dimensions, and it is necessary to measure the force on it vectorially, again in the appropriate number of dimensions. Provided that the deflecting forces are independent in the sensing directions, the resulting outputs can be added vectorially to generate independent values for flow speed and direction. Target flowmeters using strain gage technology have been used by industry, utilities, aerospace, and research laboratories. They have been used to successfully measure the flow of uni- and bidirectional liquids (including cryogenic), gases, and steam (both saturated and superheated) for almost half a century.

Despite these advantages, the target flowmeter appears to have been neglected in favor of more complex and sophisticated devices. The authors have sought to remedy this neglect by developing a sensor suitable for measuring multidirectional flows in two dimensions, instead of measuring only bidirectional flows in a single dimension.

### Design of the Flow Sensor

The sensor described in this chapter section is ideally suited for environmental flow measurement. The operation is based on strain measurement of deformation of an elastic rubber cantilever, to which a force is applied by a spherically symmetrical drag element (Figure 28.85). This sensor has many advantages, including compactness and a simple construction requiring no infrastructure other than a rigid support, and it can cope with fluids containing solid matter such as sludge and slurries provided that they do not tangle with the drag element or the rubber beam.

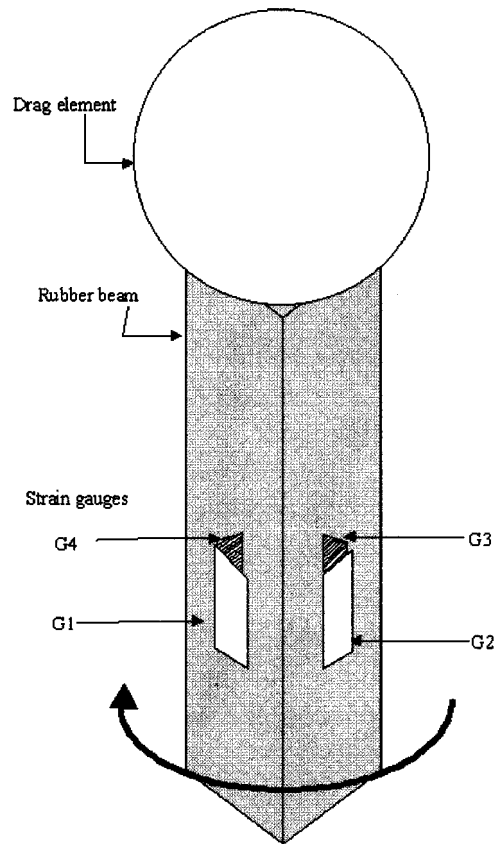


FIGURE 28.85 Schematic of the electric resistance strain gage drag force flow sensor.

According to Clarke [1], the ideal drag element is a flat disk, because this configuration gives a drag coefficient independent of flow rate. Using a spherical drag element, which departs from the ideal of a flat disk [1], the drag coefficient is likely to vary with flow speed, and therefore the gage must be calibrated and optimized for the conditions of intended use. In this discussion, a gage is developed for air flows in the range normally encountered in the natural environment.

The strain measurement can be performed with conventional strain gages, but this limits the applications of the device to conditions where corrosion of the metal-resistive track of the strain gage can be avoided. Therefore, an optical fiber strain gage has been developed as an alternative.

### Principle of Fluid Flow Measurement

The drag force  $F_D$  exerted by a fluid on a solid object exposed to it is given by the *drag equation*, which from incompressible fluid dynamics is:

$$F_D = \frac{C_D \rho AV^2}{2} \quad (28.146)$$

where  $\rho$  = Fluid density

$V$  = Fluid's velocity at the point of measurement

$A$  = Projected area of the body normal to the flow

$C_D$  = Overall drag coefficient

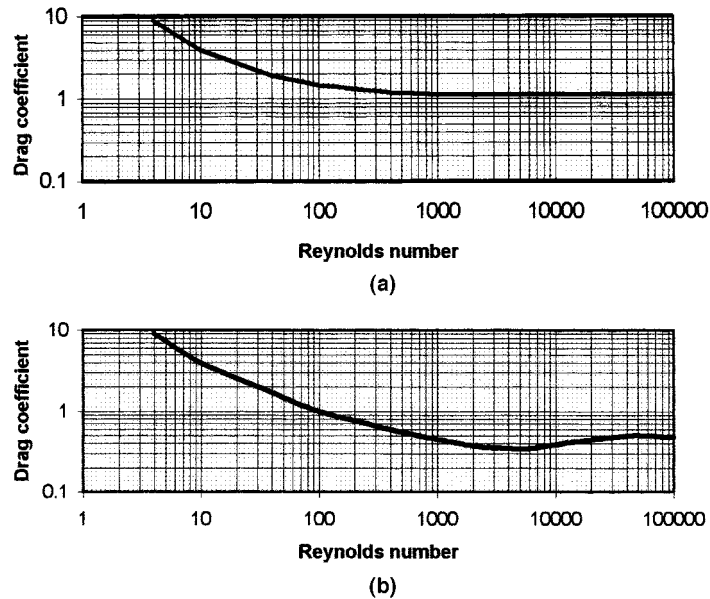


FIGURE 28.86 Graph shows drag coefficient  $C_D$  plotted against Reynolds number  $Re$  for (a) a flat disk and (b) a sphere.

$C_D$  is a dimensionless factor, whose magnitude depends primarily on the physical shape of the object and its orientation relative to the fluid stream. The drag coefficient  $C_D$  for a sphere is related to the Reynolds number ( $Re$ ), another dimensionless factor, given by:

$$Re = \rho V A / \eta \quad (28.147)$$

where  $\eta$  = viscosity of the fluid.

A graph of  $C_D$  against Reynolds number (derived from Clarke [1]) is shown in Figure 28.86(a) for a flat disk and Figure 28.86(b) for a sphere, from which it is evident that the value of  $C_D$ , although not constant, is not subject to wide variation over the range of the graph.

Now consider the effect of the force  $F_D$  on an elastic beam to which the drag element is attached (as in Figure 28.85). If the mass of the beam can be ignored, the deflection of the beam will be due only to force exerted on the drag element by the fluid. From the theory of elasticity for a cantilever beam of length  $L$  with point load at its end [2], the shear force  $P$  will be constant along the beam. The bending moment,  $M$  at a point  $x$  along the beam will be  $P(L-x)$  so that it varies linearly from  $PL$  at  $x = 0$  to 0 at  $x = L$ . The distance  $y$  is measured from the neutral plane, which for a rectangular section is the mid-plane.

The inverse of the radius of curvature is given by:

$$\frac{1}{\rho} = \frac{M}{EI} \quad (28.148)$$

where  $E$  is the modulus of elasticity or the Young's modulus and  $I$  is the moment of inertia of the cross-section where it is assumed that the force is applied perpendicular to the broad face of width  $b$ .

$$I = \frac{b a^3}{12} \quad (28.149)$$

Through the thickness  $a$  of the beam, the strain is  $\epsilon_x$ .

$$\epsilon_x = \frac{\sigma_x}{E} = \frac{Y}{\rho} \quad (28.150)$$

Substituting Equation 28.148 in Equation 28.150 gives:

$$\epsilon_x = \frac{YM}{EI} \quad (28.151)$$

The strain at the surfaces is:

$$\epsilon_x = \frac{a}{2\rho} = \frac{YM}{2EI} \quad (28.152)$$

Substituting Equation 28.149 and the bending moment into Equation 28.151 gives:

$$\epsilon_x = \frac{6P(L-x)}{Ea^2b} \quad (28.153)$$

or, the shear force  $P$  is:

$$P = \frac{\epsilon E a^2 b}{6(L-x)} \quad (28.154)$$

Consequently,

$$\frac{C_D \rho AV^2}{2} = \frac{\epsilon E a^2 b}{6(L-x)} \quad (28.155)$$

Therefore, the strain is:

$$\epsilon = \frac{3C_D \rho AV^2 (L-x)}{Ea^2b} \quad (28.156)$$

From Equation 28.156, the strain is a square law function of fluid speed.

For most fluid flows in the natural environment, a two-dimensional measurement is necessary as the flow in the natural environment is almost always two-dimensional. For a measurement of flow speed and direction, it is necessary to relate wind speed to strain measured in two orthogonal directions, on the assumption (which has been justified by experiment) that the velocity vector has a zero component along (parallel to) the rubber beam support (i.e.,  $U_z = 0$ ). The wind speed  $U$  has orthogonal components  $U_x$  and  $U_y$  that are proportional to the strain measured in the  $x$  (strain <sub>$x$</sub> ) and  $y$  directions (strain <sub>$y$</sub> ), respectively. Since  $U_x$  is proportional to  $\sqrt{\text{strain}_x}$  and  $U_y$  is proportional to  $\sqrt{\text{strain}_y}$ , then the velocity magnitude  $|U|$  can be written as

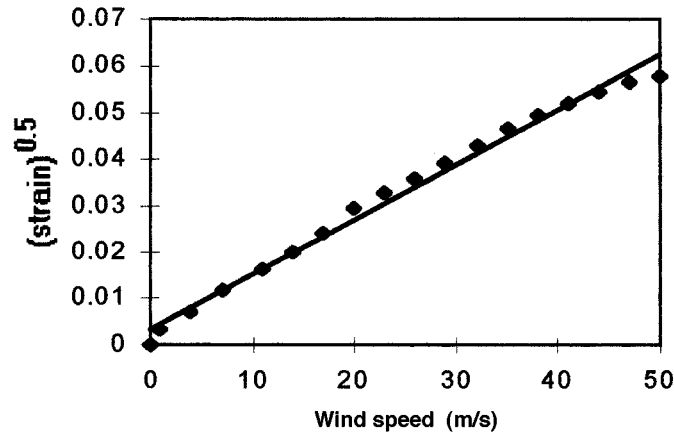


FIGURE 28.87 Root strain vs. wind speed for one dimensional air flow measurement.

$$|U| = \sqrt{U_x^2 + U_y^2} \quad (28.157)$$

thus, 
$$|U| \propto \sqrt{\text{strain}_x + \text{strain}_y} \quad (28.158)$$

Therefore, the magnitude of the velocity,  $|U|$ , is proportional to the square root of the sum of the orthogonal strain components,  $\text{strain}_x$  and  $\text{strain}_y$ . The velocity direction,  $\theta$ , is calculated using the relation:

$$\theta = \tan^{-1} \left[ \frac{\sqrt{\text{strain}_y}}{\sqrt{\text{strain}_x}} \right] \quad (28.159)$$

### Implementation Using Resistive Strain Gages

A sensor was constructed for measuring one-dimensional flows by bonding two strain gages onto the opposite sides of a square-sectioned elastic beam, 165 mm long and 13.5 mm square, made from polybutadiene polymer (unfilled vulcanized rubber) supplied by the Malaysian Rubber Products Research Association. The modulus of the beam, at approximately  $1.2 \times 10^6 \text{ N m}^{-2}$ , was relatively low in order to achieve good sensitivity. The drag element was a table tennis ball of diameter 20 mm, glued to the end of the rubber beam. The strain gages were cupro-nickel alloy on a polyimide film, and were bonded to the rubber beam with epoxy resin. The two gage elements were connected in a half-bridge configuration, and the output was taken to a digital strain-gage indicator reading directly in microstrain units.

The sensor was mounted in a calibrated wind tunnel, in such a way that one gage underwent compression and the other gage underwent extension. The wind speed was set at different values and the corresponding strain readings were noted. Results were plotted as wind speed against square root of strain (Figure 28.87). The graph obtained was linear with a correlation co-efficient of 0.98. The linearity shows that the strain is a square-law function of speed, which confirms the theory above.

In this first prototype of the sensor, the range was limited by beam oscillations at speeds greater than  $23 \text{ m s}^{-1}$ , causing spurious signals. In principle, however, much greater speeds up to  $50 \text{ m s}^{-1}$  can be monitored by this sensor, if the construction is suitable.

A second sensor was constructed for measuring two-dimensional flows, in which a square-sectioned rubber beam similar to the previous one was set up with four strain gages attached to the four longitudinal

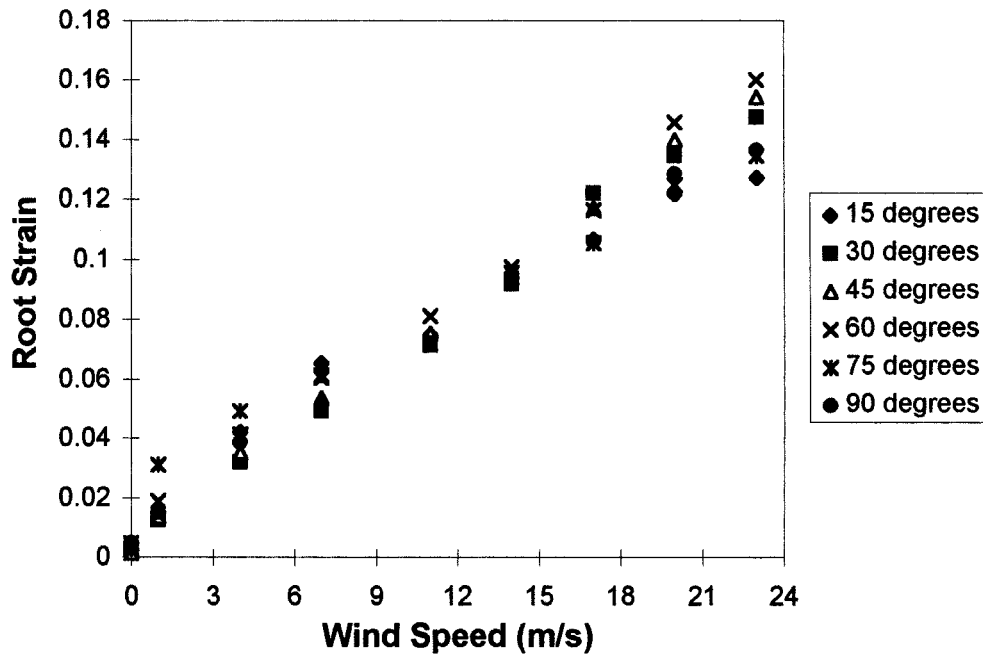


FIGURE 28.88 Root strain plotted against wind speed with the flowmeter oriented at various angles to wind flow.

surfaces of the beam. Each opposite pair of strain gage elements was connected in a half-bridge configuration as before. The two outputs were taken to instrumentation amplifiers and then to a data acquisition board interfaced to the LabView instrumentation software package (National Instruments Corporation). After appropriate signal processing by the software, the values of  $\text{strain}_x$  and  $\text{strain}_y$  from both the channels are added and then the square root of the absolute value of this sum is found.

The device was clamped on a turntable and this was rotated about its longitudinal axis from  $0^\circ$  to  $90^\circ$  at  $15^\circ$  intervals. At each angle, the  $x$  and  $y$  strain gage outputs were recorded as a function of velocity, over a range from 0 to  $23 \text{ m s}^{-1}$ . The graph of speed vs.  $(\text{strain}_x + \text{strain}_y)^{1/2}$  for different angles is shown in Figure 28.88. The data presented in Figure 28.88 can be used to obtain a speed calibration curve for the sensor, which will be valid for multidirectional air flow.

The direction of wind flow was calculated according to Equation 28.159 for the different wind speeds. Figure 28.89 shows the plots of the wind flow direction at different wind speeds for various sensor positions. Several authors have published the inability of calculating the wind direction accurately at low wind speeds. The situation is similar in this case and the readings get more accurate as the wind speed increases, especially beyond  $11 \text{ m s}^{-1}$ .

For the measurement of gusts, the time response of the sensor becomes a critical parameter. Experiments were performed to measure the response time by dropping known weights on the free end of the sensor and using a specially written program in Labview to acquire and record the response. The sensor indicated a 95% response time of 50 ms and a time constant of 30 ms.

### Optical Fiber Strain Gage Drag Force Flowmeter

Optical fibers have been applied to measurement of fluid flow, and strain measurement, using interferometric techniques and bending losses [3–5]. The instrument described in the previous sections can be adapted to use optical strain measurement instead of resistive strain gages. In this way, the advantages of the instrument can be preserved; in addition, the flowmeter has the usual benefits of optical fiber sensors such as immunity to electromagnetic interference and intrinsic safety in hazardous environments.



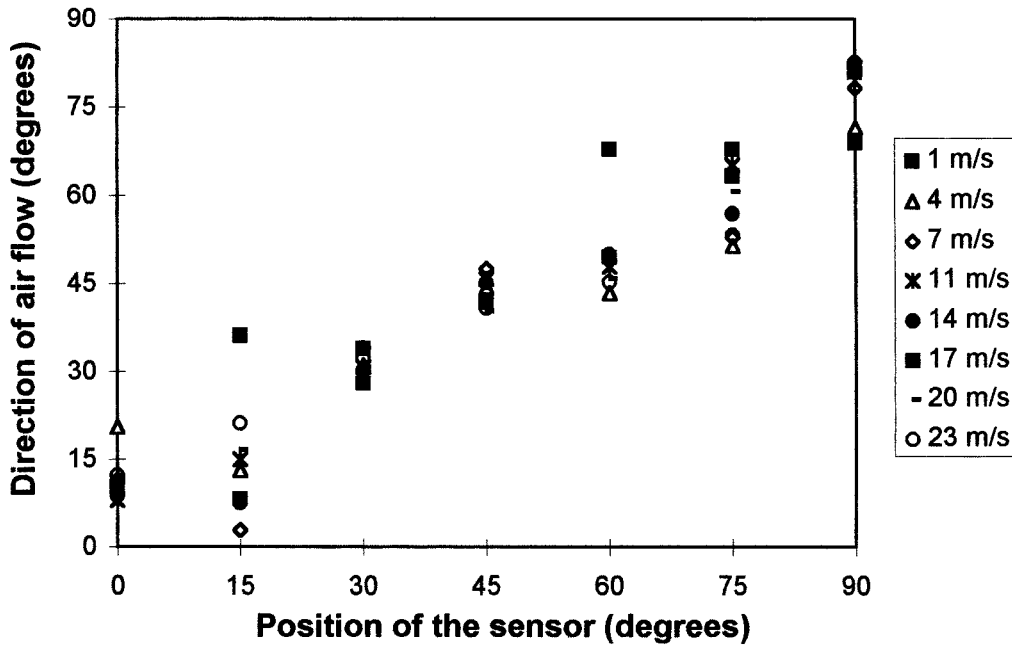


FIGURE 28.89 Calculated direction of wind velocity at different wind speeds.

The principle of an optical fiber strain gage is based on the effect of one or more grooves inserted radially into a 1 mm diameter PMMA fiber, which cause a loss in light transmission. As the optical fiber is bent, as in a cantilever, the angle of the grooves varies. These changes of angle cause light to be attenuated at each groove. The intensity variation can be related to the change of the angle of the groove caused by the bending of the cantilever.

To develop an analogy between the optical strain measurement and the resistive strain measurement, the optical strain was calculated using the formula:

$$\text{Strain}_{\text{opt}} = \frac{\text{Change in power output}}{\text{Original power output}} = \frac{\Delta P}{P} \quad (28.160)$$

Hence,

$$\text{Strain}_x = \frac{\Delta P_x}{P_x} \quad \text{and} \quad \text{strain}_y = \frac{\Delta P_y}{P_y} \quad (28.161)$$

Therefore, the magnitude of the velocity,  $|U|$  is given by:

$$|U| = \sqrt{U_x^2 + U_y^2} = \sqrt{\text{strain}_x + \text{strain}_y}$$

Substituting Equation 28.161 in  $|U|$ , the optical root strain magnitude is:

$$|U| = \sqrt{\left( \frac{\Delta P_x}{P_x} + \frac{\Delta P_y}{P_y} \right)} \quad (28.162)$$

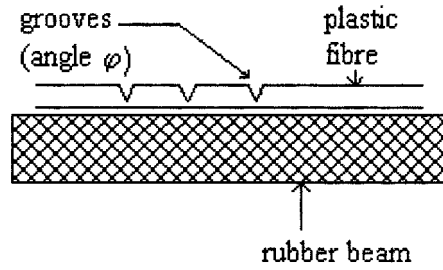


FIGURE 28.90 Principle of operation of the fiber optic drag force flow sensor.

and the direction of wind velocity,  $\theta$ :

$$\theta = \tan^{-1} \left[ U_y / U_x \right] = \tan^{-1} \sqrt{\frac{\text{Strain}_y}{\text{Strain}_x}} \quad (28.163)$$

Substituting Equation 28.161 in  $\theta$ , the optical strain direction is:

$$\theta = \tan^{-1} \frac{\sqrt{\left( \frac{\Delta P_y}{P_y} \right)}}{\sqrt{\left( \frac{\Delta P_x}{P_x} \right)}} \quad (28.164)$$

Two types of the optical fiber flow sensor are described here. In the first type, the rubber beam is used as the deflected device with optical fiber strain gages attached to the deflected beam. The second version of this flow sensor uses an unsupported sensitised 1 mm diameter plastic optical fiber that undergoes deflection in the airflow.

### Fiber Optic Flow Sensor WITH Rubber Beam

The sensor has been built using a rectangular cross-sectioned rubber beam and a spherical drag element with a 1 mm plastic optical fiber glued to the beam with epoxy. The fiber is looped inside the drag element to enhance the sensitivity of the device. Grooves have been made in the fiber surface that extends into the core of the fiber to increase the losses as a function of the bending of the rubber beam (Figure 28.90).

The grooves are normal to the rubber beam on its outside face, and their depths affect only the cladding of the fiber. As the cantilever bends due to the force exerted by the air flow, the angle of the grooves vary. The groove angle increases when the air flow is facing the sensor, and vice versa. These changes of groove angle cause an intensity modulation of the light transmitted through the fiber because light is lost at each groove. Changes in intensity can be related to changes in the angle caused by the force inducing the bending of the cantilever, and therefore to the velocity of the fluid.

The orthogonal components of strain were measured by attaching two grooved optical fibers on adjacent sides of the rubber beam, orthogonal to each other, as illustrated in Figure 28.91. These two fibers measured the  $x$  and  $y$  components of optical strain.

Light from a 1 mW helium-neon laser of peak wavelength 633 nm was split into equal components using a cubic beam splitter, and coupled into each fiber. The transmitted intensity through each of the two fibers was monitored using a power meter. The signals from the power meter were sent to a 486 DX2 laptop computer via a data acquisition card to be acquired and processed by Labview. Experiments indicated that this version of the flow sensor could measure wind speeds up to  $30 \text{ m s}^{-1}$  with a resolution of  $1.3 \text{ m s}^{-1}$ .

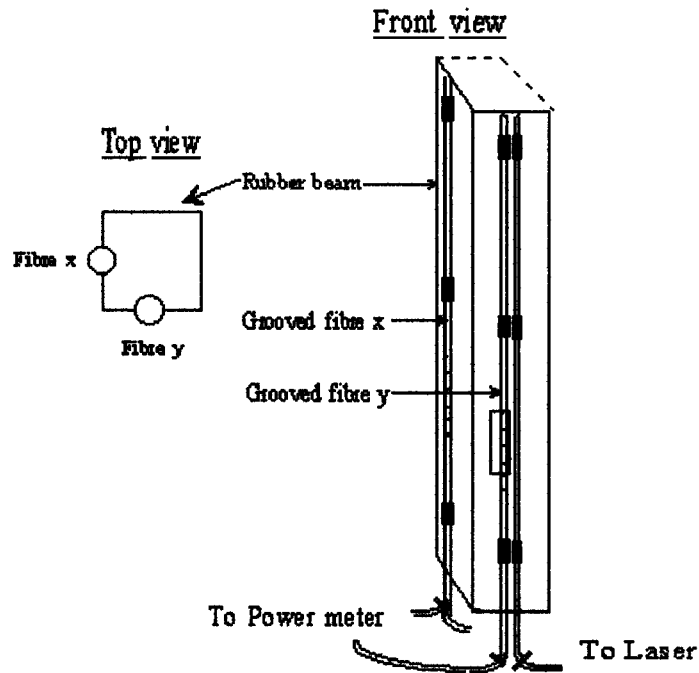


**FIGURE 28.91** Front and top views of a section of the fiber optic drag force flow sensor used to measure the two dimensional fluid flow.

### Fiber Optic Flow Sensor WITHOUT Rubber Beam

This version of the sensor uses 1 mm diameter polymer fiber as the deflection element, with a core diameter of 0.980 mm, and a thin cladding layer of approximately 20  $\mu\text{m}$  [6]. Multiple grooves were etched radially into the fiber surface to a depth of 0.5 mm, extending into the core of the fiber, using a hot scalpel, and a manufactured V-groove template to ensure uniformity of grooves. Six grooves were determined as the optimum number to achieve a compromise between insertion losses and strain sensitivity, spaced 0.4 cm apart, over a length of 2.5 cm.

In order to measure strain in two orthogonal directions, perpendicular to the longitudinal axis of the fiber, two fibers were used, as shown in Figure 28.92, with the grooves oriented at  $90^\circ$  to each other. This was achieved by positioning the fibers on two adjacent faces of a beam of square cross-section. This beam was short enough to prevent any restriction to the deflection and yet long enough to hold and support the optical fibers. The fibers were looped around so that the looped ends acted as drag elements. The grooved portion of the fiber was unsupported and free to deflect in the air stream. Wind tunnel calibration indicated that the sensor could measure two-dimensional flow up to  $35 \text{ m s}^{-1}$  with a resolution of  $0.96 \text{ m s}^{-1}$ .

### Conclusion

The measurement of one- and two-dimensional fluid velocity, using both optical fiber and conventional strain gages on a deflected beam, for a range of 0 to  $30 \text{ m s}^{-1}$ , has been demonstrated experimentally. Although flow visualization and modeling techniques are well advanced in engineering, there is still a need for real measurements, especially in the natural environment. The sensors described in this study are particularly suited for such measurements, which are almost always two-dimensional. The outputs

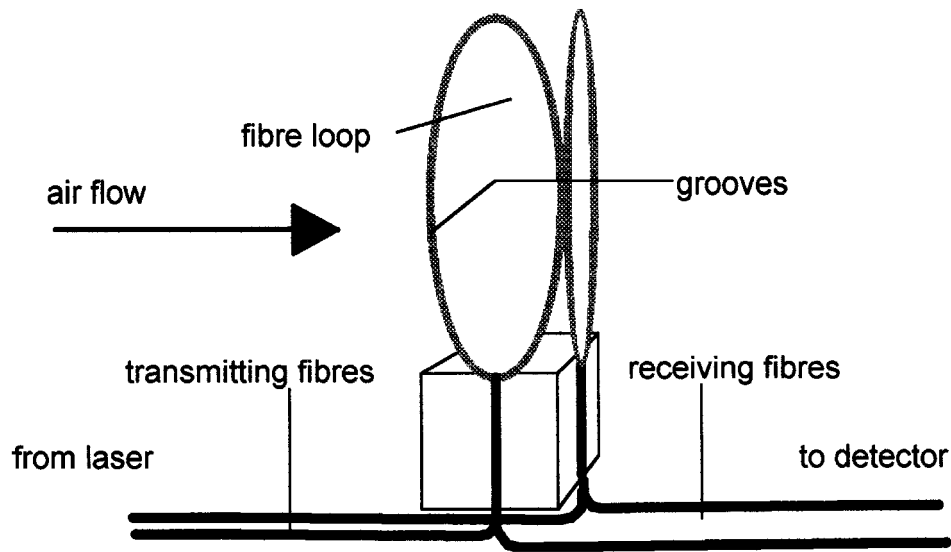


FIGURE 28.92 Optical fiber drag force flow sensor without rubber beam.

of the sensor representing speed and direction of fluid flow are independent of each other, so the sensor is suitable for environmental applications such as wind measurement or river flow, where the fluid forms gusts and can change direction as well as speed. One noteworthy feature of this sensor is its quick response time of 50 ms, which easily enables the measurement of gusts. The dimensions and materials of the sensor must be chosen to suit the fluid. In terms of sensitivity and resolution, the resistive strain gage sensor is a better option, but replacing the conventional strain gages with optical fiber strain gages ensures electrical noise immunity and intrinsic safety for use in hazardous environments.

## References

1. T. Clarke, Design and operation of target flowmeters, *Encyclopedia of Fluid Mechanics*, Vol 1, Houston, TX: Gulf Publishing Company, 1986.
2. F. H. Newman and V. H. L. Searle, The general properties of matter. Edward Arnold, 1948.
3. S. Webster, R. McBride, J. S. Barton, and J. D. C. Jones, Air flow measurement by vortex shedding from multimode and monomode fibres. *Measurement, Science and Technology*, 3, 210-216, 1992.
4. J. S. Barton and M. Saudi, A fibre optic vortex flowmeter. *J. Phys. E: Sci. Instrum.* 19, 64-66, 1986.
5. N. Narendran, A. Shukla, and S. Letcher, Optical fibre interferometric strain sensor using a single fibre, *Experimental Techniques*, 16(2), 33-36, 1992.
6. R. Philip-Chandy, Ph.D. thesis, *Fluid flow measurement using electrical and optical fibre strain gauges*, Liverpool John Moores University, UK, 1997.